Cellular and molecular mechanisms of VEGF-induced dose-dependent angiogenesis

Inauguraldissertation

zur
Erlangung der Würde eines Doktors der Philosophie
vorgelegt der
Philosophisch-Naturwissenschaftlichen Fakultät
der Universität Basel

von

Marianna Trani

aus **Italien**

Basel, 2012

Genehmigt von der Philosophisch-Naturwissenschaftlichen Fakultät

auf Antrag von

Prof. Dr. Markus Affolter   Dr. Andrea Banfi   Prof. Dr. Michael Heberer

Basel, den 26 Juni 2012

Prof. Dr. Martin Spiess

Table of Contents

Molecular mechanisms of angiogenesis

1.1 Hallmarks of vessel formation

The development of the vascular system is a complex process, which requires the fine interplay of several factors and molecular signals. During embryonic development, the vascular system develops shortly after gastrulation and plays a pivotal role, providing both signals for organ morphogenesis and carrying oxygen to distant districts. In the adult, blood vessels are essential for the maintenance of the tissue metabolism and for the repair process during wound healing. Inadequate blood vessel growth causes several pathological conditions, such as myocardial infarction and stroke. On the other hand, excessive and abnormal blood vessel outgrowth can trigger inflammatory disorders and cancer. In order to develop novel therapies for the treatment of such pathologies, a better understanding of the processes governing blood vessel formation is required.

1.1.1. Blood vessels in embryonic development

In the developing embryo, initial blood vessels appear through a process known as *vasculogenesis*, in which blood vessels form *de novo* by differentiation and coalescence of individual progenitor cells [1]. These progenitors are mesoderm-derived and can generate only endothelial cells (angioblasts) in response to vascular endothelial growth factor (VEGF), or can differentiate both in endothelial and hematopoietic cells (hemangioblasts) [2]. After commitment to the endothelial lineage, angioblasts generate specialized structures, called blood islands, which can then fuse and remodel in response to

haemodynamic forces to generate the first primitive plexus of vessels [3]. Later in development, during differentiation, endothelial cells in the plexus become committed to either arterial or venous fate (Figure 1). Originally, it was thought that only genetic pre-determination as well as differences in blood flow and pressure controlled the specification in arteries or veins [4]. Recent studies identified several signalling pathways controlling arterial and venous identities of endothelial cells, such as the complex Eph-Ephrin system [4, 5]. In addition, VEGF, Notch, angiopoietins, platelet derived growth factor (PDGF) and transforming growth factor (TGF)-beta are also key molecular determinants of vascular morphogenesis both in embryo and in adults [6]. After endothelial cell specification, the vascular plexus expands giving rise to a functional network of vessels by sprouting.
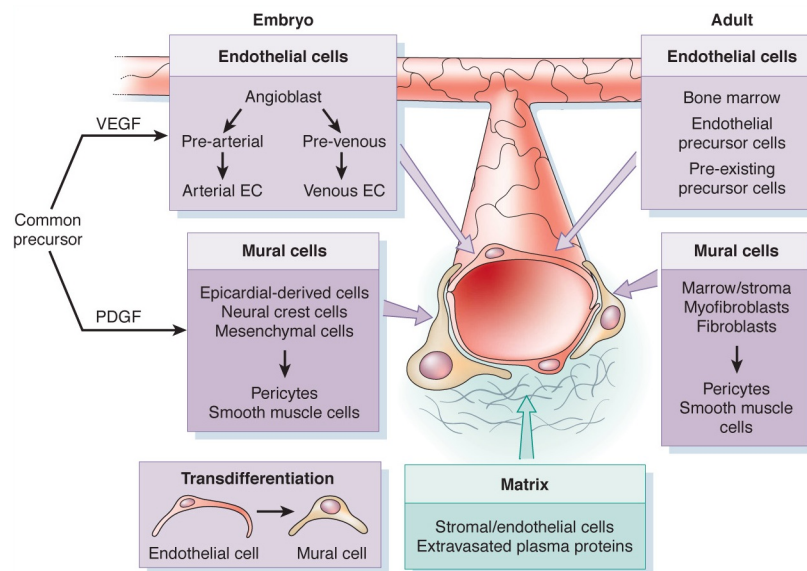
Figure 1. Cell components of growing blood vessels (adapted from Jain RK, Nature Medicine 2003)

After the formation of the immature plexus, mural cells that interact with the outer surface of the vessel are recruited (Figure 1). Most often, these cells are pericytes and invest the vast majority of capillary-size vessels in the body. Smooth muscle cells indeed cover large vessels, such as arteries and veins. Mural cells originate from multiple sources during development. In the embryo, the first smooth muscle cells originate directly from the endothelium in response to TGF-β3 [7]. Later, some of them arise from the neural crest [8, 9] and some others are indeed of mesodermal origin [10, 11]. Recently, it has been demonstrated that there are common vascular progenitors, Flk1+ embryonic stem cells, which can differentiate in endothelial cells in response to VEGF, or develop in smooth muscle cells when exposed to PDGF-BB [12].

1.1.2. Blood vessels in adult life

During adult life, neovascularization occurs predominantly through *angiogenesis*, the growth of blood vessels from pre-existing capillaries. Blood vessel formation by angiogenesis is an extremely complex multistep process, which requires the tight control and coordination of endothelial cell behavior in all its phases [3]. Angiogenesis can occur by sprouting or by intussusception, as will be discussed in detail in the next paragraph. The generation of new capillaries from pre-existing ones can be represented as a process in two phases: 1) tube formation, in which endothelial cells react to growth factor gradients and local concentration, migrating, proliferating and generating the new sprout and 2) vascular maturation, in which the nascent vessels are then stabilized by recruiting mural

cells (pericytes or vascular smooth muscle cells) and by generating extracellular matrix (ECM). Pericytes play a crucial role in regulating the physiology of the microvasculature. Their association with the newly-induced vessels render them independent of VEGF stimulus, whereas vessels lacking perictyes tend to regress following VEGF withdrawal [13, 14]. Pericyte recruitment is strictly regulated by PDGF-BB that is secreted directly by endothelial cells upon VEGF stimulation and signals through its receptor PDGFR-β expressed by mural cells. Important evidences supporting the compelling role of PDGF-BB during vascular maturation come from genetic studies. Using PDGF-b and PDGFR-β deficient mice, it has been demonstrated that lack of pericytes causes endothelial cell hyperplasia associated with an abnormal shape and morphological signs of increased permeability [15]. Besides PDGF-BB/ PDGFR-β axis, the regulatory function of pericytes on endothelial cells takes place through cell-to-cell contact and secreted factors. Among them, TGF-β signaling pathway, angiopoietins and VEGF have been shown to contribute to the molecular cross-talk between endothelial cells and mural cells. [11, 16, 17].

In adult life, neovascularization is not only due to angiogenesis. Recent studies revealed that postnatal vasculogenesis can occur through the recruitment of endothelial progenitors cells (EPC) circulating in peripheral blood [18]. These cells can be recruited at the site of revascularization and incorporated within the forming vasculature in distant organs in various disorders, such as hypoxic conditions or tumors [19-21]. Most of these circulating EPCs reside in the bone marrow and can be mobilized in response to various stimuli including VEGF, GM-CSF, FGF-2 and angiopoietins [19, 22-24]. In addition, it has been reported that bone marrow derived-macrophages can also contribute to neovascularization by in situ transdifferentiation to endothelial cells [25]. Recently, another

population of recruited bone-marrow circulating cells (RBCCs) has been described. These cells do not function as EPC but contribute to neovessel formation. Their homing and retention in close proximity of angiogenic vessels is mediated by VEGF and SDF1, a chemokine induced by VEGF. These cells are able to enhance in situ proliferation of resident endothelial cells and therefore to promote adult neovascularization [26].

1.2 Molecular regulation of angiogenesis

The first suggestion of the existence of angiogenic factors comes from the pioneering work of Gordon Ide and collaborators in the early 20th century. Using a transparent chamber inserted into the rabbit ear as a model of tumor transplantation, they observed that tumor growth was accompanied by a strong angiogenic response [27]. This observation led them to postulate for the first time that tumor cells released growth factors able to induce vessels growth. Subsequently, several other studies contributed to the discovery and characterization of numerous angiogenic factors such as VEGF, angiopoietins, TGF-β, fibroblast growth factor (FGF), hepatocyte growth factor (HGF) [28, 29]. Among them, VEGF is the most potent and specific angiogenic factor. In 1989, it was isolated for the first time from medium conditioned by bovine pituitary follicular cells as specific endothelial cell mitogen [30]. At the same time, other research groups reported the identification of a protein that induced vascular leakage that was named tumor vascular permeability factor (VPF) [31] and isolated an endothelial mitogen from mouse pituitary cell line called "vasculotropin" [32]. Later on, cloning and sequencing of those molecules revealed that

VEGF and VPF were the same molecule whereas vasculotropin was the mouse orthologue of VEGF.

1.2.1 Vascular Endothelial Growth Factors and receptors

The mammalian vascular endothelial growth factor (VEGF) family consists of five mammalian different polypeptides: VEGF-A, VEGF-B, VEGF-C, VEGF-D and placental growth factor (PlGF) (Figure 2). Besides them, there are other related factors, such as VEGF-E that is an Orf virus-encoded VEGF protein [33] and VEGF-F that is snake venom-derived [34]. These are proteins of invertebrate origin that bind VEGFRs in a different way than the mammalian VEGFs. The main receptors involved in initiating the signal transduction cascades upon VEGF binding are three tyrosine kinase receptors termed VEGFR-1 (Flt-1), VEGFR-2 (Flk-1) and VEGFR-3 (Flt-3). In addition, there are accessory receptors such as neuropilins, which seem to modulate the binding of VEGFs to the main receptors. Their ability to signal independently is still not understood. VEGFRs share the same structure and are composed by an extracellular domain organized in seven immunoglobulin (Ig)-like folds, followed by a single transmembrane region, a juxta-membrane domain, a split tyrosine-kinase domain interrupted by a kinase insert and a C-terminal tail. Only VEGFR-3 has a disulfide bridge replacing the fifth Ig domain [35]. VEGFR-1 binds VEGF-A, VEGF-B and PlGF and is expressed in two variants: a full length form and a soluble form (sFlt1), often considered a decoy for VEGF.
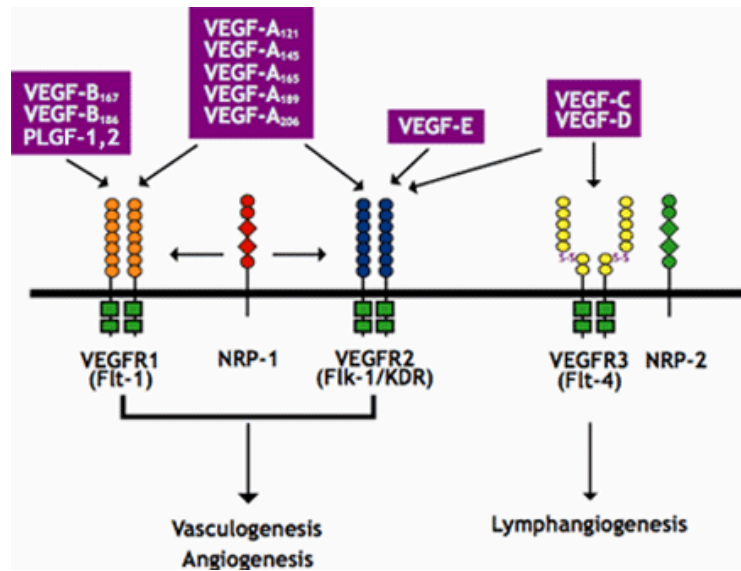
Figure 2. Vascular Endothelial Growth Factors and receptors (Hicklin DJ, Ellis LM. *J Clin Oncol.* 2005;23:1011-1027)

Despite having the highest affinity for VEGF, VEGFR-1 kinase activity is weak as confirmed by the lack of mitogenic response in endothelial cells upon VEGF stimulation [36]. The functions of VEGFR-1 have been dissected using specific knockout models. Embryonic lethality and increased cell proliferation resulted from VEGFR-1 knockout suggesting that it might act as a negative regulator in vascular development, dampening the proangiogenic effects of VEGFR-2 activation [37-39]. On the other hand, VEGFR-2 is the first vascular marker to appear during development. It binds VEGF-A with less affinity than VEGFR-1. However, it shows a strong kinase activity that results in mitogenic, prosurvival and chemotactic signals in several cell types. VEGFR-2 binds also the processed form of VEGF-C and VEGF-D. Its central role in vascular development and angiogenesis has been suggested by VEGFR-2 gene targeting studies. Indeed, embryos

lacking VEGFR-2 die and fail to form blood islands and to complete hematopoietic and endothelial development. VEGFR-3 binds VEGF-C and VEGF-D and it is expressed in lymphatic endothelial precursors and mature cells as well as in blood vascular endothelial cells. It is considered an important regulator of lymphangiogenesis [40].

Among the mammalian VEGFs, VEGF-A (also referred to simply as VEGF) is the most potent and characterized angiogenic factor and plays a pivotal role in both physiological and pathological conditions [41]. It binds VEGFR-1 and VEGFR-2 as well as neuropilin-1 (Nrp-1) and neuropilin-2 (Nrp-2). VEGF-B selectively binds VEGFR-1 and Nrp-1 and it exists in two different isoforms, VEGF-B$_{167}$ and VEGF-B$_{186}$. It exerts a less pronounced role in the vascular system, being involved mainly in the maintenance of newly formed vessels in pathological conditions rather than in their formation [42]. Recently, it has been demonstrated that its angiogenic effect is restricted to the heart where it induces revascularization and preserves cardiac function after myocardial infarction [43, 44]. VEGF-C and VEGF-D are indeed mostly involved in lymphangiogenesis and their different isoforms do not arise from alternative splicing but derive form proteolytic processing in both N-terminal and C-terminal of a precursor protein. Both VEGFs have also mitogenic activity for endothelial cells [45, 46] and bind VEGFR-3. PlGF has been discovered in the placenta and exists in three isoforms (PlGF-1, -2, and -3) generated by alternative splicing. It signals through VEGFR-1 stimulating angiogenesis and collateral growth in ischemic limb and heart [47].

The human VEGF-A gene is composed by eight exons divided by seven introns. VEGF mRNA expression can be regulated by several factors such as hypoxia. VEGF is an oxygen sensitive molecule and its transcription is under the control of hypoxia-inducible factor

(HIF)-1. HIF-1 is composed by two peptides, HIF-1α and HIF-1β. In normoxic conditions, HIF-1α is rapidly degraded through hydroxylation of proline residues, ubiquitination and targeting to the proteosome. On the other hand, in hypoxic conditions this peptide dimerizes with HIF-1β. This complex is able to bind and activate a specific region of the VEGF promoter driving its transcription. This mechanism of regulation has been largely investigated and appears to be common in many types of tumors or in wound healing processes [48]. Besides hypoxia, it has been demonstrated that several growth factors and oncogenes can induce VEGF gene expression [41].

The VEGF molecule exists in several isoforms generated by alternative splicing events occurring predominantly in exons 6 and 7, encoding for two different heparin-binding domains [36, 45]. Among them, $VEGF_{121}$, $VEGF_{165}$ and $VEGF_{189}$ are the predominant ones secreted by several cell types [49]. They differ from each other in the size of the heparin-binding domain. Whereas $VEGF_{121}$ lacks both heparin-binding domains and is therefore highly diffusible, $VEGF_{165}$ and $VEGF_{189}$ have only one or both binding regions respectively and display increasing affinity for extracellular matrix. As a consequence, $VEGF_{165}$ is partially soluble and is able to generate gradients of intermediate steepness, whereas $VEGF_{189}$ that remains tightly bound to the extracellular matrix [50], generates very steep gradients. The different biological functions of these splicing variants have been largely characterized in vivo in the mouse hindbrain and in the retina using isoform specific genetic manipulations and using specific VEGF knockout mice. Mice expressing only $VEGF_{120}$ died soon after birth, developed severe cardiomyopathy [51] and showed impaired angiogenesis characterized by reduced vascular branching and increased capillary diameter. The number of endothelia filopodia processes was greatly reduced and their

orientation was compromised [52]. Opposite effects were observed when mice expressed only the strongest heparin-binding isoform, VEGF$_{188}$. Increased branching and very thin microvessels characterized the vasculature. Furthermore, mice displayed impaired arteriolar development and almost 50% of them died at birth [52, 53]. Instead, mice that expressed only VEGF$_{164}$, the partially soluble isoform, were viable and healthy and exhibited a normal vessel network. The same effect was detected also in heterozygous mice, which expressed both VEGF$_{120}$ and VEGF$_{188}$, but no VEGF$_{164}$ [52]. In agreement with these findings, expression of VEGF$_{120}$ in the retina was sufficient to drive endothelial cell proliferation at the same extent as VEGF$_{164}$, but failed to guide tip cells properly [54]. These results imply that VEGF signaling through receptors is not enough to establish a directional sprouting through tip cells migration and emphasize that well-shaped and directional gradients are indeed essentials to induce endothelial cells to form branched networks.

1.2.2 *The role of VEGF in physiological and pathological angiogenesis*

There are considerable evidences that VEGF is a major player in embryonic and early postnatal development of the vascular system. However, VEGF upregulation is important also in other physiological processes, such as corpus luteum development and endochondral bone formation [41]. On the other hand, VEGF disregulation is associated with various pathological conditions. It is known that VEGF is also a tumor angiogenesis factor and its expression is often upregulated in many human tumors [55]. Several studies

showed that inhibiting VEGF activity in tumors results in suppression of their growth in animal models. These findings have been confirmed by several clinical trials using small molecule inhibitors or humanized monoclonal antibodies [56, 57]. Uncontrolled neovascularization is also associated with proliferative retinopathy, and increased VEGF levels were described in the humor vitreous and aqueous of eyes of patients affected by such pathology [58]. Furthermore, several studies have demonstrated that age-related macular degeneration (AMD) is caused by neovascularization and vascular leakage [59]. Several anti-VEGF therapies using humanized VEGF-specific Fab or aptamers, are being explored. These strategies showed benefits in a primate model of AMD reducing angiogenesis and vascular leakage and are currently in phase 3 clinical trials [41].

1.2.3 Sprouting angiogenesis: tip and stalk specification

Sprouting angiogenesis is the best understood process of vessel growth. It is a reiterative process that involves a tight regulation of endothelial cell behavior in space and time. Vessel sprouting is characterized by endothelial heterogeneity and initiates with the specification and selection of two cell types, named tip and stalk cells [54]. In response to specific pro-angiogenesis signals such as VEGF, the first event occurring is the detachment of pericytes from the vessel wall and the loosening of endothelial cell junctions. Meanwhile, matrix metalloproteases (MMPs) mediate proteolytic degradation of the basement membrane and some endothelial cells acquire a motile and invasive phenotype necessary to initiate vessel sprouting (Figure 3). These cells are called tip cells

and are not lumenized and respond to VEGF gradients mainly extending filopodia and migrating outward from the parent vessel. On the other hand, stalk cells form behind the tip and respond to the growth factor concentration by proliferating and promoting the increase of the surface of the trunk [54]. It is thought that the cells designated to behave as tip cells are the ones that experience higher angiogenic factor signaling than neighboring cells. Once selected, tip cells signal back to the adjacent endothelial cells preventing them from sprouting and specifically directing their patterning [60].
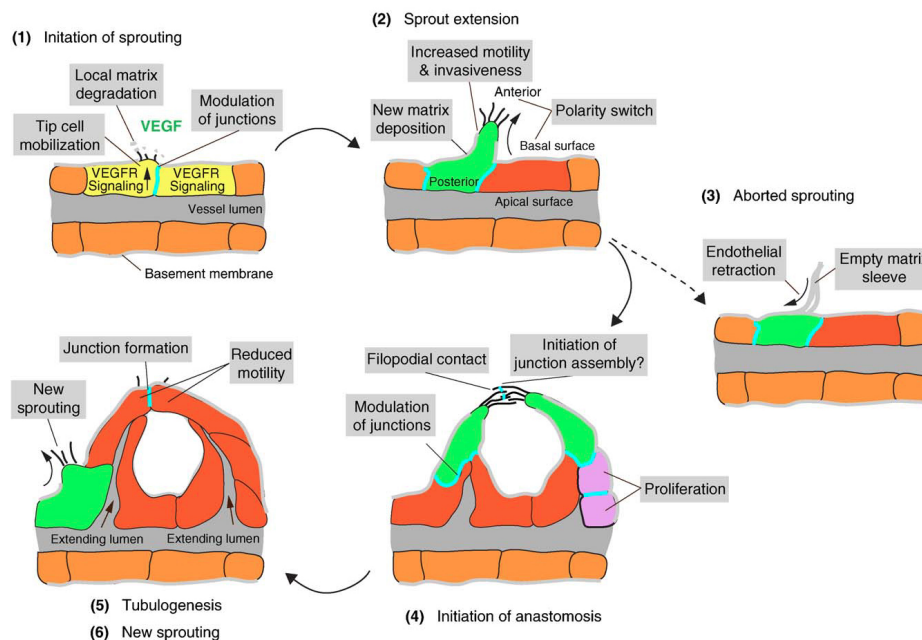
Figure 3. Sprouting angiogenesis (adapted from Eilkan H & Adams R, *Current Opinion in Cell Biology 2010*)

One of the most important guidance cues for sprout formation is VEGF. It guides angiogenic sprouting by directing tip cell migration, polarization and directional filopodia extension depending on its local distribution and therefore on the generation of

extracellular gradients. Although filopodia formation is induced by all VEGF isoforms, their morphology and the following vascular patterning appear to be isoform specific [52, 54]. Recent evidences showed that local VEGF gradients can be further refined by endothelial cells close to the nascent sprout that upregulate the expression of soluble VEGFR-1. The increased levels of soluble VEGFR-1 act by limiting VEGF availability in the regions adjacent to the sprout. This creates a more directional and shaped path for tip cells that guide the sprout away from the parental vessel in an easier way. [61] However, extracellular distribution of VEGF not only affects tip cell behavior but it controls also the proliferation of stalk cells. Its local availability and concentration, rather than its spatial distribution, determine cell division. In principle, almost all endothelial cells in the growing vascular network can respond to VEGF by proliferation. However, it has been demonstrated that the pattern of endothelial cell proliferation in the mouse retina is not accidental but follows a specific pattern. In fact, the vast majority of proliferating cells were localized close to regions of low oxygenation, where the local VEGF production was higher [62]. To be functional, a new sprout needs to acquire a lumen and this often happens after the fusion of a tip cell with a target vessel or sprout. When a tip cell approaches a potential fusion site, the target cell extends protrusions and start to interact engaging filopodia from the sprouting tip cell. At the same time, it has been demonstrated that this is accompanied by an increase in cell-cell junctions that contribute to strengthen tip cells connections [60].

Experimental evidences demonstrate that sprout fusion can also be regulated by macrophages that are localized close to the fusion site where they act as a bridge between filopodia of the two tip cells [63]. To complete the sprouting process, after tip cells fusion

and the generation of a stably connected new vessel segment, lumen formation occurs. The lumen is confined to the stalk region and extends just behind tip cells. The mechanisms of lumen formation are still not fully understood. However, it seems that blood flow and polarization of endothelial cells are essential to set up morphological changes that will give rise to the vascular lumen [64].

1.2.4 Intussusceptive angiogenesis

Intussusceptive angiogenesis is a mode of vessel growth, distinct form sprouting, often referred to also as splitting angiogenesis. It defines a process in which the capillary network expands "within itself" [65]. The hallmark of intussusception is the formation of transluminal tissue pillars that arise within the endothelium of pre-existing vessels. After fusion of pillars, new vascular entities are delineated and the vasculature can be further remodeled.
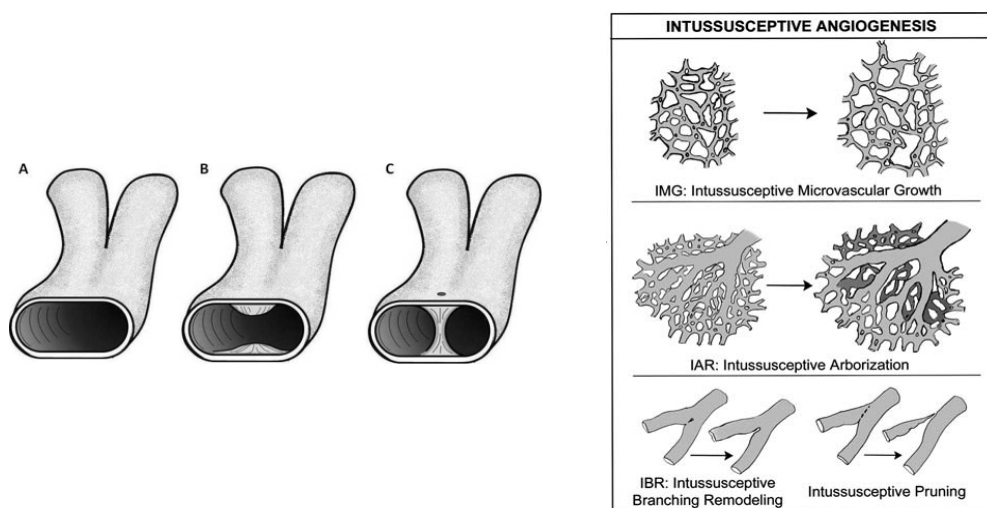
Figure 4. Intussusceptive angiogenesis (adapted from Djonov and Makanya, 2009)

17

The concept of intussusceptive angiogenesis was first described in the developing lung vasculature [66] and later several other studies demonstrated that intussusception occurs in many other organs [65]. The formation of pillars follows a precise dynamics and can be divided in four consecutive steps. During stage I, two endothelial leaflets of opposite capillary walls contact each other. Subsequently, in stage II, junctions between endothelial cells reorganize and the bilayer is pierced in the center, indicating the beginning of the pillar formation. In the next step, an interstitial pillar core is formed and invaded by cytoplasmic processes of fibroblasts, pericytes or myofibroblasts that deposit matrix. During the last stage, pillars start to grow and increase in diameter without changing their structure. Several other alternative modes of transcapillary pillar formation have been then described following experimental observations in the chicken chorioallantoic membrane (CAM) [67]. Intussusceptive angiogenesis is divided in three main phases including intussusceptive microvascular growth (IMG), intussusceptive arborization (IAR) and intussusceptive branching remodeling (IBR) (Figure 4).

Intussusceptive microvascular growth refers to the process of pillar initiation and expansion that results in an increase of the complexity of the vascular network. On the other hand, the process of splitting of large vessels such as arteries and veins and the subsequent generation of a feeding functional vascular tree is defined as intussusceptive arborization. IAR is initiated with the formation of several "vertical" pillars that delimit future perfused vessels. Remaining bridges that interconnect new vascular entities are then removed by formation of horizontal pillar folds. Intussusceptive branching remodeling is indeed intended as the process by which the branching geometry of the vessels is optimized to adapt to local requirements. This is accomplished by transluminal

pillar formation close to arterial and venous bifurcation sites. In addition, IBR can also serve as a vascular pruning system to remove superfluous vessels [68]. Unlike sprouting, intussusception is a rather fast process that does not rely on massive endothelial cell proliferation and is achieved at low vascular permeability and several studies revealed that sprouting often precedes IA. This highlights that the two processes are complementary and might occur in the same organ although in different times. The role of IA in pathological conditions is being studied, in particular in tumors. As showed in a recent study, radiotherapy or anti-VEGF treatments of tumors result in a transient reduction of tumor volume followed by a relapse characterized by broad IA [69]. The molecular mechanisms governing intussusceptive angiogenesis are still poorly understood. It has been proved that VEGF can directly promote intussusception in the CAM [70] and it has also been demonstrated that intussusception can be driven by blood flow [71]. In muscle, increased blood flow triggers capillary growth through intraluminal splitting rather than by sprouting [72].

1.2.5 Notch signaling pathway

The Notch signaling pathway is evolutionarily conserved and plays multiple roles in several physiological processes both in development and in adult life [73]. In mammals, the Notch family encompasses four receptors (Notch1-4) and five ligands, namely Delta-like 1 (Dll1), Delta-like 3 (Dll3), Delta-like 4 (Dll4), Jagged-1 (Jag1) and Jagged-2 (Jag2). Notch receptors are single-pass type I transmembrane proteins with a large extracellular

domain constituted by tandem repeats of epidermal growth factor (EGF)-like motifs and a membrane-tethered intracellular domain. Like the receptors, Notch ligands are transmembrane proteins. A hallmark of Notch signaling is its mechanism of signal transduction that requires cell-cell contact (juxtacrine signaling). It initiates when a ligand expressed on the surface of a cell (signal-sending cell) physically interacts with a receptor expressed on the surface of another cell (signal-receiving cell) (Figure 5).
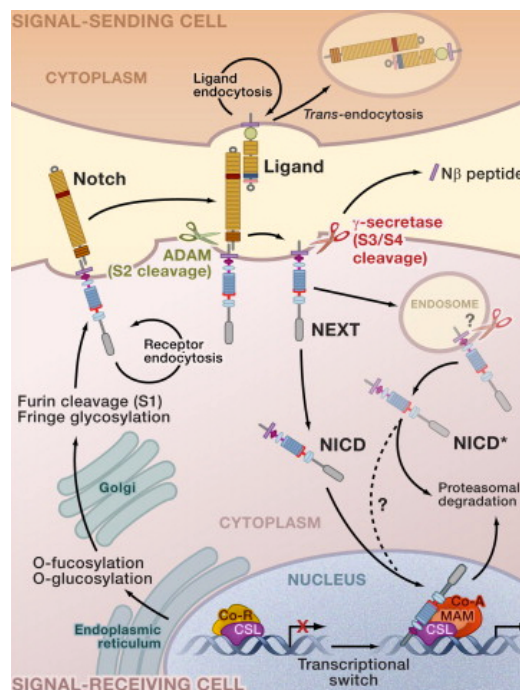
Figure 5. Notch signaling pathway (adapted from Kopan et al, Cell 2009)

Upon cell-cell contact and ligand binding, the receptor undergoes two proteolytic cleavages operated by proteases of the ADAM family [[(a disintegrin and metalloproteinase)/TACE (tumor necrosis factor-α) converting enzyme] and γ-secretase enzyme, respectively. The first cleavage results in a conformational change, whereas the

second one is responsible for the formation and release of the Notch intracellular domain (NICD). Afterwards, this domain translocates to the nucleus of the receiving cell where it leads to the transcriptional activation of specific Notch target genes such as basic helix-loop-helix (bHLH) transcriptional repressors of the Hes/Hey family. On the other hand, the extracellular domain that remains bound to the ligand expressing cell is internalized by endocytosis and degraded [74]. Besides *trans*-interactions (cell-cell interactions) known to activate Notch signaling, Notch ligands suppress the signaling through *cis*-interactions, binding Notch receptors in the same cell [75]. This is considered the "canonical" Notch pathway. However, a "non-canonical" pathway has been also described [76]. It can be initiated by non-canonical ligands or may not require cleavage of Notch receptors. It has been largely described for its role in antagonizing Wnt/β-catenin signaling [77]. Notch receptors can be glycosylated by the glycosyltransferase Fringe in the Golgi and this modification can also modulate Notch signaling [78].

1.2.6 Notch and VEGF: cross-talk in angiogenesis

The Notch pathway plays a pivotal role in angiogenesis as demonstrated by several studies that provided insights in its role both in development and in adults. Besides being involved in arteriovenous differentiation during development [4], recent studies in the mouse retina, in zebrafish, in tumor angiogenesis and in 3D in vitro assays demonstrated that Dll4/Notch signaling is implicated in endothelial sprouting by regulating tip and stalk cells specification [79-86] . It has been found that upon VEGF stimulation, Notch signaling acts through lateral inhibition giving rise to a heterogeneous population of

endothelial cells. These cells compete via bilateral Dll4-Notch signaling for tip cell specification generating a VEGF-Notch feedback loop (Figure 6). In response to VEGF, some endothelial cells react increasing the transcription of VEGFR-2, upregulating Dll4 and therefore acquiring a tip cell phenotype. On the other hand, Dll4 upregulation in tip cells results in Notch activation in the adjacent endothelial cell that becomes a stalk cell. Notch signaling efficiently suppresses tip cell fate by negatively regulating VEGF signaling in stalk cell. High Notch levels result in the inhibition of VEGFR-2 activity that render stalk cells less responsive to VEGF and therefore exclude them from becoming tip cells [79, 85]. Recently, it has been found that during sprouting angiogenesis endothelial cells dynamically compete for the tip cell position by fine-tuning the expression of VEGFR-1 and VEGFR-2 [87]. Furthermore, it has been proved that activation of VEGFR-3 by VEGF-C produced by macrophages is able to reinforce Notch signaling and to promote the conversion of tip in stalk cells [88].
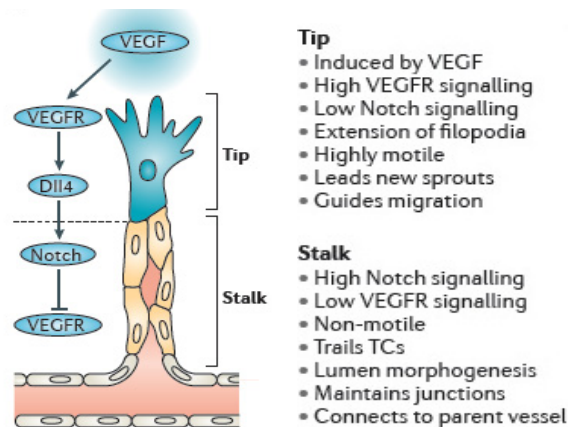
Figure 6. Tip and stalk cell specification by Dll4/Notch signaling (adapted from Herbert et al, Nature 2011)

Dll4 is not the only Notch ligand involved in sprouting angiogenesis. Recent studies in the retinal vasculature have demonstrated that Jag1 is a potent proangiogenic regulator in mice and that Dll4 and Jag1 have opposing effects on angiogenesis. It antagonizes Dll4-Notch signaling in cells expressing glycosyltransferases of the family Fringe. When the receptor gets glycosylated, Jag1 competes with Dll4 for the binding and acts as an antagonist [89]. Studies in the mouse retina and in zebrafish demonstrated that suppression of Notch signaling by γ-secretase inhibitors and blocking of Dll4 expression by genetic means or protein knockdown, leads to excessive tip cells formation and enhanced sprouting [79, 80, 85, 86]. By contrast, ectopic activation of Notch after administration of a soluble Jag1 peptide resulted in reduced vascular density, with less and shorter filopodia [79]. Besides its role in the development of the vascular system and in sprouting angiogenesis, Dll4 is highly expressed also in tumor endothelial cells and appears to be a good target for anti-angiogenic therapies. Strikingly, VEGF blockade and Dll4 blockade showed paradoxically distinct and unrelated effects on tumor vasculature. When treated with an anti-VEGF antibody, the vasculature of tumors was pruned and normalized and overall this resulted in a decreased tumor perfusion and in a remarkable decrease of tumor size. Conversely, blockade of Dll4/Notch signaling with Dll4-neutralizing antibodies or modified Dll4 proteins promoted sprouting and increased the vessel density of tumors. However, the newly induced vasculature was abnormal, less efficient and not functional. This led to a reduction in the perfusion, increased hypoxia and therefore reduction of the tumor size [82, 83, 90]. Dll4 blockade has been largely tested also in tumor resistant to anti-VEGF treatment and appears to be effective in most cases [82].

Bibliography

1. Swift MR, Weinstein BM. Arterial-venous specification during development. *Circulation research*. 2009;104:576-588
2. Carmeliet P. Developmental biology. One cell, two fates. *Nature*. 2000;408:43, 45
3. Herbert SP, Stainier DY. Molecular control of endothelial cell behaviour during blood vessel morphogenesis. *Nature reviews. Molecular cell biology*. 2011;12:551-564
4. Rocha SF, Adams RH. Molecular differentiation and specialization of vascular beds. *Angiogenesis*. 2009;12:139-147
5. Carmeliet P. Angiogenesis in health and disease. *Nature medicine*. 2003;9:653-660
6. Carmeliet P, Jain RK. Molecular mechanisms and clinical applications of angiogenesis. *Nature*. 2011;473:298-307
7. Nakajima Y, Mironov V, Yamagishi T, Nakamura H, Markwald RR. Expression of smooth muscle alpha-actin in mesenchymal cells during formation of avian endocardial cushion tissue: A role for transforming growth factor beta3. *Developmental dynamics : an official publication of the American Association of Anatomists*. 1997;209:296-309
8. Gittenberger-de Groot AC, DeRuiter MC, Bergwerff M, Poelmann RE. Smooth muscle cell origin and its relation to heterogeneity in development and disease. *Arteriosclerosis, thrombosis, and vascular biology*. 1999;19:1589-1594
9. Bautch VL. Stem cells and the vasculature. *Nature medicine*. 2011;17:1437-1443
10. Hellstrom M, Kalen M, Lindahl P, Abramsson A, Betsholtz C. Role of pdgf-b and pdgfr-beta in recruitment of vascular smooth muscle cells and pericytes during embryonic blood vessel formation in the mouse. *Development*. 1999;126:3047-3055
11. Hirschi KK, Rohovsky SA, D'Amore PA. Pdgf, tgf-beta, and heterotypic cell-cell interactions mediate endothelial cell-induced recruitment of 10t1/2 cells and their differentiation to a smooth muscle fate. *The Journal of cell biology*. 1998;141:805-814
12. Yamashita J, Itoh H, Hirashima M, Ogawa M, Nishikawa S, Yurugi T, Naito M, Nakao K, Nishikawa S. Flk1-positive cells derived from embryonic stem cells serve as vascular progenitors. *Nature*. 2000;408:92-96
13. Benjamin LE, Hemo I, Keshet E. A plasticity window for blood vessel remodelling is defined by pericyte coverage of the preformed endothelial network and is regulated by pdgf-b and vegf. *Development*. 1998;125:1591-1598
14. Benjamin LE, Golijanin D, Itin A, Pode D, Keshet E. Selective ablation of immature blood vessels in established human tumors follows vascular endothelial growth factor withdrawal. *The Journal of clinical investigation*. 1999;103:159-165
15. Hellstrom M, Gerhardt H, Kalen M, Li X, Eriksson U, Wolburg H, Betsholtz C. Lack of pericytes leads to endothelial hyperplasia and abnormal vascular morphogenesis. *The Journal of cell biology*. 2001;153:543-553

16. Hirschi KK, Rohovsky SA, Beck LH, Smith SR, D'Amore PA. Endothelial cells modulate the proliferation of mural cell precursors via platelet-derived growth factor-bb and heterotypic cell contact. *Circulation research*. 1999;84:298-305

17. Jain RK. Molecular regulation of vessel maturation. *Nature medicine*. 2003;9:685-693

18. Luttun A, Carmeliet G, Carmeliet P. Vascular progenitors: From biology to treatment. *Trends in cardiovascular medicine*. 2002;12:88-96

19. Asahara T, Masuda H, Takahashi T, Kalka C, Pastore C, Silver M, Kearne M, Magner M, Isner JM. Bone marrow origin of endothelial progenitor cells responsible for postnatal vasculogenesis in physiological and pathological neovascularization. *Circulation research*. 1999;85:221-228

20. Lyden D, Hattori K, Dias S, Costa C, Blaikie P, Butros L, Chadburn A, Heissig B, Marks W, Witte L, Wu Y, Hicklin D, Zhu Z, Hackett NR, Crystal RG, Moore MA, Hajjar KA, Manova K, Benezra R, Rafii S. Impaired recruitment of bone-marrow-derived endothelial and hematopoietic precursor cells blocks tumor angiogenesis and growth. *Nature medicine*. 2001;7:1194-1201

21. Rafii S, Lyden D. Therapeutic stem and progenitor cell transplantation for organ vascularization and regeneration. *Nature medicine*. 2003;9:702-712

22. Takahashi T, Kalka C, Masuda H, Chen D, Silver M, Kearney M, Magner M, Isner JM, Asahara T. Ischemia- and cytokine-induced mobilization of bone marrow-derived endothelial progenitor cells for neovascularization. *Nature medicine*. 1999;5:434-438

23. Schatteman GC, Hanlon HD, Jiao C, Dodds SG, Christy BA. Blood-derived angioblasts accelerate blood-flow restoration in diabetic mice. *The Journal of clinical investigation*. 2000;106:571-578

24. Kalka C, Masuda H, Takahashi T, Kalka-Moll WM, Silver M, Kearney M, Li T, Isner JM, Asahara T. Transplantation of ex vivo expanded endothelial progenitor cells for therapeutic neovascularization. *Proceedings of the National Academy of Sciences of the United States of America*. 2000;97:3422-3427

25. Schmeisser A, Garlichs CD, Zhang H, Eskafi S, Graffy C, Ludwig J, Strasser RH, Daniel WG. Monocytes coexpress endothelial and macrophagocytic lineage markers and form cord-like structures in matrigel under angiogenic conditions. *Cardiovascular research*. 2001;49:671-680

26. Grunewald M, Avraham I, Dor Y, Bachar-Lustig E, Itin A, Jung S, Chimenti S, Landsman L, Abramovitch R, Keshet E. Vegf-induced adult neovascularization: Recruitment, retention, and role of accessory cells. *Cell*. 2006;124:175-189

27. Ide AG BN, Warren SL. Vascularization of the brown pearce rabbit epithelioma transplant as seen in the transplant ear chamber. *Am. J. Roentgenol.* . 1939;42:891-899

28. Ferrara N. Vegf and the quest for tumour angiogenesis factors. *Nature reviews. Cancer*. 2002;2:795-803

29. Yancopoulos GD, Davis S, Gale NW, Rudge JS, Wiegand SJ, Holash J. Vascular-specific growth factors and blood vessel formation. *Nature*. 2000;407:242-248

30. Ferrara N, Henzel WJ. Pituitary follicular cells secrete a novel heparin-binding growth factor specific for vascular endothelial cells. *Biochemical and biophysical research communications*. 1989;161:851-858

31. Senger DR, Galli SJ, Dvorak AM, Perruzzi CA, Harvey VS, Dvorak HF. Tumor cells secrete a vascular permeability factor that promotes accumulation of ascites fluid. *Science*. 1983;219:983-985

32. Plouet J, Schilling J, Gospodarowicz D. Isolation and characterization of a newly identified endothelial cell mitogen produced by att-20 cells. *The EMBO journal*. 1989;8:3801-3806

33. Takahashi H, Shibuya M. The vascular endothelial growth factor (vegf)/vegf receptor system and its role under physiological and pathological conditions. *Clin Sci (Lond)*. 2005;109:227-241

34. Suto K, Yamazaki Y, Morita T, Mizuno H. Crystal structures of novel vascular endothelial growth factors (vegf) from snake venoms: Insight into selective vegf binding to kinase insert domain-containing receptor but not to fms-like tyrosine kinase-1. *The Journal of biological chemistry*. 2005;280:2126-2131

35. Olsson AK, Dimberg A, Kreuger J, Claesson-Welsh L. Vegf receptor signalling - in control of vascular function. *Nature reviews. Molecular cell biology*. 2006;7:359-371

36. Hoeben A, Landuyt B, Highley MS, Wildiers H, Van Oosterom AT, De Bruijn EA. Vascular endothelial growth factor and angiogenesis. *Pharmacological reviews*. 2004;56:549-580

37. Fong GH, Rossant J, Gertsenstein M, Breitman ML. Role of the flt-1 receptor tyrosine kinase in regulating the assembly of vascular endothelium. *Nature*. 1995;376:66-70

38. Kearney JB, Ambler CA, Monaco KA, Johnson N, Rapoport RG, Bautch VL. Vascular endothelial growth factor receptor flt-1 negatively regulates developmental blood vessel formation by modulating endothelial cell division. *Blood*. 2002;99:2397-2407

39. Dvorak HF. Vascular permeability factor/vascular endothelial growth factor: A critical cytokine in tumor angiogenesis and a potential target for diagnosis and therapy. *Journal of clinical oncology : official journal of the American Society of Clinical Oncology*. 2002;20:4368-4380

40. Karpanen T, Alitalo K. Molecular biology and pathology of lymphangiogenesis. *Annual review of pathology*. 2008;3:367-397

41. Ferrara N, Gerber HP, LeCouter J. The biology of vegf and its receptors. *Nature medicine*. 2003;9:669-676

42. Zhang F, Tang Z, Hou X, Lennartsson J, Li Y, Koch AW, Scotney P, Lee C, Arjunan P, Dong L, Kumar A, Rissanen TT, Wang B, Nagai N, Fons P, Fariss R, Zhang Y, Wawrousek E, Tansey G, Raber J, Fong GH, Ding H, Greenberg DA, Becker KG, Herbert JM, Nash A, Yla-Herttuala S, Cao Y, Watts RJ, Li X. Vegf-b is dispensable for blood vessel growth but critical for their survival, and vegf-b targeting inhibits pathological angiogenesis. *Proceedings of the National Academy of Sciences of the United States of America*. 2009;106:6152-6157

43. Li X, Tjwa M, Van Hove I, Enholm B, Neven E, Paavonen K, Jeltsch M, Juan TD, Sievers RE, Chorianopoulos E, Wada H, Vanwildemeersch M, Noel A, Foidart JM, Springer ML, von Degenfeld G, Dewerchin M, Blau HM, Alitalo K, Eriksson U, Carmeliet P, Moons L. Reevaluation of the role of vegf-b suggests a restricted role in the revascularization of the ischemic myocardium. *Arteriosclerosis, thrombosis, and vascular biology*. 2008;28:1614-1620

44. Zentilin L, Puligadda U, Lionetti V, Zacchigna S, Collesi C, Pattarini L, Ruozi G, Camporesi S, Sinagra G, Pepe M, Recchia FA, Giacca M. Cardiomyocyte vegfr-1 activation by vegf-b induces compensatory hypertrophy and preserves cardiac function after myocardial infarction. *FASEB journal : official publication of the Federation of American Societies for Experimental Biology*. 2010;24:1467-1478

45. Tammela T, Enholm B, Alitalo K, Paavonen K. The biology of vascular endothelial growth factors. *Cardiovascular research*. 2005;65:550-563

46. Saharinen P, Tammela T, Karkkainen MJ, Alitalo K. Lymphatic vasculature: Development, molecular regulation and role in tumor metastasis and inflammation. *Trends in immunology*. 2004;25:387-395

47. Luttun A, Tjwa M, Carmeliet P. Placental growth factor (plgf) and its receptor flt-1 (vegfr-1): Novel therapeutic targets for angiogenic disorders. *Annals of the New York Academy of Sciences*. 2002;979:80-93

48. Nagy JA, Dvorak AM, Dvorak HF. Vegf-a and the induction of pathological angiogenesis. *Annual review of pathology*. 2007;2:251-275

49. Robinson CJ, Stringer SE. The splice variants of vascular endothelial growth factor (vegf) and their receptors. *Journal of cell science*. 2001;114:853-865

50. Park JE, Keller GA, Ferrara N. The vascular endothelial growth factor (vegf) isoforms: Differential deposition into the subepithelial extracellular matrix and bioactivity of extracellular matrix-bound vegf. *Molecular biology of the cell*. 1993;4:1317-1326

51. Carmeliet P, Ng YS, Nuyens D, Theilmeier G, Brusselmans K, Cornelissen I, Ehler E, Kakkar VV, Stalmans I, Mattot V, Perriard JC, Dewerchin M, Flameng W, Nagy A, Lupu F, Moons L, Collen D, D'Amore PA, Shima DT. Impaired myocardial angiogenesis and ischemic cardiomyopathy in mice lacking the vascular endothelial growth factor isoforms vegf164 and vegf188. *Nature medicine*. 1999;5:495-502

52. Ruhrberg C, Gerhardt H, Golding M, Watson R, Ioannidou S, Fujisawa H, Betsholtz C, Shima DT. Spatially restricted patterning cues provided by heparin-binding vegf-a control blood vessel branching morphogenesis. *Genes & development*. 2002;16:2684-2698

53. Stalmans I, Ng YS, Rohan R, Fruttiger M, Bouche A, Yuce A, Fujisawa H, Hermans B, Shani M, Jansen S, Hicklin D, Anderson DJ, Gardiner T, Hammes HP, Moons L, Dewerchin M, Collen D, Carmeliet P, D'Amore PA. Arteriolar and venular patterning in retinas of mice selectively expressing vegf isoforms. *The Journal of clinical investigation*. 2002;109:327-336

54. Gerhardt H, Golding M, Fruttiger M, Ruhrberg C, Lundkvist A, Abramsson A, Jeltsch M, Mitchell C, Alitalo K, Shima D, Betsholtz C. Vegf guides angiogenic sprouting

utilizing endothelial tip cell filopodia. *The Journal of cell biology*. 2003;161:1163-1177

55. Dvorak HF, Brown LF, Detmar M, Dvorak AM. Vascular permeability factor/vascular endothelial growth factor, microvascular hyperpermeability, and angiogenesis. *The American journal of pathology*. 1995;146:1029-1039

56. Presta LG, Chen H, O'Connor SJ, Chisholm V, Meng YG, Krummen L, Winkler M, Ferrara N. Humanization of an anti-vascular endothelial growth factor monoclonal antibody for the therapy of solid tumors and other disorders. *Cancer research*. 1997;57:4593-4599

57. Wood JM, Bold G, Buchdunger E, Cozens R, Ferrari S, Frei J, Hofmann F, Mestan J, Mett H, O'Reilly T, Persohn E, Rosel J, Schnell C, Stover D, Theuer A, Towbin H, Wenger F, Woods-Cook K, Menrad A, Siemeister G, Schirner M, Thierauch KH, Schneider MR, Drevs J, Martiny-Baron G, Totzke F. Ptk787/zk 222584, a novel and potent inhibitor of vascular endothelial growth factor receptor tyrosine kinases, impairs vascular endothelial growth factor-induced responses and tumor growth after oral administration. *Cancer research*. 2000;60:2178-2189

58. Adamis AP, Miller JW, Bernal MT, D'Amico DJ, Folkman J, Yeo TK, Yeo KT. Increased vascular endothelial growth factor levels in the vitreous of eyes with proliferative diabetic retinopathy. *American journal of ophthalmology*. 1994;118:445-450

59. Kvanta A, Algvere PV, Berglin L, Seregard S. Subfoveal fibrovascular membranes in age-related macular degeneration express vascular endothelial growth factor. *Investigative ophthalmology & visual science*. 1996;37:1929-1934

60. Chappell JC, Wiley DM, Bautch VL. Regulation of blood vessel sprouting. *Seminars in cell & developmental biology*. 2011;22:1005-1011

61. Chappell JC, Taylor SM, Ferrara N, Bautch VL. Local guidance of emerging vessel sprouts requires soluble flt-1. *Developmental cell*. 2009;17:377-386

62. Claxton S, Fruttiger M. Oxygen modifies artery differentiation and network morphogenesis in the retinal vasculature. *Developmental dynamics : an official publication of the American Association of Anatomists*. 2005;233:822-828

63. Fantin A, Vieira JM, Gestri G, Denti L, Schwarz Q, Prykhozhij S, Peri F, Wilson SW, Ruhrberg C. Tissue macrophages act as cellular chaperones for vascular anastomosis downstream of vegf-mediated endothelial tip cell induction. *Blood*. 2010;116:829-840

64. Iruela-Arispe ML, Davis GE. Cellular and molecular mechanisms of vascular lumen formation. *Developmental cell*. 2009;16:222-231

65. Makanya AN, Hlushchuk R, Djonov VG. Intussusceptive angiogenesis and its role in vascular morphogenesis, patterning, and remodeling. *Angiogenesis*. 2009;12:113-123

66. Caduff JH, Fischer LC, Burri PH. Scanning electron microscope study of the developing microvasculature in the postnatal rat lung. *The Anatomical record*. 1986;216:154-164

67. Patan S, Haenni B, Burri PH. Implementation of intussusceptive microvascular growth in the chicken chorioallantoic membrane (cam). *Microvascular research*. 1997;53:33-52

68.	Burri PH, Hlushchuk R, Djonov V. Intussusceptive angiogenesis: Its emergence, its characteristics, and its significance. *Developmental dynamics : an official publication of the American Association of Anatomists*. 2004;231:474-488

69.	Hlushchuk R, Riesterer O, Baum O, Wood J, Gruber G, Pruschy M, Djonov V. Tumor recovery by angiogenic switch from sprouting to intussusceptive angiogenesis after treatment with ptk787/zk222584 or ionizing radiation. *The American journal of pathology*. 2008;173:1173-1185

70.	Baum O, Suter F, Gerber B, Tschanz SA, Buergy R, Blank F, Hlushchuk R, Djonov V. Vegf-a promotes intussusceptive angiogenesis in the developing chicken chorioallantoic membrane. *Microcirculation*. 2010;17:447-457

71.	Djonov VG, Kurz H, Burri PH. Optimality in the developing vascular system: Branching remodeling by means of intussusception as an efficient adaptation mechanism. *Developmental dynamics : an official publication of the American Association of Anatomists*. 2002;224:391-402

72.	Egginton S, Zhou AL, Brown MD, Hudlicka O. Unorthodox angiogenesis in skeletal muscle. *Cardiovascular research*. 2001;49:634-646

73.	Phng LK, Gerhardt H. Angiogenesis: A team effort coordinated by notch. *Developmental cell*. 2009;16:196-208

74.	Roca C, Adams RH. Regulation of vascular morphogenesis by notch signaling. *Genes & development*. 2007;21:2511-2524

75.	Fiuza UM, Arias AM. Cell and molecular biology of notch. *The Journal of endocrinology*. 2007;194:459-474

76.	Kume T. Novel insights into the differential functions of notch ligands in vascular formation. *Journal of angiogenesis research*. 2009;1:8

77.	Andersen P, Uosaki H, Shenje LT, Kwon C. Non-canonical notch signaling: Emerging role and mechanism. *Trends in cell biology*. 2012;22:257-265

78.	Bray SJ. Notch signalling: A simple pathway becomes complex. *Nature reviews. Molecular cell biology*. 2006;7:678-689

79.	Hellstrom M, Phng LK, Hofmann JJ, Wallgard E, Coultas L, Lindblom P, Alva J, Nilsson AK, Karlsson L, Gaiano N, Yoon K, Rossant J, Iruela-Arispe ML, Kalen M, Gerhardt H, Betsholtz C. Dll4 signalling through notch1 regulates formation of tip cells during angiogenesis. *Nature*. 2007;445:776-780

80.	Leslie JD, Ariza-McNaughton L, Bermange AL, McAdow R, Johnson SL, Lewis J. Endothelial signalling by the notch ligand delta-like 4 restricts angiogenesis. *Development*. 2007;134:839-844

81.	Lobov IB, Renard RA, Papadopoulos N, Gale NW, Thurston G, Yancopoulos GD, Wiegand SJ. Delta-like ligand 4 (dll4) is induced by vegf as a negative regulator of angiogenic sprouting. *Proceedings of the National Academy of Sciences of the United States of America*. 2007;104:3219-3224

82.	Noguera-Troise I, Daly C, Papadopoulos NJ, Coetzee S, Boland P, Gale NW, Lin HC, Yancopoulos GD, Thurston G. Blockade of dll4 inhibits tumour growth by promoting non-productive angiogenesis. *Nature*. 2006;444:1032-1037

83.	Ridgway J, Zhang G, Wu Y, Stawicki S, Liang WC, Chanthery Y, Kowalski J, Watts RJ, Callahan C, Kasman I, Singh M, Chien M, Tan C, Hongo JA, de Sauvage F, Plowman

G, Yan M. Inhibition of dll4 signalling inhibits tumour growth by deregulating angiogenesis. *Nature*. 2006;444:1083-1087

84. Sainson RC, Aoto J, Nakatsu MN, Holderfield M, Conn E, Koller E, Hughes CC. Cell-autonomous notch signaling regulates endothelial cell branching and proliferation during vascular tubulogenesis. *FASEB journal : official publication of the Federation of American Societies for Experimental Biology*. 2005;19:1027-1029

85. Siekmann AF, Lawson ND. Notch signalling limits angiogenic cell behaviour in developing zebrafish arteries. *Nature*. 2007;445:781-784

86. Suchting S, Freitas C, le Noble F, Benedito R, Breant C, Duarte A, Eichmann A. The notch ligand delta-like 4 negatively regulates endothelial tip cell formation and vessel branching. *Proceedings of the National Academy of Sciences of the United States of America*. 2007;104:3225-3230

87. Jakobsson L, Franco CA, Bentley K, Collins RT, Ponsioen B, Aspalter IM, Rosewell I, Busse M, Thurston G, Medvinsky A, Schulte-Merker S, Gerhardt H. Endothelial cells dynamically compete for the tip cell position during angiogenic sprouting. *Nature cell biology*. 2010;12:943-953

88. Tammela T, Zarkada G, Nurmi H, Jakobsson L, Heinolainen K, Tvorogov D, Zheng W, Franco CA, Murtomaki A, Aranda E, Miura N, Yla-Herttuala S, Fruttiger M, Makinen T, Eichmann A, Pollard JW, Gerhardt H, Alitalo K. Vegfr-3 controls tip to stalk conversion at vessel fusion sites by reinforcing notch signalling. *Nature cell biology*. 2011;13:1202-1213

89. Benedito R, Roca C, Sorensen I, Adams S, Gossler A, Fruttiger M, Adams RH. The notch ligands dll4 and jagged1 have opposing effects on angiogenesis. *Cell*. 2009;137:1124-1135

90. Scehnet JS, Jiang W, Kumar SR, Krasnoperov V, Trindade A, Benedito R, Djokovic D, Borges C, Ley EJ, Duarte A, Gill PS. Inhibition of dll4-mediated signaling induces proliferation of immature vessels and results in poor tissue perfusion. *Blood*. 2007;109:4753-4760

Chapter | 2

VEGF and its limitations for therapeutic angiogenesis

Atherosclerotic cardiovascular diseases, including peripheral artery disease (PAD) and coronary artery disease (CAD) are the leading cause of death in the western world, despite advances in medical and surgical therapy. In most cases, pharmacological therapy with vasodilators and antiplatelet agents is not enough to cure such pathologies. As the disease progresses, surgical intervention is often required. Unfortunately, many patients with advanced atherosclerosis are not amenable to these surgical procedures and fail other treatments. In the last decades, therapeutic angiogenesis has emerged as an attractive alternative. The goal is to restore blood supply by delivering growth factors that control the formation of new vessels by means of gene or cell-based approaches. In the last years, several studies delivering various growth factors alone or in different combinations have been performed disclosing some limitations of this approach. Further investigation is required in order to translate it into a fully applicable therapeutic strategy.

2.1 Limitations of VEGF delivery for therapeutic angiogenesis

2.1.1. Toxicity of VEGF gene delivery

The first experimental and clinical studies of gene therapy for cardiovascular diseases were carried out using plasmid DNA. Compared to viral delivery, plasmid DNA is easy to produce and it is safer. This technology was initially employed in small uncontrolled clinical trials and yielded promising results. However, larger clinical trials highlighted that gene transfer efficacy of DNA *in vivo* is very low and can only be slightly improved using

carrier molecules such as liposome complexes or cationic polymers and physical methods such as electroporation. On the other hand, although considered safe, some reports showed that plasmid DNA delivery could also cause transient inflammation or fever [1]. Besides, intramyocardial injection of DNA expressing VEGF in a myocardial infarction model in rat, resulted in the growth of macroscopic angioma-like structures at the site of injection. Furthermore, the treatment did not result in any functional improvement [2]. The induction of vascular tumors (hemangioma) as a consequence of excessive VEGF expression in the myocardium has also been reported using myoblast-based VEGF delivery. In this study, continuous expression of VEGF caused the formation of intramural vascular tumors at the site of implantation and animal death [3]. The deleterious effects of uncontrolled VEGF expression have been largely observed also in skeletal muscle. In 1998, hemangioma formation was first reported after implantation of retrovirally-transduced myoblasts overexpressing VEGF [4]. Few years later, it has been described that injection of an adenoviral vector engineered to express VEGF induced a dose-dependent angiogenic response in skeletal muscle and in other tissues and caused angioma formation [5]. In addition, intramuscular VEGF gene transfer in animals with critical limb ischemia resulted in increased leakiness of blood vessels, severe edema and accelerated limb amputation [6]. Although uncontrolled levels and long-term expression of VEGF are dangerous due to serious side effects, short-term expression has been shown to be insufficient for the formation of a functional vasculature. Induced vessels were unstable and immediately regressed after the cessation of VEGF stimulus [7]. These results emphasize the importance of being able to tightly regulate VEGF expression for

therapeutic angiogenesis in order to exploit its therapeutic potential while avoiding its deleterious effects.

2.1.2. Cell-based VEGF delivery for therapeutic angiogenesis

Skeletal muscle is the target tissue of therapeutic angiogenesis approaches and has several features that make it suitable for both *in vivo* and *ex vivo* gene delivery approaches. *In vivo* approaches are characterized by injection of engineered viral vectors such as adenoviruses, adeno-associated viruses, retroviruses, lentiviruses or naked DNA plasmid directly into muscle tissue. This strategy has been used extensively uncovering several limitations of this approach [1]. On the other hand, muscle tissue is also suited for *ex vivo* approaches such as cell-based gene delivery. Skeletal muscle is highly accessible and vascularized and composes a large mass of the body. It is constituted by myofibers that are formed during development by the fusion of mononucleated precursor cells called myoblasts. The fusion process is not restricted to development but continues throughout adult life. In particular, after muscle injury myoblasts help regeneration of the tissue by fusing to preexisting muscle fibers. Myoblasts are retained as satellite cells, residing between the basal lamina and the plasma membrane of the muscle fibers, and can be readily isolated and expanded in culture. Besides, they can be transduced at high efficiency with viral vectors such as retroviruses encoding the therapeutic protein and characterized *in vitro*. Upon intramuscular injection, they are incorporated in resident muscle fibers. The gene of interest is therefore expressed only by the muscle fiber itself,

which is the direct target of therapeutic angiogenesis approaches. This makes myoblasts ideal as a cell-based gene delivery platform to skeletal muscle. Furthermore, myoblast-based strategy allows a form of "adult transgenesis" and can be also used to study the effects of the delivery of multiple angiogenic factors. In fact, multiple transduction steps can be performed to introduce additional genes without impairing the myoblast differentiation potential *in vitro* and fusion ability *in vivo* [8].
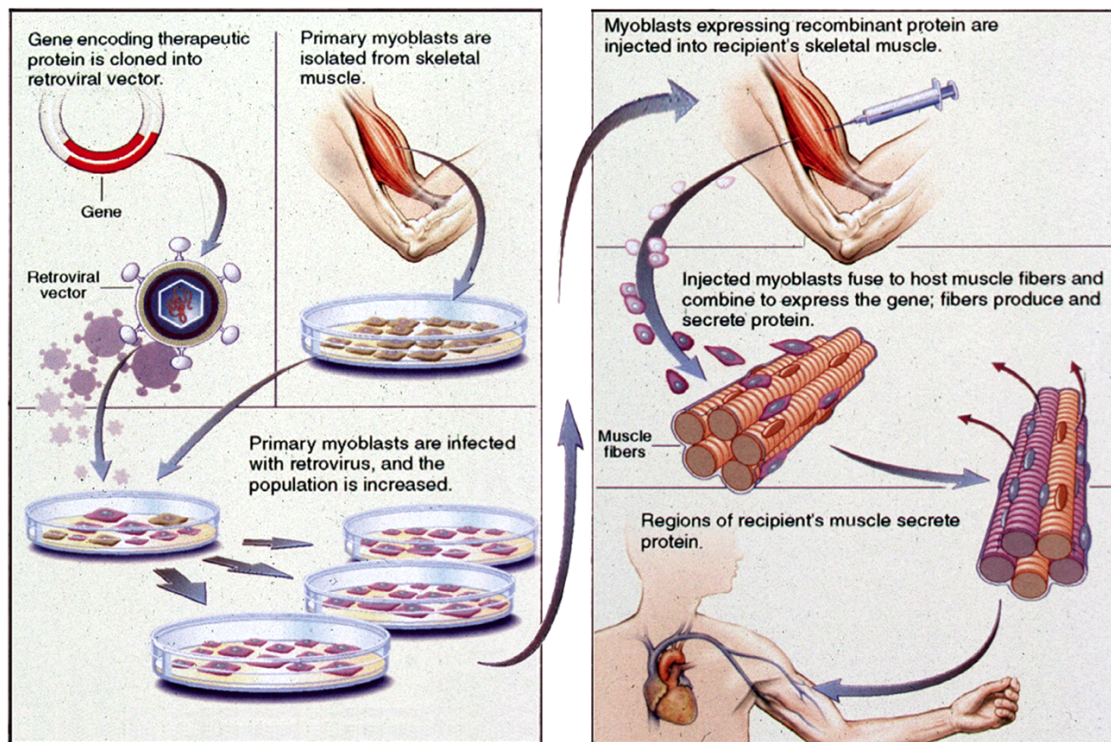
Figure 7. **Myoblast-mediated gene delivery approach** (adapted from Blau H, 1995)

Another advantage of the myoblast-based *ex vivo* approach derives from the possibility to measure the expression of the gene product *in vitro* before implantation. In addition, modifications of this approach allow the possibility to control the levels and duration of

transgene expression. This modulation can be pursued by generating tetracycline-inducible systems [9] that allow switching on and off the transgene expression in any moment, or by isolating clonal populations of transduced myoblasts that homogeneously express specific transgene levels [10]. Myoblast-mediated gene transfer has been used to rigorously investigate the dose-dependent effects of long-term expression of VEGF on vessel morphology and functionality in skeletal muscle [4, 10, 11].

2.1.3. VEGF dose: total versus microenvironmental

Several clinical trials in the past have tested the potential of VEGF delivery for achieving therapeutic angiogenesis but failed to show clear clinical efficacy [12]. Retrospective analyses have found that clinical delivery of VEGF appears to have a narrow therapeutic window: while low vector doses appear to be mostly inefficacious, higher doses become rapidly unsafe leading to the growth of hemangioma-like structures [2, 4]. Over the past several years, work in our group rigorously investigated the dose-dependent effects of VEGF in skeletal muscle, focusing on its therapeutic window, by using retrovirally-transduced myoblasts. Single myoblast clones were isolated from a transduced heterogeneous population, which homogeneously expressed various specific VEGF levels, ranging from 5 to 200 $ng/10^6$ cells/day. The effects of different VEGF doses were investigated by using two separate strategies, controlling either the total or the microenvironmental level of VEGF. The total dose was reduced by implanting lower numbers of the heterogeneous VEGF myoblast population that caused the formation of

hemangiomas. With this approach, the aberrant vascular growth could not be avoided even when a total dose low as 5 ng/10^6 cells/days was delivered. By contrast, when VEGF expression was controlled in each cell by implanting clonal populations, a dose-dependent threshold between normal and aberrant angiogenesis was discovered. Indeed, VEGF levels from 5 to 60 ng/10^6 cells/days induced only normal, stable and pericyte-covered capillaries, whereas higher levels (100 to 200 ng/10^6 cells/days) resulted in abnormal tortuous vessels and induced the growth of large hemangiomas. Therefore, the induction of normal or aberrant angiogenesis by VEGF strictly depends on its amount in the microenvironment around each secreting cell *in vivo* and not on the total dose delivered, as different levels will not average with each other in the tissue [10] (Figure 8).
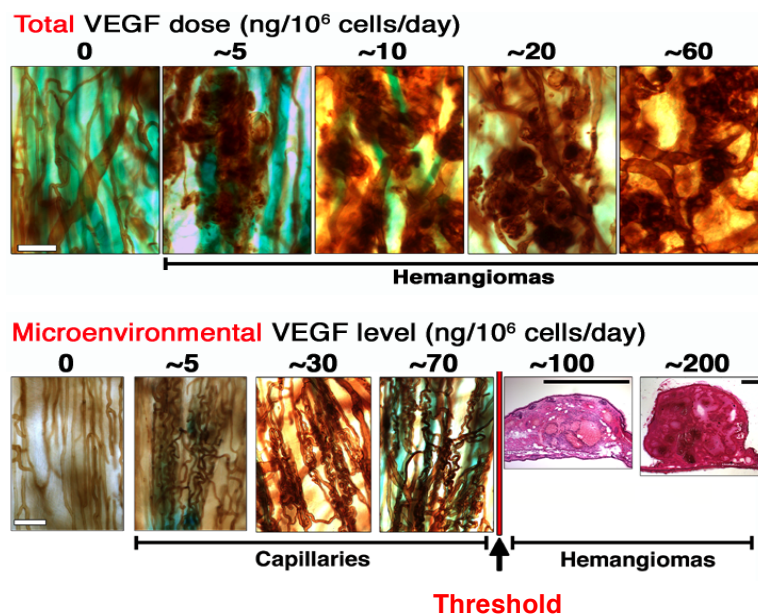
Figure 8. **Microenvironmental VEGF concentration, not total dose, determines a threshold between normal and aberrant angiogenesis** (adapted from Ozawa, 2004).

Furthermore, it has been demonstrated that only homogeneous and controlled levels of VEGF below the threshold are able to induce functional and stable angiogenesis in ischemic conditions, showing that the control over the microenvironmental distribution of VEGF levels is critical to improving both efficacy and safety in ischemia [11]. These findings can partially explain the disappointing results obtained in clinical trials of VEGF gene delivery. In fact, gene therapy approaches using viral vectors enable only the manipulation of the total VEGF dose, by reducing the titer of viral particles delivered. On the contrary, the cell-based gene delivery system described here allows a tight control on the microenvironmental level of VEGF. While providing a proof-of-principle, this approach is not feasible in clinical practice because it is time-consuming and it would require the isolation and characterization of libraries of clones for each patient. To overcome this limitation, our group has recently developed a FACS-based high-throughput technology to predict the level of VEGF expression in single cells and to rapidly purify populations homogeneously expressing specific levels. This was achieved by linking VEGF expression quantitatively to that of a syngenic marker (truncated CD8a), which can be detected and quantified on the cell surface by fluorescence-activated cells sorting. A single round of sorting with a suitably designed gate yielded a purified population that induced robust, normal and stable angiogenesis [13]. The safety of controlled VEGF expression by this approach was further tested in a rat model of chronic hindlimb ischemia. Purified transduced myoblasts could ensure the induction of only normal and stable angiogenesis and the avoidance of any aberrant vascular growth also in ischemic tissue [14].

2.2   Retroviral and lentiviral vectors for gene and cell-based therapies

2.2.1 Retroviral vectors safety for clinical applications

Retroviruses comprise a large family of enveloped RNA viruses. They have the ability to integrate efficiently into the genomic DNA of animal cells and to be stably replicated and transmitted to the progeny. This feature provided a strong incentive for the development of efficient retroviral gene transfer vectors. The first approaches for retrovirus-based gene transfer were initiated about 30 years ago to deliver genes for the treatment of genetic and acquired diseases [15]. Nowadays, retroviral-based gene therapy represents about 20% of all gene therapy trials. In most cases, the hematopoietic and immune systems are the targets for retroviral gene therapy. Successful clinical results were obtained for the treatment of severe combined immunodeficiencies (SCID), in particular SCID-ADA, in which the adenosine deaminase (ADA) enzyme is malfunctional due to a single autosomal gene defect that is recessively inherited [16, 17]. Although successful in the treatment of different genetic diseases, retroviral vectors have some important limitations. Retroviruses are unable to efficiently infect non-dividing cells and their limited genome only allows the incorporation of expression cassettes of small size. Furthermore, it is preferable to insert cassettes without introns because of possible interference with the reverse transcription step. In addition, it has been observed in several cases that the expression of the transgene can be limited by methylation of the retroviral LTR promoter sequences, resulting in transcriptional shut-off. On the other hand, vectors derived from retrovirusesc integrate randomly in the genome. The fact that

retroviruses infect only actively proliferating cells can favor integration into chromatin sites that may be shut-off once cells exit the cell cycle. Besides these considerations, the use of retroviruses in the clinical practice has been largely abandoned in recent years because of safety concerns. Insertional mutagenesis is the most important and it has been first reported in animal models in which leukemia was induced by retroviral gene marking [18]. Moreover, insertional mutagenesis has been also described in some patients treated with engineered hematopoietic stem cells. A proportion of them developed leukemias because of clonal transformation of some transduced cells due to the activation of endogenous oncogenes by the strong retroviral LTR promoter [19, 20]. To improve safety of retroviral vectors, self-inactivating (SIN) vectors have been developed. SIN vectors harbor a deletion within 3' U3 region in which enhancer/promoter activity resides. During reverse transcription reaction, this deletion is copied to the 5'-LTR. LTR-promoter activity of the provirus is therefore abolished, allowing the introduction of an internal promoter of choice to drive transgene expression. Despite these safety improvements and although in other progenitor classes, such as skin stem cells, retroviral gene therapy showed very promising results without revealing any side effect [21], regulatory bodies in Europe and USA are currently restricting the use of retroviral vectors for clinical applications in favor of lentiviral vectors, which appear to be safer and more efficacious.

2.2.2 Lentiviral vectors safety for clinical applications

Lentiviruses are distinct members of the Retroviridae family of viruses from which different gene transfer vectors have been derived because of their attractive features. Among these, their ability to infect both dividing and non-dividing cells [22] is considered a great advantage compared to retroviruses and makes these vectors useful to transduce a wide variety of primary cells and mammalian cell lines with high efficiency [23]. Furthermore, lentiviral vectors allow for stable long-term expression of the transgene since no evidence of transcriptional shut-off has been reported in a variety of target tissues. This difference between retroviruses and lentiviruses may reside in an intrinsic difference in the viral LTRs and in the different integration profile of such viruses. It has been demonstrated that while retroviruses cluster in the proximity of the transcriptional start site, CpG islands and DNase I hypersensitive sites, lentiviruses tend to integrate within all transcription unit [24, 25]. Furthermore, lentiviruses are able to accommodate larger transgenes (up to 10 kilobases) and to drive a lower level of transgene expression when compared with enhancer-deleted retroviral based vectors carrying the same expression cassette [26]. In the last years, several studies have been initiated to compare the genotoxic potential of lentiviral vectors and retroviral vectors. In 2006, using a tumor-prone mouse model, it has been demonstrated that retroviral vectors triggered dose-dependent acceleration of tumor onset, whereas lentiviral vectors did not affect tumorigenicity despite a stronger expression of lentiviral vectors in all hematopoietic lineages [27]. These results uncovered a lower oncogenic potential of lentivirus-derived vectors and were confirmed by several other studies, indicating a promising safety profile

for lentiviral vectors [28-30]. In addition, further studies revealed that the genotoxic potential of viral vectors is strongly modulated by vector design [31]. Besides the use of SIN vectors that significantly reduces the likelihood of transactivation of nearby endogenous oncogenes, recent reports showed that the use of a cellular enhancer-promoter could greatly reduce the genotoxic potential of integrating vectors [32]. These findings have been further supported by clinical studies in which no oncogenic events were observed [33-35]. Lentiviruses have been extensively used for both *in vivo* and *ex vivo* gene delivery. The first efficient transduction and stable expression of the transgene in vivo by lentiviral vectors was observed in the central nervous system of adult rats [36]. Sustained transgene expression was achieved also by lentiviral transduction of the liver and skeletal muscle [37]. As an alternative to direct intramuscular injection, lentiviral vectors can be used in cell-based approaches to transduce muscle stem cells such as myoblasts or mesoangioblasts that, once *in vivo*, are able to differentiate and fuse to pre-existing fibers. In particular, it has been shown that lentivirally transduced mesoangioblasts can functionally repair dystrophic muscle after their systemic injection in both mouse and dog dystrophic models [38, 39]. The promising results obtained in several gene and cell-based approaches using lentiviral vectors prompted the scientific community to further refine their design and to improve their safety profile. For this purpose, it has been shown that the incorporation of cell type-specific microRNAs downstream of a transgene can help to restrict its expression in those particular cells [40, 41]. In conclusion, lentiviral vectors are potent and versatile vectors for *ex vivo* or *in vivo* gene transfer and their improved safety and efficacy make them ideal candidates for successful applications both in clinical practice and in therapeutic angiogenesis approaches.

Bibliography

1.   Rissanen TT, Yla-Herttuala S. Current status of cardiovascular gene therapy. *Molecular therapy : the journal of the American Society of Gene Therapy*. 2007;15:1233-1247

2.   Schwarz ER, Speakman MT, Patterson M, Hale SS, Isner JM, Kedes LH, Kloner RA. Evaluation of the effects of intramyocardial injection of DNA expressing vascular endothelial growth factor (vegf) in a myocardial infarction model in the rat-- angiogenesis and angioma formation. *Journal of the American College of Cardiology*. 2000;35:1323-1330

3.   Lee RJ, Springer ML, Blanco-Bose WE, Shaw R, Ursell PC, Blau HM. Vegf gene delivery to myocardium: Deleterious effects of unregulated expression. *Circulation*. 2000;102:898-901

4.   Springer ML, Chen AS, Kraft PE, Bednarski M, Blau HM. Vegf gene delivery to muscle: Potential role for vasculogenesis in adults. *Molecular cell*. 1998;2:549-558

5.   Pettersson A, Nagy JA, Brown LF, Sundberg C, Morgan E, Jungles S, Carter R, Krieger JE, Manseau EJ, Harvey VS, Eckelhoefer IA, Feng D, Dvorak AM, Mulligan RC, Dvorak HF. Heterogeneity of the angiogenic response induced in different normal adult tissues by vascular permeability factor/vascular endothelial growth factor. *Laboratory investigation; a journal of technical methods and pathology*. 2000;80:99-115

6.   Masaki I, Yonemitsu Y, Yamashita A, Sata S, Tanii M, Komori K, Nakagawa K, Hou X, Nagai Y, Hasegawa M, Sugimachi K, Sueishi K. Angiogenic gene therapy for experimental critical limb ischemia: Acceleration of limb loss by overexpression of vascular endothelial growth factor 165 but not of fibroblast growth factor-2. *Circulation research*. 2002;90:966-973

7.   Dor Y, Djonov V, Abramovitch R, Itin A, Fishman GI, Carmeliet P, Goelman G, Keshet E. Conditional switching of vegf provides new insights into adult neovascularization and pro-angiogenic therapy. *The EMBO journal*. 2002;21:1939-1947

8.   von Degenfeld G, Banfi A, Springer ML, Blau HM. Myoblast-mediated gene transfer for therapeutic angiogenesis and arteriogenesis. *British journal of pharmacology*. 2003;140:620-626

9.   Blau HM, Rossi FM. Tet b or not tet b: Advances in tetracycline-inducible gene expression. *Proceedings of the National Academy of Sciences of the United States of America*. 1999;96:797-799

10.   Ozawa CR, Banfi A, Glazer NL, Thurston G, Springer ML, Kraft PE, McDonald DM, Blau HM. Microenvironmental vegf concentration, not total dose, determines a threshold between normal and aberrant angiogenesis. *The Journal of clinical investigation*. 2004;113:516-527

11.   von Degenfeld G, Banfi A, Springer ML, Wagner RA, Jacobi J, Ozawa CR, Merchant MJ, Cooke JP, Blau HM. Microenvironmental vegf distribution is critical for stable and functional vessel growth in ischemia. *FASEB journal : official publication of the Federation of American Societies for Experimental Biology*. 2006;20:2657-2659

12. Simons M, Ware JA. Therapeutic angiogenesis in cardiovascular disease. *Nature reviews. Drug discovery*. 2003;2:863-871

13. Misteli H, Wolff T, Fuglistaler P, Gianni-Barrera R, Gurke L, Heberer M, Banfi A. High-throughput flow cytometry purification of transduced progenitors expressing defined levels of vascular endothelial growth factor induces controlled angiogenesis in vivo. *Stem Cells*. 2010;28:611-619

14. Wolff T, Mujagic E, Gianni-Barrera R, Fueglistaler P, Helmrich U, Misteli H, Gurke L, Heberer M, Banfi A. Facs-purified myoblasts producing controlled vegf levels induce safe and stable angiogenesis in chronic hind limb ischemia. *Journal of cellular and molecular medicine*. 2012;16:107-117

15. Coffin JM, Hughes SH, Varmus HE. The interactions of retroviruses and their hosts. In: Coffin JM, Hughes SH, Varmus HE, eds. *Retroviruses*. Cold Spring Harbor (NY); 1997.

16. Aiuti A, Slavin S, Aker M, Ficara F, Deola S, Mortellaro A, Morecki S, Andolfi G, Tabucchi A, Carlucci F, Marinello E, Cattaneo F, Vai S, Servida P, Miniero R, Roncarolo MG, Bordignon C. Correction of ada-scid by stem cell gene therapy combined with nonmyeloablative conditioning. *Science*. 2002;296:2410-2413

17. Aiuti A, Cattaneo F, Galimberti S, Benninghoff U, Cassani B, Callegaro L, Scaramuzza S, Andolfi G, Mirolo M, Brigida I, Tabucchi A, Carlucci F, Eibl M, Aker M, Slavin S, Al-Mousa H, Al Ghonaium A, Ferster A, Duppenthaler A, Notarangelo L, Wintergerst U, Buckley RH, Bregni M, Marktel S, Valsecchi MG, Rossi P, Ciceri F, Miniero R, Bordignon C, Roncarolo MG. Gene therapy for immunodeficiency due to adenosine deaminase deficiency. *The New England journal of medicine*. 2009;360:447-458

18. Li Z, Dullmann J, Schiedlmeier B, Schmidt M, von Kalle C, Meyer J, Forster M, Stocking C, Wahlers A, Frank O, Ostertag W, Kuhlcke K, Eckert HG, Fehse B, Baum C. Murine leukemia induced by retroviral gene marking. *Science*. 2002;296:497

19. Hacein-Bey-Abina S, Garrigue A, Wang GP, Soulier J, Lim A, Morillon E, Clappier E, Caccavelli L, Delabesse E, Beldjord K, Asnafi V, MacIntyre E, Dal Cortivo L, Radford I, Brousse N, Sigaux F, Moshous D, Hauer J, Borkhardt A, Belohradsky BH, Wintergerst U, Velez MC, Leiva L, Sorensen R, Wulffraat N, Blanche S, Bushman FD, Fischer A, Cavazzana-Calvo M. Insertional oncogenesis in 4 patients after retrovirus-mediated gene therapy of scid-x1. *The Journal of clinical investigation*. 2008;118:3132-3142

20. Baum C, Dullmann J, Li Z, Fehse B, Meyer J, Williams DA, von Kalle C. Side effects of retroviral gene transfer into hematopoietic stem cells. *Blood*. 2003;101:2099-2114

21. Mavilio F, Pellegrini G, Ferrari S, Di Nunzio F, Di Iorio E, Recchia A, Maruggi G, Ferrari G, Provasi E, Bonini C, Capurro S, Conti A, Magnoni C, Giannetti A, De Luca M. Correction of junctional epidermolysis bullosa by transplantation of genetically modified epidermal stem cells. *Nature medicine*. 2006;12:1397-1402

22. Naldini L, Blomer U, Gallay P, Ory D, Mulligan R, Gage FH, Verma IM, Trono D. In vivo gene delivery and stable transduction of nondividing cells by a lentiviral vector. *Science*. 1996;272:263-267

23. Dropulic B. Lentiviral vectors: Their molecular design, safety, and use in laboratory and preclinical research. *Human gene therapy*. 2011;22:649-657

24. Mitchell RS, Beitzel BF, Schroder AR, Shinn P, Chen H, Berry CC, Ecker JR, Bushman FD. Retroviral DNA integration: Aslv, hiv, and mlv show distinct target site preferences. *PLoS biology*. 2004;2:E234

25. Wu X, Li Y, Crise B, Burgess SM. Transcription start regions in the human genome are favored targets for mlv integration. *Science*. 2003;300:1749-1751

26. Vigna E, Naldini L. Lentiviral vectors: Excellent tools for experimental gene transfer and promising candidates for gene therapy. *The journal of gene medicine*. 2000;2:308-316

27. Montini E, Cesana D, Schmidt M, Sanvito F, Ponzoni M, Bartholomae C, Sergi Sergi L, Benedicenti F, Ambrosi A, Di Serio C, Doglioni C, von Kalle C, Naldini L. Hematopoietic stem cell gene transfer in a tumor-prone mouse model uncovers low genotoxicity of lentiviral vector integration. *Nature biotechnology*. 2006;24:687-696

28. Maruggi G, Porcellini S, Facchini G, Perna SK, Cattoglio C, Sartori D, Ambrosi A, Schambach A, Baum C, Bonini C, Bovolenta C, Mavilio F, Recchia A. Transcriptional enhancers induce insertional gene deregulation independently from the vector type and design. *Molecular therapy : the journal of the American Society of Gene Therapy*. 2009;17:851-856

29. Modlich U, Baum C. Preventing and exploiting the oncogenic potential of integrating gene vectors. *The Journal of clinical investigation*. 2009;119:755-758

30. Modlich U, Navarro S, Zychlinski D, Maetzig T, Knoess S, Brugman MH, Schambach A, Charrier S, Galy A, Thrasher AJ, Bueren J, Baum C. Insertional transformation of hematopoietic cells by self-inactivating lentiviral and gammaretroviral vectors. *Molecular therapy : the journal of the American Society of Gene Therapy*. 2009;17:1919-1928

31. Montini E, Cesana D, Schmidt M, Sanvito F, Bartholomae CC, Ranzani M, Benedicenti F, Sergi LS, Ambrosi A, Ponzoni M, Doglioni C, Di Serio C, von Kalle C, Naldini L. The genotoxic potential of retroviral vectors is strongly modulated by vector design and integration site selection in a mouse model of hsc gene therapy. *The Journal of clinical investigation*. 2009;119:964-975

32. Zychlinski D, Schambach A, Modlich U, Maetzig T, Meyer J, Grassman E, Mishra A, Baum C. Physiological promoters reduce the genotoxic risk of integrating gene vectors. *Molecular therapy : the journal of the American Society of Gene Therapy*. 2008;16:718-725

33. Cartier N, Hacein-Bey-Abina S, Bartholomae CC, Veres G, Schmidt M, Kutschera I, Vidaud M, Abel U, Dal-Cortivo L, Caccavelli L, Mahlaoui N, Kiermer V, Mittelstaedt D, Bellesme C, Lahlou N, Lefrere F, Blanche S, Audit M, Payen E, Leboulch P, l'Homme B, Bougneres P, Von Kalle C, Fischer A, Cavazzana-Calvo M, Aubourg P. Hematopoietic stem cell gene therapy with a lentiviral vector in x-linked adrenoleukodystrophy. *Science*. 2009;326:818-823

34. Cavazzana-Calvo M, Payen E, Negre O, Wang G, Hehir K, Fusil F, Down J, Denaro M, Brady T, Westerman K, Cavallesco R, Gillet-Legrand B, Caccavelli L, Sgarra R, Maouche-Chretien L, Bernaudin F, Girot R, Dorazio R, Mulder GJ, Polack A, Bank A, Soulier J, Larghero J, Kabbara N, Dalle B, Gourmel B, Socie G, Chretien S, Cartier N, Aubourg P, Fischer A, Cornetta K, Galacteros F, Beuzard Y, Gluckman E, Bushman

F, Hacein-Bey-Abina S, Leboulch P. Transfusion independence and hmga2 activation after gene therapy of human beta-thalassaemia. *Nature*. 2010;467:318-322

35. Levine BL, Humeau LM, Boyer J, MacGregor RR, Rebello T, Lu X, Binder GK, Slepushkin V, Lemiale F, Mascola JR, Bushman FD, Dropulic B, June CH. Gene transfer in humans using a conditionally replicating lentiviral vector. *Proceedings of the National Academy of Sciences of the United States of America*. 2006;103:17372-17377

36. Naldini L, Blomer U, Gage FH, Trono D, Verma IM. Efficient transfer, integration, and sustained long-term expression of the transgene in adult rat brains injected with a lentiviral vector. *Proceedings of the National Academy of Sciences of the United States of America*. 1996;93:11382-11388

37. Kafri T, Blomer U, Peterson DA, Gage FH, Verma IM. Sustained expression of genes delivered directly into liver and muscle by lentiviral vectors. *Nature genetics*. 1997;17:314-317

38. Sampaolesi M, Blot S, D'Antona G, Granger N, Tonlorenzi R, Innocenzi A, Mognol P, Thibaud JL, Galvez BG, Barthelemy I, Perani L, Mantero S, Guttinger M, Pansarasa O, Rinaldi C, Cusella De Angelis MG, Torrente Y, Bordignon C, Bottinelli R, Cossu G. Mesoangioblast stem cells ameliorate muscle function in dystrophic dogs. *Nature*. 2006;444:574-579

39. Sampaolesi M, Torrente Y, Innocenzi A, Tonlorenzi R, D'Antona G, Pellegrino MA, Barresi R, Bresolin N, De Angelis MG, Campbell KP, Bottinelli R, Cossu G. Cell therapy of alpha-sarcoglycan null dystrophic mice through intra-arterial delivery of mesoangioblasts. *Science*. 2003;301:487-492

40. Brown BD, Naldini L. Exploiting and antagonizing microrna regulation for therapeutic and experimental applications. *Nature reviews. Genetics*. 2009;10:578-585

41. Brown BD, Cantore A, Annoni A, Sergi LS, Lombardo A, Della Valle P, D'Angelo A, Naldini L. A microrna-regulated lentiviral vector mediates stable correction of hemophilia b mice. *Blood*. 2007;110:4144-4152

Aim of thesis

Angiogenesis is a complex process that is tightly controlled in all its phases by the fine interplay of different signaling pathways. Perturbations of this delicate balance are often associated with pathological conditions that are not always amenable to surgical or pharmacological treatment. In such cases, therapeutic angiogenesis is an attractive alternative. However, the results of clinical trials using gene therapy strategies to over-express VEGF have been disappointing. One of the reasons for those negative results relies on the narrow therapeutic window that VEGF has *in vivo* and on the need to tightly control its dose in the microenvironment, as discussed in the previous Chapter. On the other hand, to further improve the therapies for peripheral and coronary artery diseases, it is also essential to elucidate which signaling pathways play a pivotal role during vascular growth and how they are regulated. The Notch signaling pathway has recently been found to be the master regulator of sprouting angiogenesis. Its role in regulating the cell fate decision between tip and stalk phenotypes has been elucidated in elegant developmental models such as the perinatal formation of the retinal vascular plexus, which is generated exclusively by endothelial cells in response to VEGF gradients. In this system pericytes are recruited in a second stage by PDGF-BB deposited in the extracellular matrix by migrating tip cells. In postnatal angiogenesis, instead, and specifically in skeletal muscle, which is the target tissue of treatments for peripheral artery disease, angiogenesis takes place by re-activation of pericyte-coated quiescent capillaries. In these conditions, VEGF over-expression can induce normal and therapeutic vascular growth or aberrant angioma formation depending on its microenvironmental dose, as described in Chapter 2. However, the role of Notch signaling in the VEGF dose-dependent transition between normal and aberrant angiogenesis is completely unknown.

Therefore, here we aimed to investigate how VEGF controls the initial morphogenic events of vascular growth in skeletal muscle. In Chapter 3, taking advantage of our myoblast-mediated approach that allows controlling microenvironmental VEGF levels, we aimed to determine the cellular mechanisms by which physiologic and aberrant vessels are induced by over-expression of different VEGF doses in adult skeletal muscle. In Chapter 4, we focused on the molecular mechanisms of the switch between normal and aberrant angiogenesis by investigating the role of endothelial cell fate regulation by Notch signaling in our *in vivo* controlled model.

Furthermore, we aimed to develop a clinically compliant platform for dose-controlled expression of human VEGF using lentivirally transduced mouse myoblasts as a delivery strategy. In Chapter 5, we used retrovirally-engineered mouse myoblasts to rigorously determine the in vivo dose-dependent effects of human $VEGF_{165}$, the real therapeutic molecule for clinical applications, in mouse skeletal muscle and to compare them to the well-characterized effects of mouse $VEGF_{164.}$ In the attempt to translate these findings into an applicable strategy, we switched to the use of lentiviral vectors, which possess a much lower oncogenic potential than retroviruses. For this purpose, in Chapter 6 we developed a new library of clones over-expressing human $VEGF_{165}$ from a lentiviral vector. Herein we aimed to evaluate if and how vector type and design affect human $VEGF_{165}$ expression and its angiogenic potential in skeletal muscle.

Chapter $\vert$ 3

VEGF$_{164}$ over-expression in skeletal muscle induces angiogenesis by intussusception and not by sprouting

3.1   Introduction

Angiogenesis, i.e. the growth of new blood vessels from pre-existing ones, is a process that can be targeted to restore blood supply to ischemic tissues. Vascular Endothelial Growth Factor (VEGF) is the master regulator of vascular growth both in development and disease and, upon expression as a single factor, is capable of initiating the cascade of events leading from endothelial activation to the generation of new functional and stable vascular networks [1]. However, we previously found that VEGF can induce the growth of either normal capillary networks or aberrant angioma-like structures depending on its expression level in the microenvironment around each producing cell *in vivo* and not on the total dose delivered, since it remains tightly bound to the extracellular matrix [2, 3]. The need to strictly control VEGF dose distribution *in vivo* poses a major challenge to its therapeutic exploitation [4-6]. Understanding how normal or aberrant vessels are formed after expression of specific VEGF doses is crucial to design new rational therapeutic strategies. Our current comprehension of the initiation of vessel growth is mostly based on powerful genetic models of developmental angiogenesis, in which new vessels sprout to invade and vascularize non-perfused tissue, such as the newborn mouse retina [7]. However, in skeletal and cardiac muscle, which are the target tissues of ischemia treatments, extensive pre-existing vascular networks are present, from which new vessels are induced therapeutically by over-expression of factors well above endogenous levels. Therefore, we took advantage of a unique and well-characterized cell-based platform for controlled gene expression in skeletal muscle [2, 3, 8] to investigate the cellular mechanisms by which specific VEGF doses induce normal or aberrant angiogenesis in clinically relevant conditions.

3.2   Materials and methods

Cell culture

Primary myoblasts isolated from C57BL/6 mice and already transduced with a retrovirus expressing the β-gal marker gene were further infected at high efficiency, as previously described [9], with a retroviral construct carrying the cDNA for murine $VEGF_{164}$ linked through an Internal Ribosomal Entry Sequence (IRES) to a truncated version of murine CD8a (trCD8a) [8]. Control CD8 cells expressed only trCD8a and no VEGF. Early passage myoblast clones were isolated using a FACS Vantage SE cell sorter (Becton Dickinson, Basel, Switzerland) and single cell isolation was confirmed visually. All myoblast populations were cultured in 5% CO_2 on collagen-coated dishes, with a growth medium consisting of 40% F10, 40% DMEM (Sigma-Aldrich Chemie GmbH, Steinheim, Germany) and 20% fetal bovine serum (HyClone, Logan, UT), supplemented with 2.5 ng/ml FGF-2 (R&D Systems, Abingdon, UK), as described [10].

Myoblast implantation into mice

Cells were implanted into 5-10 week-old immunodeficient SCID CB.17 mice (Charles River Laboratories, Sulzfeld, Germany) in order to avoid an immunological response to β-galactosidase-expressing myoblasts. Animals were treated in accordance with Swiss Federal guidelines for animal welfare and the study protocol was approved by the Veterinary Office of the Canton Basel-Stadt (Basel, Switzerland). Myoblasts were dissociated in trypsin and resuspended at a concentration of 10^8 cells/ml in sterile PBS with 0.5% BSA. 1×10^6 cells in 10 μl were implanted into the posterior auricular muscle,

midway up the dorsal aspect of the external ear, or into the tibialis anterior (TA) and gastrocnemius (GC) muscles of the leg, using a syringe with a $29^1/_2$G needle, as previously described [2].

Recombinant adenovirus production

Recombinant adenoviruses expressing either mouse $VEGF_{164}$ linked to truncated CD8a in a bicistronic cassette, or only CD8a as control, were produced using the Adeno-X™ Expression System (Clontech, Saint-Germain-en-Laye, France) according to manufacturer's recommendations. Briefly, target genes were cloned into the pShuttle vector, sub-cloned into the Adeno-X viral DNA and used to transfect HEK 293 cells with Fugene HD reagent (Roche Applied Science, Basel, Switzerland). After 1 week, viral particles were collected from transfected cells by repeated freezing–thawing and used for re-infection of fresh HEK 293. After 4–5 lysis and infection cycles, viral particles were collected and purified by a double cesium chloride gradient. Viral titer was determined as infectious units after serial infection of HEK 293 cells at different multiplicities of infection, as previously described [11]. Adenoviral vectors were diluted in physiological solution and 20 μl were injected in Tibialis Anterior muscles of SCID mice at the titer of $5x10^9$ infectious units/ml.

Tissue staining

The entire vascular network of the ear could be visualized after intravascular staining with a biotinylated *Lycopersicon esculentum* (tomato) lectin (Vector Laboratories, Burlingame, CA) that binds the luminal surface of all blood vessels, as previously

described [2]. Tissues were stained with avidin-biotin complex-diaminobenzidine histochemistry (Vector Laboratories, Burlingame, CA), dehydrated through an alcohol series, cleared with toluene and whole-mounted on glass slides with Permount embedding medium (Fisher Scientific, Wholen, Switzerland). Myoblast engraftment was revealed by X-Gal staining. Immunofluorescence staining was performed on 12 μm-thick frozen sections of muscles tissues, cut along the longitudinal axis. The following primary antibodies and dilutions were used: rat anti-CD31 (clone MEC 13.3, BD Biosciences, Basel, Switzerland) at 1:100; mouse anti-α-SMA (clone 1A4, MP Biomedicals, Basel, Switzerland) at 1:400; rabbit anti-NG2 (Chemicon International, Hampshire, UK) at 1:200; rabbit anti-Ki67 (Abcam, Cambridge, UK) at 1:100. Fluorescently labeled secondary antibodies (Invitrogen, Basel, Switzerland) were used at 1:200. Fluorescence images were taken with 40x or 63x objectives on a Carl Zeiss LSM710 3-laser scanning confocal microscope (Carl Zeiss, Feldbach, Switzerland). All image analyses were performed with LSM software Zen 2010 (Carl Zeiss, Feldbach, Switzerland).

Vessel measurements

Vessel diameters were measured in whole mounts of ears stained with intravascular *L. esculentum* lectin perfusion as described [2]. Briefly, vessel diameters were measured by overlaying captured microscopic images with a square grid. Squares were randomly chosen, and the diameter of each vessel (if any) in the center of selected squares was measured. About 200 total vessel diameter measurements were obtained from 6 ears per group (n=6). All images were taken with a 10x objective on an Olympus BX61 microscope

(Olympus, Volketswil, Switzerland) and analyses were performed with AnalySIS D software (Soft Imaging System Gmbh, Münster, Germany).

Vascular casting

Vascular casts were prepared similarly to the previously described technique [12]. Briefly, the vasculature was perfused with a freshly prepared solution of PU4ii polymer (vasQtec, Zurich, Switzerland). One hour after perfusion, the samples were transferred to 7.5% potassium hydroxide for dissolution of tissue, which was completed over 2 to 3 weeks. After washing, the casts were freeze-dried and glued onto the aluminum sample stabs. The samples were then sputtered with gold to a thickness of 10 nm and examined in a Philips XL-30 SFEG scanning electron microscope.

Semi-thin serial sectioning

For the preparation of semi-thin sections of implanted muscles mice were perfused with 2.5% (v/v) glutaraldehyde solution buffered with 0.03 M potassium phosphate (pH 7.4, 370 mOsm). The samples were then harvested and left overnight in the same solution. They were then post-fixed in 1% $OsO4$ buffered with 0.1 M sodium cacodylate (pH 7.4, 340 mOsm), dehydrated in ethanol, and embedded in epoxy resin (Sigma-Aldrich Co., St. Louis, MO). One-µm-thick serial sections were prepared using glass knives and stained with Toluidine Blue (Sigma-Aldrich Co., St. Louis, MO). The serial sections were viewed with a Leica DMRB light microscope (Leica microsystems, Heerbrugg, Switzerland) and the images of implantation sites were captured with a 40x objective using SIS ColorView 3U Camera (Olympus Europe Holding GmbH, Hamburg, Germany).

The set of images obtained was aligned using Photoshop CS3 software (Adobe Systems, San Jose, CA) and imported as a stack into Imaris Software (Bitplane, Zürich, Switzerland) for 3D-reconstruction and image analysis.

Total RNA isolation and quantitative Real-Time PCR

Whole fresh mouse muscles were disrupted using a Qiagen Tissue Lyser (Qiagen, Hombrechtikon, Switzerland) to extract total RNA with a RNA Mini kit (Qiagen, Hombrechtikon, Switzerland), according to the manufacturer's instructions. Total RNA was reverse-transcribed into cDNA with the Omniscript Reverse Transcription kit (Qiagen, Hombrechtikon, Switzerland) at 37 °C for 60 minutes. Quantitative Real-Time PCR (qRT-PCR) was performed on an ABI 7300 Real-Time PCR system (Applied Biosystems, Zug, Switzerland). To determine the expression of the genes of interest the following TaqMan gene expression assays (Applied Biosystems, Zug, Switzerland) were used: Nos3 (Mm00435217_m1), Klf2 (Mm01244979_g1) and Gapdh housekeeping gene (Mm03302249_g1). The cycling parameters were: 50°C for 2 minutes, followed by 95°C for 10 minutes and 40 cycles of denaturation at 95°C for 15 seconds and annealing/extension at 60°C for 1 minute. Reactions were performed in triplicate for each template, averaged, and normalized to expression of the Gapdh housekeeping gene.

Statistical analysis

Data are presented as means ± standard error. The significance of differences was evaluated using analysis of variance (ANOVA) followed by the Bonferroni test (for

multiple comparisons), or using a Student's t-test (for single comparisons). $P < 0.05$ was considered statistically significant.

3.3 Results

VEGF over-expression induces both normal and aberrant angiogenesis through initial vascular enlargement

We investigated the initial vascular response to different doses of murine $VEGF_{164}$ in non-ischemic ear and leg skeletal muscle of SCID mice, to avoid the confounding effects of endogenous factor upregulation and inflammation that occur in ischemic tissue. To address this point, we took advantage of a well-characterized pool of monoclonal populations of retrovirally transduced mouse myoblast and selected 2 clones expressing specific low and high $VEGF_{164}$ doses (V_{Low}=61.0±2.9 and V_{High}=121.0±14.6 ng/10^6 cells/day), previously shown to induce normal and therapeutic angiogenesis, or aberrant angioma growth, respectively [2, 3, 8]. Myoblasts transduced with the empty retroviral vector were used as control. As expected control myoblasts did not alter the pre-existing vasculature at any time-point and were surrounded by morphologically normal capillaries (Fig. 1a and Fig. 1e), covered with pericytes positive for nerve/glial antigen 2 (NG2) (Fig. 2a and Fig. 2d). Four days after myoblast implantation both clones induced a marked enlargement of the pre-existing vessels (Fig. 1b-c) compared with controls. Quantification of vessel diameters showed that the degree of vascular enlargement was proportional to VEGF dose (ctrl=13.0±0.4 µm, V_{Low}=23.5±0.9 µm and V_{High}=35.1±1.0 µm; p<0.0001 for all the comparison; Fig. 1d). However, by 7 days enlarged vessels remodeled differently depending on VEGF dose, generating either normal capillary networks (Fig. 1f, V_{Low}), which showed well-attached NG2-positive pericytes (Fig. 2e), or aberrant angioma-like structures (Fig. 1g, V_{High}), which lacked NG2-positive pericytes and were coated

59

instead by a thick α-SMA-positive smooth muscle layer (Fig. 2f). At 4 days, enlarged

vessels retained NG2-positive pericytes in the presence of low VEGF (Fig. 2b), whereas

many vascular stretches were devoid of mural cells with high VEGF (Fig. 2c). Careful

analysis of the enlarged vessel walls did not reveal any evidence of sprouting, such as

filopodia-bearing endothelial tip cells, whereas clear intravascular holes were evident in

all enlarged structures at 4 days, suggestive of vascular splitting, or intussusception (Fig.

2g-h)
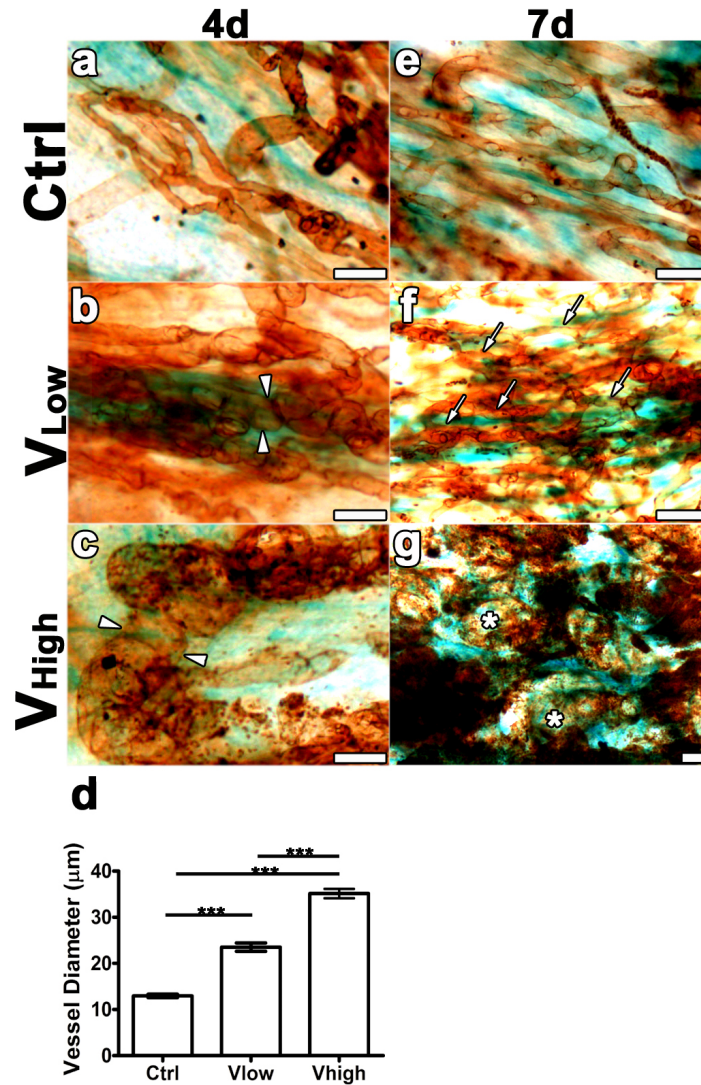
Figure 1. Vascular morphology 4 and 7 days after over-expression of different VEGF doses. Two clonal populations of transduced myoblasts expressing either a low or a high VEGF dose (V_{low} and V_{high}, respectively), and control myoblasts expressing only CD8 (ctrl) were injected in the posterior auricularis muscle. The angiogenic response was analyzed in tissue whole-mounts by lectin staining (brown) and myoblast engraftment was tracked by X-Gal staining (blue). **a-c** Vascular morphology 4 days after cell implantation. Arrowheads indicate the diameters of markedly enlarged vessels at the sites of VEGF over-expression. **d** Vessel diameter quantification showed that the degree of vascular enlargement was dependent on VEGF dose; ***P<0.0001 for all the comparisons. **e-g** By 7 days, control myoblasts did not alter the pre-existing vasculature, whereas enlarged vessels remodelled into morphologically normal capillaries (arrows, V_{Low}) or aberrant angioma-like structures (stars, V_{High}). n = 6; size bars = 50 μm

CD31-NG2-SMA-Nuclei
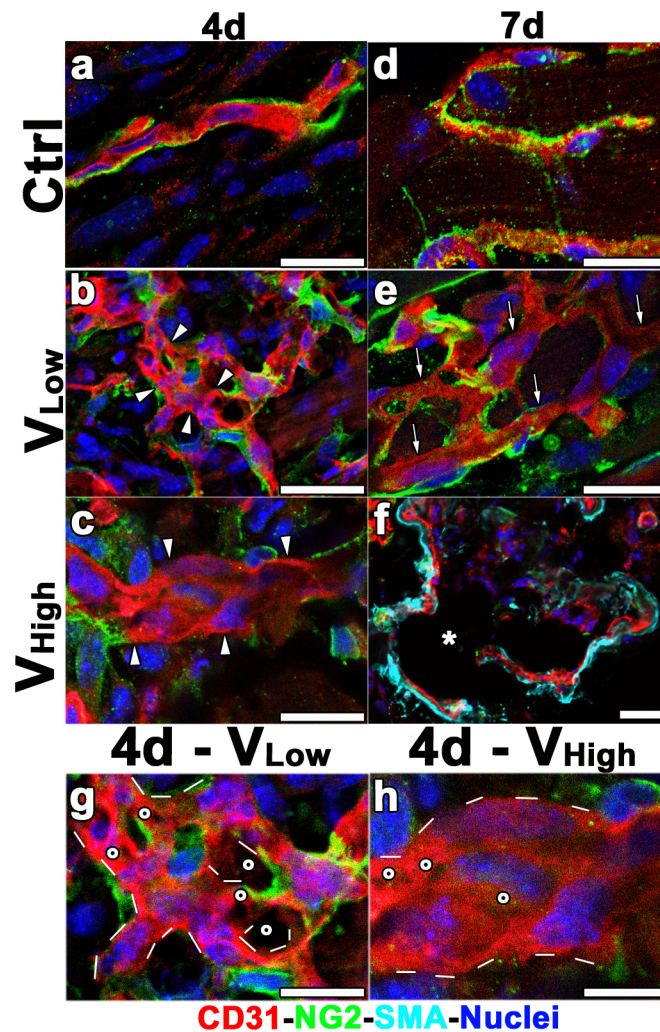
Figure 2. Mural cell coverage and endothelial morphology during vascular remodeling. Vessels induced by implantation of V_{Low} and V_{High} myoblast clones were immunostained with antibodies against CD31 (endothelial cells, red), NG2 (pericytes, green), α-SMA (smooth muscle cells, cyan) and with DAPI (nuclei, blue) in cryosections of implanted muscles. **a-c** By 4 days ,VEGF caused vascular enlargements (arrowheads) which were associated with normal NG2+ pericytes (V_{Low}) or were mainly devoid of mural cell (V_{High}), depending on VEGF dose. **d-f** By 7 days, these vascular enlargements remodeled in networks of mature capillaries, as shown by the NG2+ pericyte coverage (arrows, V_{Low}) or into aberrant dilated angioma-like structures, which lacked pericytes and were covered with a thick smooth muscle coat (star, V_{High}). **g-h** At 4 days enlarged vessels (outlined by dashed lines) showed no evidence of sprout formation and were pierced by numerous trans-luminal holes at both VEGF doses (white dots). n = 3; size bars = 20 μm

61

Vascular enlargements undergo intussusceptive angiogenesis

Characteristic for the process of intussusception is the formation of transluminal tissue pillars, which fuse progressively together and split the affected vascular segment longitudinally [13]. We addressed whether intussusception was occurring by the gold-standard analysis of vascular corrosion casts [14]. V_{Low} and V_{High} myoblast clones and control cells were implanted into tibialis anterior and gastrocnemius muscles of SCID mice. Four and seven days later the entire vasculature was cast by perfusion of polyurethane resin and the detailed microvascular morphology was observed by scanning electron microscopy. Control myoblasts did not perturb the pre-existing vasculature at any time-point (Fig. 3a-b and Fig. 3g-h). At 4 days, enlarged vessels induced by both VEGF doses displayed numerous tiny holes that pierced through the vessel casts (Fig. 3c-f), caused by the initial formation of transluminal pillars. By 7 days, vascular casts showed clear evidence of segregation of new capillary segments by intussusceptive pillar fusion and splitting in the presence of low VEGF (Fig. 3i-j). In contrast, the aberrant bulbous angioma-like structures induced by high VEGF no longer showed any signs of either pillar formation or splitting (Fig. 3k-l). To determine the morphological substrate of the holes observed in the vascular casts, 3D reconstruction of vascular structures was performed from serial semi-thin sections. This analysis confirmed the absence of vascular sprouts and that the visible holes represented transluminal pillars (Fig. 4). At 4 days, enlarged vessels displayed the presence of both incipient and mature transluminal pillars, indicated by arrowheads and arrows, respectively, in Fig. 4a-f. By 7 days, fusion of adjacent pillars led to splitting into regular capillary segments with low VEGF (Fig. 4g-i), whereas aberrant structures induced by

high VEGF displayed only rare fully mature pillars separating large vascular lacunae (Fig.

4j-l).
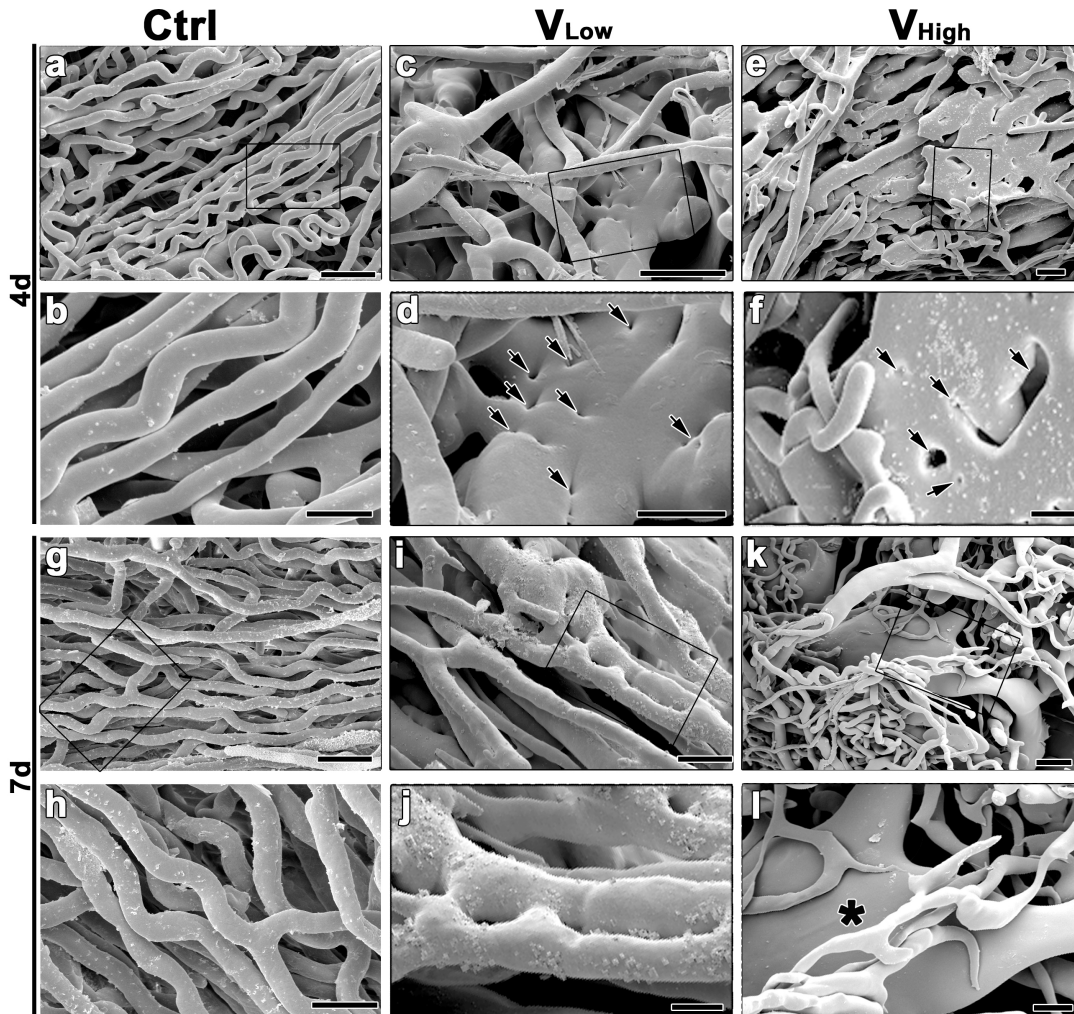
Figure 3. Scanning electron microscopy analysis of vascular casts. Control cells, V_{Low} and V_{High} myoblast clones were implanted in hindlimb muscles of SCID mice and vascular corrosion casts of the entire legs were performed 4 and 7 days post-implantation. **a-f** At 4 days, enlarged vessels displayed clear signs of transluminal tissue pillar formation, represented by the numerous small indentations and holes indicated by the black arrows. **g-l** At 7 days, low VEGF formed normal capillary networks by intussusceptive splitting (V_{Low}), whereas angioma-like structures caused by high VEGF (star, V_{High}) did not show any further signs of pillar formation. n = 3-4. Panels **b, d, f, h, j** and **l (**size bars = 10 μm) show higher magnification views of the areas indicated by the black squares in panels **a, c, e, g, i** and **k**, respectively (size bars = 25 μm)
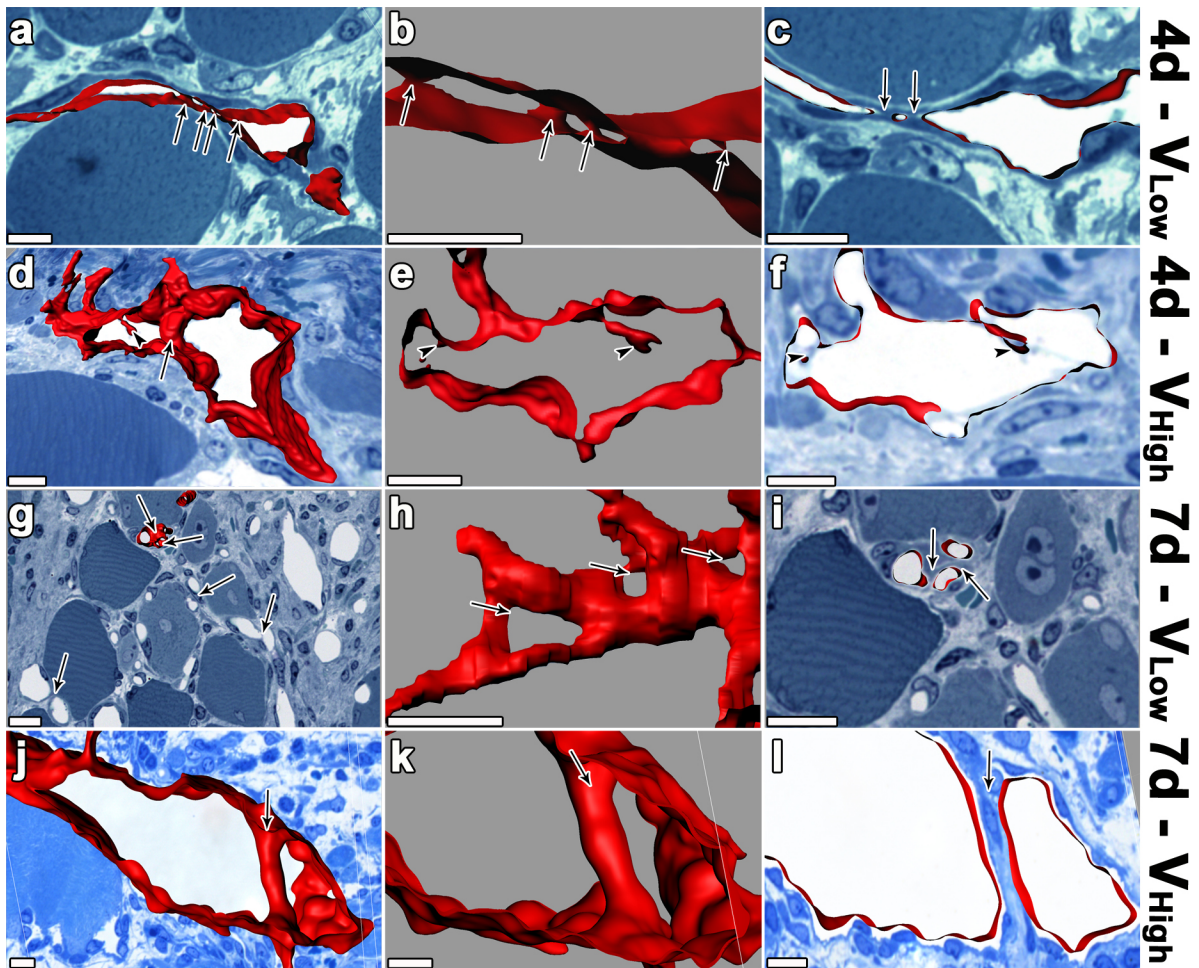
Figure 4. 3D reconstructions from serial semi-thin sections. Four and seven days after injection of V_{Low} and V_{High} clones, hundreds of serial semi-thin sections were obtained from each muscle and the corresponding 3D stacks were generated from the individual images. **a-f** At 4 days, reconstructed lumen borders (red) of enlarged vessels display mature trans-luminal pillars (arrows) and emerging pillars (arrowheads) built by intraluminal endothelial protrusions. **g-l** At 7 days, trans-luminal mature pillars (arrows) segregate new normal capillary segments with low VEGF (V_{Low}) and separate large aberrant vascular lacunae with high VEGF (V_{High}). The panels in the left column display overviews of the areas of effect, the panels in the middle column display reconstructed surfaces at a higher magnification from a different perspective, and panels in the right column display a virtual section through the obtained 3D stacks. n = 3; size bars = 10 μm

Vascular enlargement is associated with endothelial proliferation and increased blood flow

Vascular enlargement can be due either to expansion of the number of endothelial cells through proliferation or to extension of their surface by thinning and spreading of individual cells, which has been described to occur in the first 24 hours after delivery of a VEGF-expressing adenovirus [15]. KI67 staining showed that the initial vascular enlargement at 4 days was induced through active endothelial proliferation (Fig. 5a-b). Quantification of the amount of proliferating endothelial nuclei showed no differences between VEGF doses (Fig. 5e, V_{Low}=81.8±0.7% and V_{High}=84.8±1.3%). By 7 days, the endothelium of normal capillary networks was almost completely quiescent, whereas that of angioma-like structures continued proliferating (Fig. 5c-e; V_{Low}=7.1±1.3% and V_{High}=50.1±2.3%, [***] $P<0.0001$).

Gene expression analysis (Fig. 6) showed that the initial vascular enlargement by both VEGF doses was associated with a markedly increased expression of the flow-dependent genes Krüppel-like factor-2 (KLF2) and Endothelial Nitric Oxide Synthase (eNOS) at 4 days, suggesting that the endothelium of these structures was exposed to increased flow and shear stress. Consistently with the observed vascular morphology, by 7 days expression of both markers remained elevated with high VEGF, but returned to control levels in the presence of low VEGF and normal capillary remodeling.
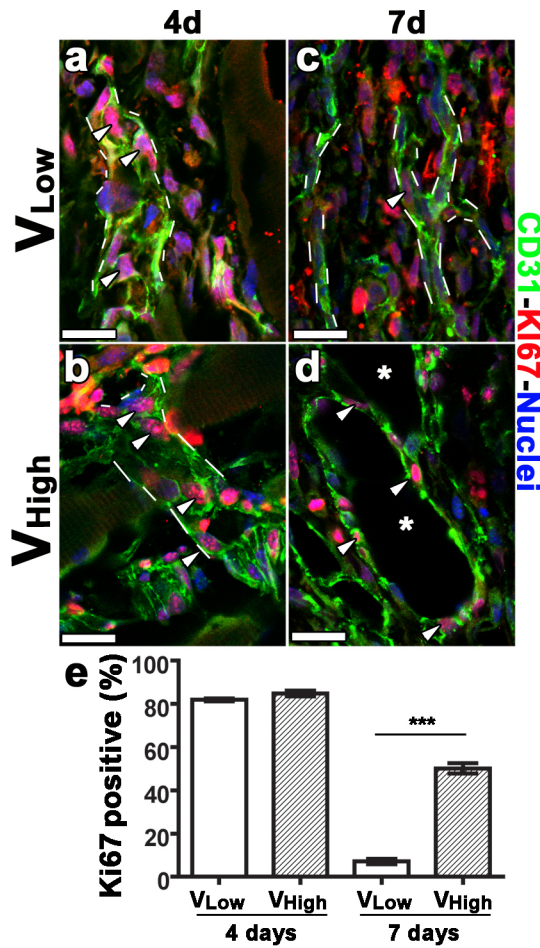
Figure 5. Vascular enlargement depends on endothelial proliferation. a-d Immunostaining with antibodies against CD31 (endothelial cells, green), KI67 (proliferating cells, red) and with DAPI (nuclei, blue) was performed on cryosections of injected muscles 4 and 7 days after myoblast implantation. Vessels are outlined by dashed lines, arrowheads point to proliferating nuclei of endothelial cells and asterisks indicate the lumens of large aberrant angioma-like structures. **e** The percentage of proliferating endothelial cells was quantified in areas of effect, [***] P<0.0001. n = 3; size bars = 20μm
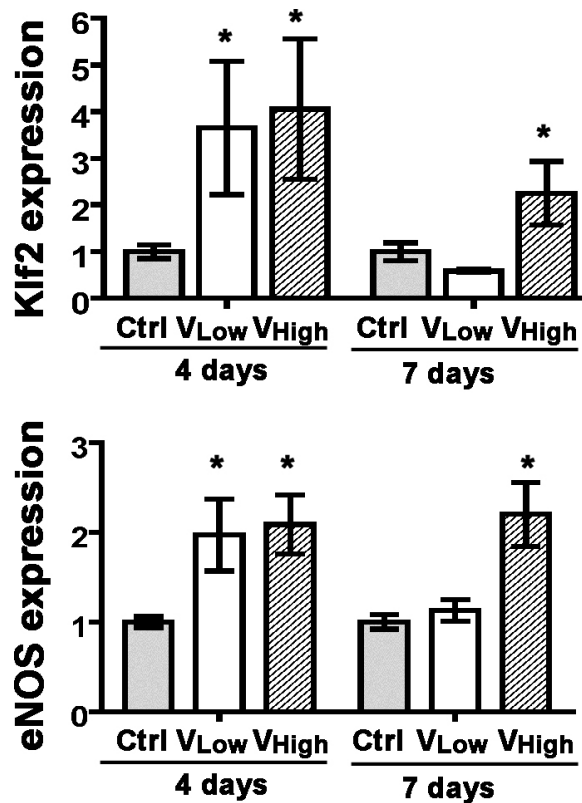
Figure 6. **Vascular enlargement causes increased flow**. Total RNA was extracted from muscles harvested 4 and 7 days after implantation with control cells (Ctrl), V_{Low} and V_{High} myoblast clones. Expression of the flow-dependent genes Klf2 and eNOS was quantified by qRT-PCR and normalized to that of the housekeeping gene GAPDH (n = 3). *p < 0.05 vs control

VEGF over-expression causes intussusceptive angiogenesis also after adenoviral delivery

Lastly, we sought to determine whether VEGF over-expression by an unrelated and clinically relevant gene delivery system would also induce angiogenesis in skeletal muscle by intussusception rather than sprouting. To test this hypothesis, adenoviral vectors, expressing $VEGF_{164}$ or just a truncated CD8 molecule as control (Ad-VEGF and Ad-CD8) [16], were implanted in tibialis anterior muscles. Immunostaining of frozen tissue

sections and confocal microscopy showed that, while Ad-CD8 did not affect the pre-existing vasculature (Fig. 7a-b), by 4 days Ad-VEGF caused vessel enlargement, without signs of sprouting, but with evidence of transluminal pillar formation (Fig. 7c). Enlarged vessels subsequently remodeled into angioma-like structures covered by a thick α-SMA-positive smooth muscle coat (Fig. 7d), similarly to the effects of high-dose VEGF expression by transduced myoblasts.
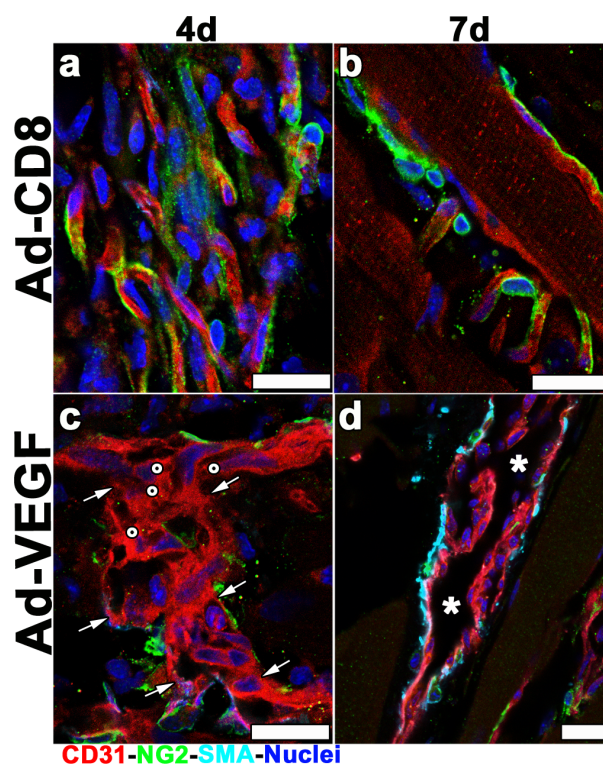
Figure 7. VEGF adenoviral delivery causes vascular enlargement and remodeling by intussusception. **a-d** Vascular morphology was analyzed 4 and 7 days after intramuscular injection of adenoviruses expressing VEGF (Ad-VEGF) or only CD8 as control (Ad-CD8) by immuno-fluorescent staining for CD31 (endothelial cells, red), NG2 (pericytes, green), α-SMA (smooth muscle cells, cyan) and DAPI (nuclei, blue) on cryosections. Ad-VEGF caused vascular enlargement (arrows in **c**), with no sprouts and many trans-luminal holes (white dots in **c**), which remodeled into angioma-like structures (asterisks in **d**). n = 3; size bars = 20

3.4   Discussion

By using a highly controlled cell-based gene delivery platform, we could study how angiogenesis is induced by over-expression of specific VEGF doses: one that we have previously shown to be therapeutic and safe in a model of hindlimb ischemia, and one that instead caused angioma growth [3]. Our data from 3 independent and complementary methods (confocal microscopy, vascular casting and 3D reconstruction of serial semi-thin sections) show that in both cases new vascular growth took place without sprouting, but rather by an initial circumferential enlargement of pre-existing vessels through VEGF-induced endothelial proliferation. This in turn was associated with increased flow and shear stress, as evidenced by the up-regulation of the transcription factor Klf2, that mediates endothelial responses to shear stress [17, 18]. These hemodynamic stimuli are potent triggers for intussusception [19]. In fact, acute increases in flow and shear stress in microvascular networks have been found to rapidly initiate transluminal pillar formation, i.e. intussusception, even without endothelial proliferation or growth factor delivery [20, 21]. We have previously shown that clamping of arterial side-branches in fully mature 16-day-old chicken chorioallantoic membranes led to a greater than 50% increase in the downstream flow rate and the appearance of transluminal pillars in capillaries as early as 40 minutes later [20]. The immediacy of the response indicates that the hemodynamic trigger is sufficient and does not require changes in gene expression to initiate the intussusceptive process. Hudlicka and coworkers further demonstrated that treatment with the α1-adrenergic receptor blocker prazosin, which increases blood flow and shear stress in the downstream microvascular networks purely through arterial vasodilation,

induced vascular growth in skeletal muscle by capillary splitting without any proliferation of endothelial cells [21].

Interestingly, our data also suggest that pericytes are not necessary to initiate intussusception. In fact, 4 days after high VEGF expression enlarged vessels were mostly devoid of pericytes, in agreement with the recently described negative regulation of pericytes by VEGF [22], yet pillar formation took place unimpeded and no NG2+ cell could be found in association with the initiating endothelial invaginations (Figure 2h).

During sprouting, specialized endothelial tip cells are formed that sense a VEGF gradient through filopodia extensions and migrate towards it, while stalk cells proliferate behind to form the new vessel lumen [7]. If a VEGF gradient is lacking, e.g. when the non-matrix-binding isoform $VEGF_{121}$ is expressed, endothelial cells proliferate without migrating and lead to vessel enlargement instead [23]. Our data indicate that over-expression of the matrix-binding $VEGF_{164}$ at two different doses induced vascular enlargement through robust endothelial proliferation in the absence of migrating tip cells, followed by transluminal pillar formation and intussusceptive remodeling. On the other hand, sprouting has been reported to take place in reparative angiogenesis after skeletal muscle ischemia [24]. The absence of any sprouting we found is likely due to differences in the VEGF dose achieved in tissue. In fact, as VEGF accumulates in the limited amount of extracellular matrix between muscle fibers, it can saturate the microenvironment and abolish the formation of a gradient capable of inducing tip cell migration. Indeed, we previously found that 3 days after induction of hind-limb ischemia the levels of endogenous VEGF moderately increased about 3-fold, whereas treatment with the low VEGF-expressing myoblast clone used here, that was both therapeutic and

safe in the same experiments, led to an 18-fold increase in muscle VEGF concentration [3]. Taken together, these results suggest that VEGF doses higher than the maximal up-regulation achieved by the endogenous response are necessary for therapeutic benefit, but induce angiogenesis by a different mechanism. In agreement with our findings, a recent dose-escalation study of adenoviral VEGF delivery to rabbit skeletal muscle showed that sprouting occurred with low VEGF and capillary enlargement with higher doses, but functional benefits were seen only with enlarged vessels [25]. In that study, the mechanisms of new vessel formation after initial enlargement could not be investigated due to the short-term duration of adenoviral expression in immunocompetent animals, but the complete switch from sprouting to vessel enlargement, as well as the maximal perfusion improvement, occurred with adenoviral titers from 10^{10} particles/ml, corresponding to about 5×10^8 infectious units/ml, and higher [25]. This is in good agreement with our results reported here that show absence of sprouting with an adenoviral titer of 5×10^9 infectious units/ml.

In conclusion, our results show that VEGF over-expression in skeletal muscle, at the doses required to induce functional benefit, induces vascular growth by intussusception and not by sprouting. Therefore, for the rational design of novel therapeutic angiogenesis approaches, it will be key to elucidate the molecular mechanisms controlling intussusception, which are still poorly understood compared to sprouting due to a paucity of appropriate models. The cell-based platform used in this work for controlled expression of specific VEGF doses in skeletal muscle, based on monoclonal populations of transduced myoblasts, may represent a useful such model to study the mechanisms of intussusceptive angiogenesis in a clinically relevant tissue.

Bibliography

1. Yla-Herttuala S, Rissanen TT, Vajanto I, Hartikainen J. Vascular endothelial growth factors: Biology and current status of clinical applications in cardiovascular medicine. *J Am Coll Cardiol*. 2007;49:1015-1026

2. Ozawa CR, Banfi A, Glazer NL, Thurston G, Springer ML, Kraft PE, McDonald DM, Blau HM. Microenvironmental vegf concentration, not total dose, determines a threshold between normal and aberrant angiogenesis. *J Clin Invest*. 2004;113:516-527

3. von Degenfeld G, Banfi A, Springer ML, Wagner RA, Jacobi J, Ozawa CR, Merchant MJ, Cooke JP, Blau HM. Microenvironmental vegf distribution is critical for stable and functional vessel growth in ischemia. *FASEB J*. 2006;20:2657-2659

4. Banfi A, von Degenfeld G, Blau HM. Critical role of microenvironmental factors in angiogenesis. *Curr Atheroscler Rep*. 2005;7:227-234

5. Karvinen H, Ylä-Herttuala S. New aspects in vascular gene therapy. *Curr Opin Pharmacol*. 2010;10:208-211

6. Yla-Herttuala S, Markkanen JE, Rissanen TT. Gene therapy for ischemic cardiovascular diseases: Some lessons learned from the first clinical trials. *Trends Cardiovasc Med*. 2004;14:295-300

7. Gerhardt H, Golding M, Fruttiger M, Ruhrberg C, Lundkvist A, Abramsson A, Jeltsch M, Mitchell C, Alitalo K, Shima D, Betsholtz C. Vegf guides angiogenic sprouting utilizing endothelial tip cell filopodia. *J Cell Biol*. 2003;161:1163-1177

8. Misteli H, Wolff T, Fuglistaler P, Gianni-Barrera R, Gurke L, Heberer M, Banfi A. High-throughput flow cytometry purification of transduced progenitors expressing defined levels of vascular endothelial growth factor induces controlled angiogenesis in vivo. *Stem Cells*. 2010;28:611-619

9. Springer ML, Blau HM. High efficiency retroviral infection of primary myoblasts. *Som. Cell Mol. Genet.* 1997;23:203-209

10. Banfi A, Springer ML, Blau HM. Myoblast-mediated gene transfer for therapeutic angiogenesis. *Methods Enzymol*. 2002;346:145-157

11. Gueret V, Negrete-Virgen JA, Lyddiatt A, Al-Rubeai M. Rapid titration of adenoviral infectivity by flow cytometry in batch culture of infected hek293 cells. *Cytotechnology*. 2002;38:87-97

12. Hlushchuk R, Ehrbar M, Reichmuth P, Heinimann N, Styp-Rekowska B, Escher R, Baum O, Lienemann P, Makanya A, Keshet E, Djonov V. Decrease in vegf expression induces intussusceptive vascular pruning. *Arterioscler Thromb Vasc Biol*. 2011;31:2836-2844

13. Makanya AN, Hlushchuk R, Djonov VG. Intussusceptive angiogenesis and its role in vascular morphogenesis, patterning, and remodeling. *Angiogenesis*. 2009;12:113-123

14. Djonov V, Burri PH. Corrosion cast analysis of blood vessels. In: Augustin H, ed. *Methods in endothelial cell biology*. Springer-Verlag, Berlin Heidelberg; 2004.

15. Pettersson A, Nagy JA, Brown LF, Sundberg C, Morgan E, Jungles S, Carter R, Krieger JE, Manseau EJ, Harvey VS, Eckelhoefer IA, Feng D, Dvorak AM, Mulligan RC, Dvorak HF. Heterogeneity of the angiogenic response induced in different

normal adult tissues by vascular permeability factor/vascular endothelial growth factor. *Lab Invest*. 2000;80:99-115

16. Banfi A, Von Degenfeld G, Gianni-Barrera R, Reginato S, Merchant MJ, McDonald DM, Blau HM. Therapeutic angiogenesis due to balanced single-vector delivery of vegf and pdgf-bb. *FASEB J*. 2012:doi:10.1096/fj.1011-197400

17. Atkins GB, Jain MK. Role of kruppel-like transcription factors in endothelial biology. *Circ Res*. 2007;100:1686-1695

18. Dekker RJ, van Thienen JV, Rohlena J, de Jager SC, Elderkamp YW, Seppen J, de Vries CJ, Biessen EA, van Berkel TJ, Pannekoek H, Horrevoets AJ. Endothelial klf2 links local arterial shear stress levels to the expression of vascular tone-regulating genes. *Am J Pathol*. 2005;167:609-618

19. Styp-Rekowska B, Hlushchuk R, Pries AR, Djonov V. Intussusceptive angiogenesis: Pillars against the blood flow. *Acta Physiol (Oxf)*. 2011;202:213-223

20. Djonov VG, Kurz H, Burri PH. Optimality in the developing vascular system: Branching remodeling by means of intussusception as an efficient adaptation mechanism. *Dev Dyn*. 2002;224:391-402

21. Egginton S, Zhou AL, Brown MD, Hudlicka O. Unorthodox angiogenesis in skeletal muscle. *Cardiovasc Res*. 2001;49:634-646

22. Greenberg JI, Shields DJ, Barillas SG, Acevedo LM, Murphy E, Huang J, Scheppke L, Stockmann C, Johnson RS, Angle N, Cheresh DA. A role for vegf as a negative regulator of pericyte function and vessel maturation. *Nature*. 2008;456:809-813

23. Ruhrberg C, Gerhardt H, Golding M, Watson R, Ioannidou S, Fujisawa H, Betsholtz C, Shima DT. Spatially restricted patterning cues provided by heparin-binding vegf-a control blood vessel branching morphogenesis. *Genes Dev*. 2002;16:2684-2698

24. Al Haj Zen A, Oikawa A, Bazan-Peregrino M, Meloni M, Emanueli C, Madeddu P. Inhibition of delta-like-4-mediated signaling impairs reparative angiogenesis after ischemia. *Circ Res*. 2010;107:283-293

25. Korpisalo P, Hytonen JP, Laitinen JT, Laidinen S, Parviainen H, Karvinen H, Siponen J, Marjomaki V, Vajanto I, Rissanen TT, Yla-Herttuala S. Capillary enlargement, not sprouting angiogenesis, determines beneficial therapeutic effects and side effects of angiogenic gene therapy. *Eur Heart J*. 2011;32:1664-1672

Chapter | 4

Synchronous activation of the Dll4/Notch1 axis by lateral induction determines intussusceptive angiogenesis after VEGF over-expression in skeletal muscle

4.1 Introduction

As presented in Chapter 2, vascular endothelial growth factor-A (VEGF) is the fundamental regulator of angiogenesis both in development and disease. However, VEGF over-expression for therapeutic purposes can induce either normal and functional capillary networks or the growth of vascular angiomas. Using a highly controlled gene transfer platform, we previously found that, based on clonal populations of transduced myoblasts expressing specific VEGF levels, the induction or normal or aberrant angiogenesis by VEGF depends strictly on the amount secreted in the microenvironment around each producing cell *in vivo* and not on the total dose delivered [1]. As discussed in Chapter 1, the angiogenesis can take place by two main mechanisms: intussusception or sprouting. Intussusception defines the process by which transluminal tissue pillars form in the pre-existing vasculature, subsequently fuse with each other and induce vascular growth through longitudinal splitting of these vessels into new ones [2]. On the other hand, sprouting angiogenesis relies on the presence of specialized endothelial cells, called tip cells, which respond to VEGF gradient and lead to the outgrowth of vessels sprouts. Endothelial cells following the tip cells are called stalk cells and, upon VEGF stimulation, start to proliferate [3] and form tight junctions to maintain the identity of the newly formed sprout[4]. The tip and stalk phenotype specification is directly regulated by the evolutionarily conserved Notch signaling pathway [5-10]. Recent data show that, during sprouting, endothelial cells dynamically compete to acquire a tip phenotype [11]. Upon VEGF stimulation, all endothelial cells respond by activating VEGFR2 (VEGF receptor 2) and inducing the upregulation of the Notch ligand Dll4 (Delta-like 4). In the competition to acquire a tip or a stalk phenotype, the cells expressing more Dll4 than their neighbours

become tip cells. Tip cells are characterized by the absence of a vascular lumen and have numerous filopodial protrusions used to sense the VEGF gradient, to sprout and migrate towards it. Concomitantly, Dll4 upregulation in tip cells induces Notch1 activation in the neighbouring cells, which causes them to become stalk cells by downregulating VEGFR2 transcription and repressing the tip phenotype. Stalk cells are indeed highly proliferative cells which are responsible for the formation of the trunk of the new vessel [6, 10, 12, 13]. Several studies show that suppression of Notch signaling in tumor angiogenesis, in zebrafish and mouse models causes an increased generation of endothelial tip cells resulting in increased sprouting and vascular branching. Moreover, pharmacological inhibition of Notch signaling pathway by DAPT treatment (γ-secretase inhibitor) causes excessive tip cells formation and induces a significant increase in the number of filopodia protrusions, although the resulting vascular networks are dysfunctional [7-9].

As shown in the previous chapter, we recently found that over-expression of VEGF in skeletal muscle induces both normal and aberrant angiogenesis without any sprouting, but rather through initial vascular enlargement followed by rapid intussusception. The whole process takes place between 4 and 7 days after VEGF delivery. However, it is unknown whether and how the role of Notch signaling pathway may regulate this process, in which not tip cells are formed. Therefore, herein we aimed to investigate how Notch signaling pathway regulates VEGF-induced intussusceptive angiogenesis in skeletal muscle, which is the target tissue of therapeutic interventions for peripheral artery disease.

4.2 Materials and Methods

Cell culture

The isolation and characterization of the clonal populations of transduced primary murine myoblasts used in these studies were previously described [14, 15]. Briefly, primary myoblasts isolated from C57BL/6 mice and already transduced with a retrovirus expressing the β-gal marker gene [16] were further infected at high efficiency as previously described[14] with a retroviral construct carrying the cDNA for murine $VEGF_{164}$ linked through an Internal Ribosomal Entry Sequence (IRES) to a truncated version of murine CD8a (trCD8a). Control CD8 cells expressed only trCD8a and no VEGF. Early passage myoblast clones were isolated using a FACS Vantage SE cell sorter (Becton Dickinson, Basel, Switzerland) and single cell isolation was confirmed visually.

Myoblast implantation in vivo

Cells were implanted into 5-10 week-old immunodeficient SCID CB.17 mice (Charles River Laboratories, Sulzfeld, Germany) in order to avoid an immunological response to β-galactosidase-expressing myoblasts. Animals were treated in accordance with Swiss Federal guidelines for animal welfare and the study protocol was approved by the Veterinary Office of the Canton of Basel-Stadt (Basel, Switzerland). Myoblasts were dissociated in trypsin and resuspended at a concentration of 10^8 cells/ml in PBS with 0.5% BSA. 1×10^6 cells in 10 μl were implanted into the posterior auricular muscle, midway up the dorsal aspect of the external ear or into the Tibialis Anterior (TA) and Gastrocnemius (GC) muscles of the leg, using a syringe with a $29^1/_2$G needle.

Tissue staining and confocal microscopy

Immunofluorescence on 12 μm-thick longitudinal cryosections of muscles was performed as previously described [1]. The following primary antibodies and dilutions were used: rat anti-mouse PECAM-1 (clone MEC 13.3, BD Biosciences, Basel, Switzerland) at 1:100; mouse monoclonal anti-mouse/human α-SMA (clone 1A4, MP Biomedicals, Basel, Switzerland) at 1:400; rabbit polyclonal anti-mouse NG2 (Chemicon International, Hampshire, UK) at 1:200, rat monoclonal anti-mouse VE-cadherin (CD144, clone 11D4.1, BD Pharmingen) at 1:100; goat polyclonal anti-mouse Dll4 (AF1389, R&D Systems Europe Ltd. UK) at 1:100; rabbit polyclonal anti-mouse activated Notch1 (Ab8923, Abcam, Cambridge). Fluorescently labeled secondary antibodies (Invitrogen, Basel, Switzerland) were used at 1:200. Z stack of all images were taken with a 40x or 63x objectives on a Carl Zeiss LSM710 3-laser scanning confocal microscope (Carl Zeiss AG, Deutschland). All images analyses were performed with LSM software Zen 2010 (Carl Zeiss AG, Deutschland).

Adenoviral production

Recombinant adenoviruses were produced using Adeno-X™ Expression System (Clontech, Mountain View, CA) according to manufacturer's recommendations. Briefly, target genes were cloned into the pShuttle vector, subcloned into the Adeno-X viral DNA and this was transfected into HEK293 cells with Fugene HD reagent (Roche, Basel, Switzerland). After 1 week, viral particles were collected from transfected cells by repeated freezing–thawing and used for infection of fresh HEK293. After 4–5 lysis-infection cycles, viral particles were collected and purified by a double caesium chloride

(CsCl) gradient. All adenoviral constructs expressed a truncated version of mouse CD8 as marker gene. Viral titer was determined as infection units (ifu) by determining the number of transduced HEK293 cells after infections at different MOIs [17]. Adenoviral vectors were diluted in physiological solution and injected in hindlimb muscles of SCID mice (Charles River Laboratories, Sulzfeld, Germany) at a titer of $1x10^8$ ifu.

Pharmacological inhibition of Notch signaling

Notch signaling was inhibited pharmacologically in *vivo* by systemic treatment with DAPT (N-[N-(3,5-Difluorophenacetyl)-L-alanyl]-S-phenylglycine t-butyl ester, Alexis Bioscience). DAPT was dissolved in 10% ethanol and 90% corn oil. Mice were treated with 100 mg/kg DAPT by intra peritoneal injections, twice per day for 4 days.

Quantification of Dll4 protein levels in vivo

Dll4 quantification was performed using Imaris 7.1.0 software. Frozen sections were co-stained with antibodies against CD31 and Dll4, as described above. Complete 1024X1024, 16 bit images of vascular enlargements in the areas of effect were collected with 40X objective lens using LSM 780 (Zeiss). Quantification of Dll4 levels was performed using the "Surface" function on Imaris software to measure total pixel intensity of endothelial-specific Dll4 immunostaining. Regions of interest (ROIs) were generated in order to quantify Dll4 intensity only in enlarged vessels. Normalization was achieved through dividing the total intensity by the endothelial volume in each vascular structure.

4.3   Results

Synchronous Dll4 expression and Notch1 activation in contiguous endothelial cells during vessel enlargment

In order to investigate the activation of the Notch signaling pathway during intussusceptive angiogenesis, we took advantage of the myoblast-based controlled gene-delivery system we previously developed to over-express specific levels of $VEGF_{164}$ [1, 15]. We selected two clonal populations expressing low and high VEGF levels (V_{low}=60±2,5 ng/10^6 cells/day; V_{high} =150±3,12 ng/10^6 cells/day) that we previously found to induce therapeutic and aberrant angiogenesis respectively [1, 18]. Four days after cell implantation, we analyzed Dll4 expression and Notch1 activation by immunofluorescent staining. To unequivocally identify endothelial cell boundaries we co-stained for VE-Cadherin (CD144), a specific adhesion molecule located at the junctions between endothelial cells. As shown in Fog.1, we found that in the initial vascular enlargements induced by both VEGF doses (V_{low} and V_{high}), Dll4 was expressed simultaneously on long stretches of several contiguous endothelial cells, in which Notch1 was also activated at the same time. Remarkably, we could never detect an alternate pattern of Dll4 expression and Notch1 activation in the growing endothelial structures, as described during sprouting angiogenesis.
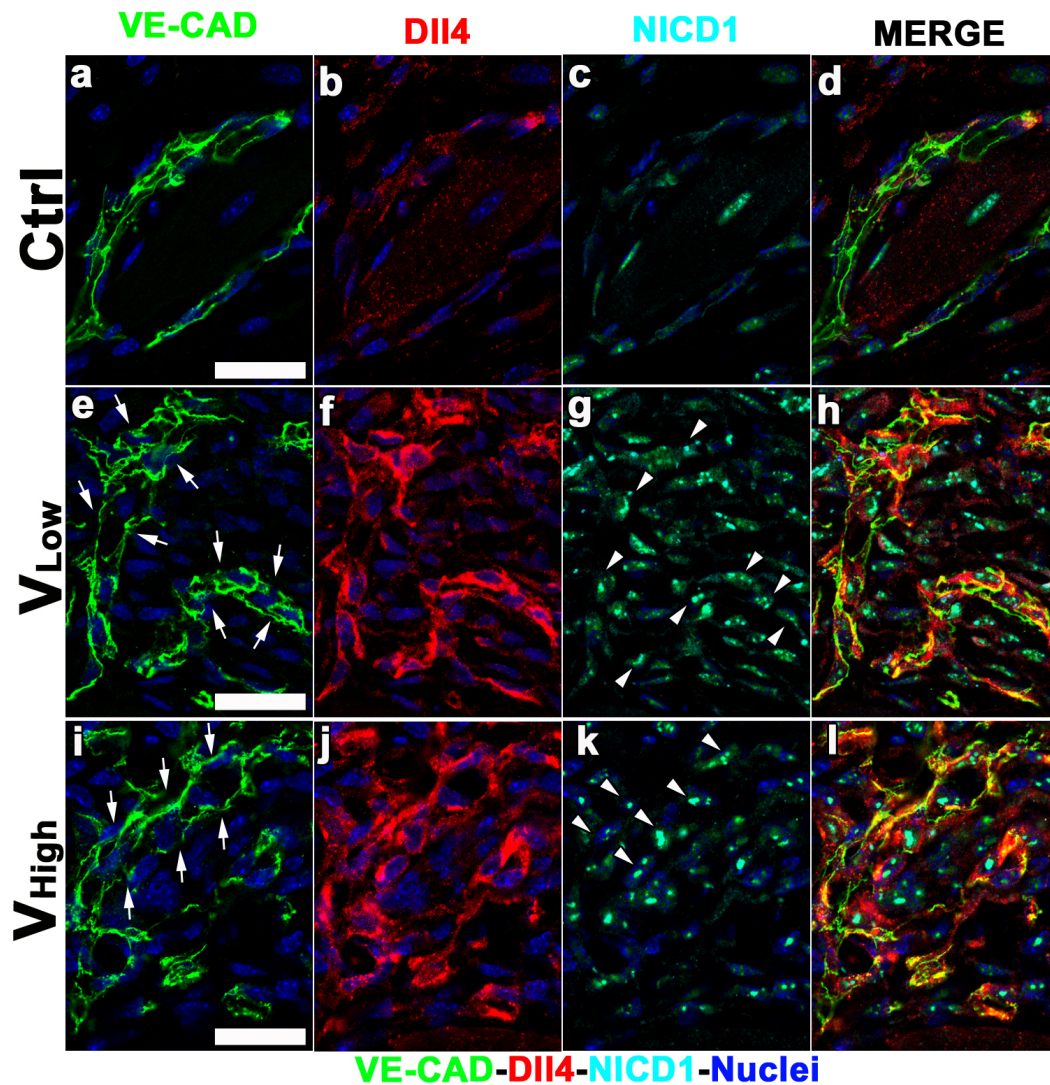
Figure 1. Dll4 expression and Notch1 activation during vascular enlargement. Vessels induced by implantation of V_{Low} and V_{High} myoblast clones were immunostained with antibodies against VE-CAD (endothelial cells, green), DLL4 (red), activated NOTCH1 (NICD1, cyan) and with DAPI (nuclei, blue) in cryosections of implanted muscles. **a-d** By 4 days, control cells did not induce any angiogenic effect. Dll4 expression and Notch1 activation were not detected. **e-l** On the other hand, both low and high VEGF levels caused vascular enlargements (arrows) which showed simultaneous Dll4 expression and Notch1 activation (arrowheads) in contiguous endothelial cells (V_{Low} and V_{High}, **h** and **l**). n = 3; size bars = 20 μm

Normal and aberrant vascular remodeling are independent of Dll4 expression and Notch1 activation.

As shown in Chapter 3, between 4 and 7 days after myoblasts implantation the initially enlarged vessels remodel to either normal capillaries or aberrant angiomas, depending on VEGF dose [19]. To investigate the expression pattern of Dll4 and activated Notch1 during vascular remodeling, V_{Low} and V_{High} myoblast clones and control cells were implanted. As expected, seven days after myoblasts implantation, into tibialis anterior and gastrocnemius muscles of SCID mice, low VEGF levels (V_{low}) induced normal capillaries, which were fully covered by $NG2^+$ pericytes (Fig.2c). However, no endothelial cell in the network of newly induced capillaries either expressed Dll4 or displayed activated Notch1 (Fig. 2d). On the other hand, high VEGF levels (V_{high}) gave rise to large angioma-like vascular structures covered by a thick layer of smooth muscle actin (SMA)-positive cells (Fig. 2e). Interestingly, also these aberrant structure did not show any Dll4 expression or Notch1 activation (Fig. 2f), suggesting that the remodeling to either normal or aberrant vessels after VEGF over-expression in skeletal muscle does not dependent on differential Dll4 expression and Notch1 activation.
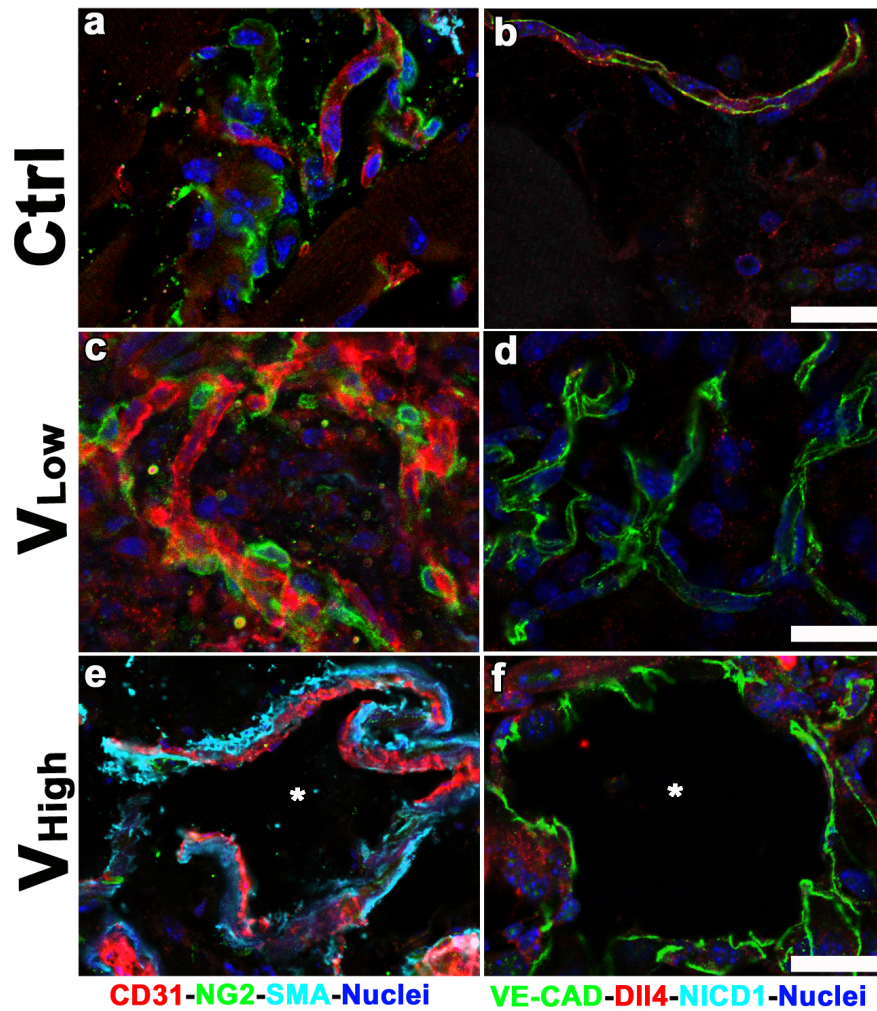
Figure 2. Intussusceptive remodeling is independent of Dll4 expression and Notch1 activation. Seven days after implantation, control cells did not induce any significant angiogenic effect (**a**) and neither Dll4 nor activated Notch1 were detected (**b**). Low VEGF levels remodelled into a network of normal capillaries, covered by pericytes (**c**) and no Dll4 or activated Notch1 were detected (**d**). High VEGF levels caused the growth of large angioma-like vascular structures (asterisks in **e** and **f**), which were covered by a thick layer of SMA+ cells (**e**) and also did not show any Dll4 expression or Notch 1 activation (**f**) n=3 in all groups; size bar = 20 µm in all panels.

Vessel enlargements are localized next to the exogenous VEGF source

In order to determine the spatial distribution of the observed angiogenic effects in relation to the VEGF source, the implanted myobalsts were tracked in tissue sections thanks to their expression of a truncated, syngenic version of CD8a, used as a cell surface marker linked to VEGF through an IRES sequence in the retroviral construct [15]. CD8 expression was specific for the transduced cells because the host SCID mice are completely deficient in B and T lymphocytes, and therefore have no endogenous CD8-positive cells. Four days after implantation, immunofluorescent staining for CD8 revealed myoblast engraftment in all conditions. As expected, no enlarged vascular structures were present in the control group. As shown in Fig.3, both V_{low} and V_{high} clones induced the enlargement of pre-existing vessels only in close proximity of the exogenous VEGF-expressing myoblasts. Again, the vascular enlargments, were composed of long stretches of contiguous endothelial cells in which Notch1 was synchronously activated. Furthermore, the immunostaining analysis revealed that Notch1 was also expressed and activated in the implanted myoblasts. This is in agreement with previous reports. In fact, Conboy and coworkers demonstrated that Notch signaling has an essential role for the regenerative potential of muscle fibers in aged muscle [20] and in particular, Notch1 activation regulates satellite cells proliferation upon injury [21].

VE-CAD-CD8-NICD1-Nuclei
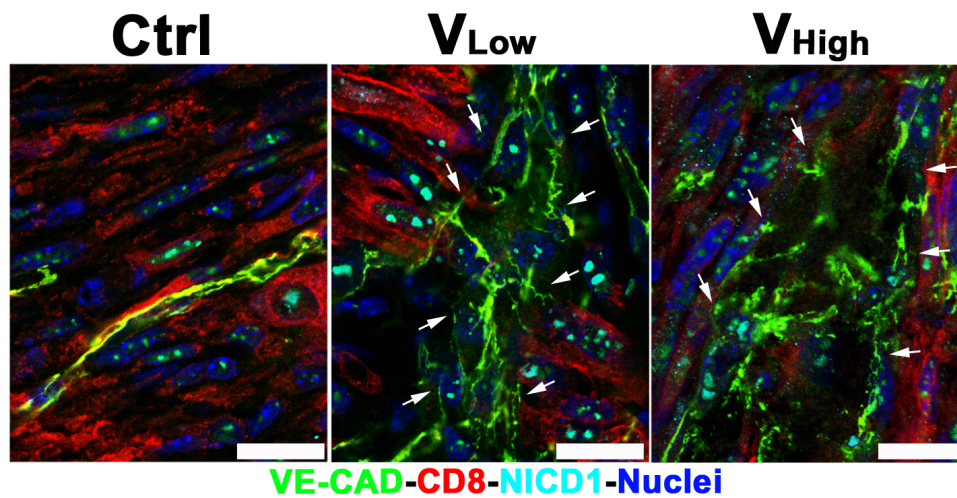
Figure 3. Angiogenic effects are localized in close proximity to the exogenous VEGF source. Arrows highlight markedly enlarged vessels (VE-cadherin) at the sites of VEGF over-expression, as illustrated by CD8 positive myoblasts (red). Both low and high VEGF levels (V_{Low} -V_{High}) showed synchronous Notch1 activation (cyan) in stretches of contiguous endothelial cells n=3; size bar = 20 μm in all panels.

VEGF-induced synchronous Notch1 activation is independent of cell-based delivery

Since myoblasts used to drive VEGF expression had activated Notch signaling and were in close contact with the induced vascular structures, we asked whether the observed pattern of Notch activation and vessel enlargement were a general property of VEGF over-expression or depended on the presence of myoblasts. To this end, VEGF was over-expressed with a cell-independent system, by direct injection of adenoviral vectors. VEGF-expressing adenoviruses (Ad.VEGF) were injected in tibialis anterior muscles of SCID mice and their angiogenic effect was evaluated four and seven days later. Control adenoviral vector expressing only CD8 (Ad.Ctrl) did not induce any angiogenic effect at either time-point, as shown by VE-Cadherin staining in Fig. 4. On the other hand, four

days after injection, VEGF-expressing adenovirus (Ad.VEGF) induced significant enlargement of pre-existing vessels, in which Dll4 and activated Notch1 were expressed simultaneously in stretches of contiguous endothelial cells. Also in this case, both Dll4 expression and Notch1 activation were lost upon remodeling by 7 days.
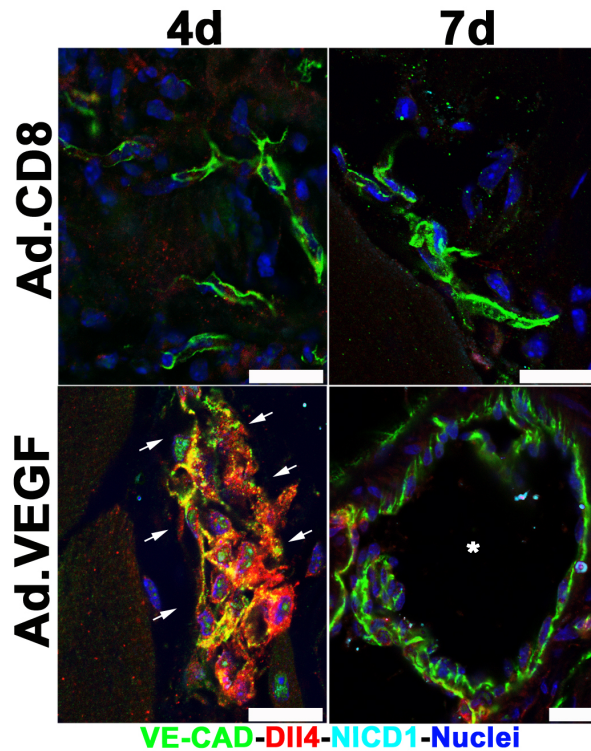
Figure 4. Angiogenic effects are specifically induced by VEGF expression. VEGF-expressing adenoviruses (Ad.VEGF) were injected in hindlimbs of SCID mice. Four days after injection, markedly enlarged vessels were detected, as highlighted by arrows. Seven days after injection, large angioma-like structures (star) were induced, which did not show any Dll4 expression and Notch1 activation (n=3 in all groups).

Notch inhibition disrupts vascular enlargements

In order to determine whether the observed pattern of Notch1 activation was the cause of VEGF-induced vascular enlargement, we performed similar experiments in presence of pharmacological inhibition of the Notch pathway by the systemic treatment

with the γ-secretase inhibitor, N-[N-(3,5-Difluorophenacetyl)-L-alanyl]-S-phenylglycine t-butyl ester (DAPT), which prevents cleavage of NICD and its translocation to the nucleus. V_{low} and V_{high} myoblast clones werw injected into tibialis anterior and gastrocnemius muscles of SCID mice and treatement with DAPT or vehicle was started 24 hours after myoblast implantation. Treatment was repeated twice per day until 3 hours before sacrificing the animals at day 4 to ensure sustained inhibition in consideration of the pharmacokinetics of the drug [22]. Immunofluorescent staining on criosections of treated muscles showed that, DAPT treatment prevented the vascular enlargement caused by both VEGF levels, which was visible in vehicle treated mice instead. As shown in Fig.5, Notch inhibition disrupted vessel enlargements and caused the formation of disorganized aggregates of endothelial cells in which no lumen was distinguishable. Remarkably, endothelial cells still expressed high levels of Dll4, whereas activated Notch1 was not detectable, confirming the effectiveness of the inhibitor treatement. In addition, we observed that in DAPT-treated mice, endothelial cells acquired a pronounced spindle and elongated shape compatible with the acquisition of a migratory phenotype (Fig. 6). Notch inhibition also caused a reduction in the number of NG2-positive pericytes and SMA-positive cells, which were almost absent around treated vessels at 4 days (Fig. 6). In conclusion, these findings suggest that Notch1 activation is essential for the initial vascular enlargement formation induced by VEGF over-expression.
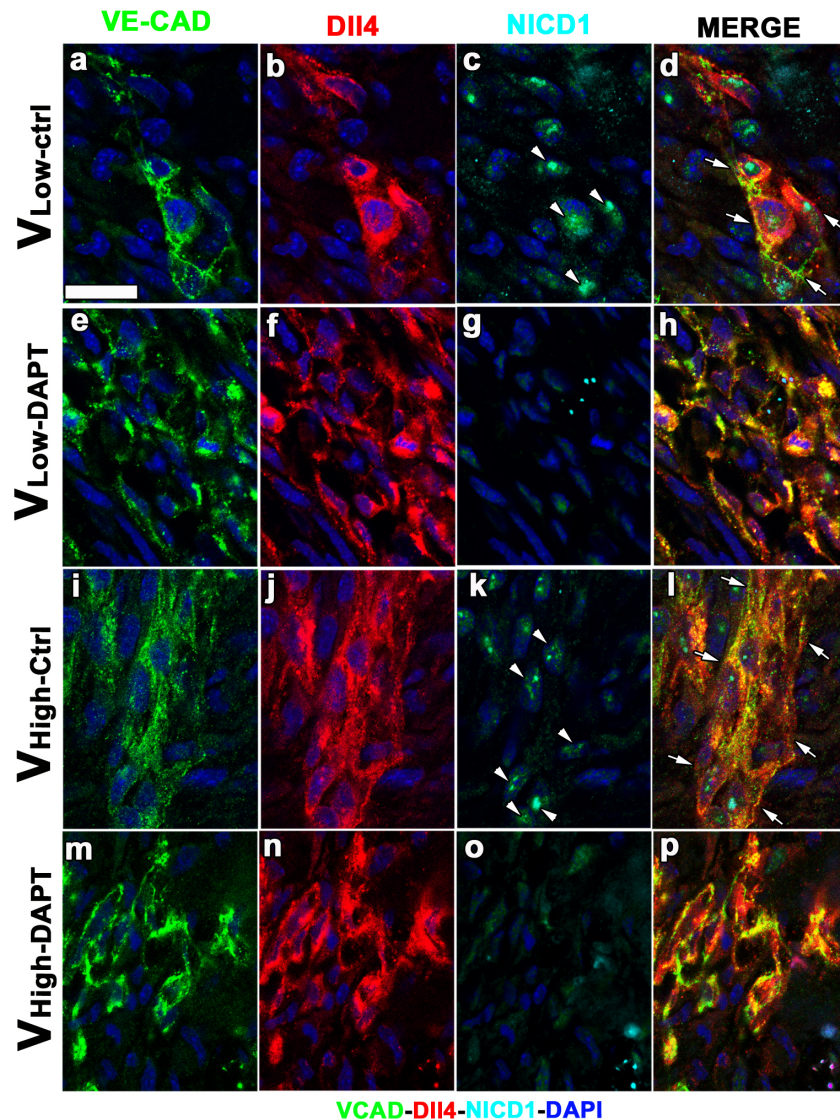
Figure 5. Inhibition of Notch signaling disrupts VEGF-induced vascular enlargement. Two clonal populations of transduced myoblasts, expressing either low or high VEGF levels, were implanted in hindlimbs of SCID mice and mice were treated with DAPT. Four days after implantation, in untreated muscles (V_{Low}-Ctrl and V_{High}-Ctrl), vessels enlargments showed Dll4 (red) expression on stretches of several contiguous endothelial cells (green), which had also activated Notch1 (cyan, arrowheads) (**a-d, i-l**). DAPT-treated muscles showed instead disorganized endothelial cells structures (arrows) but any Notch1 activation (arrowheads) both with low and high VEGF levels (**e-h, m-p**) n=3 in all groups; size bar = 20 μm in all panels.
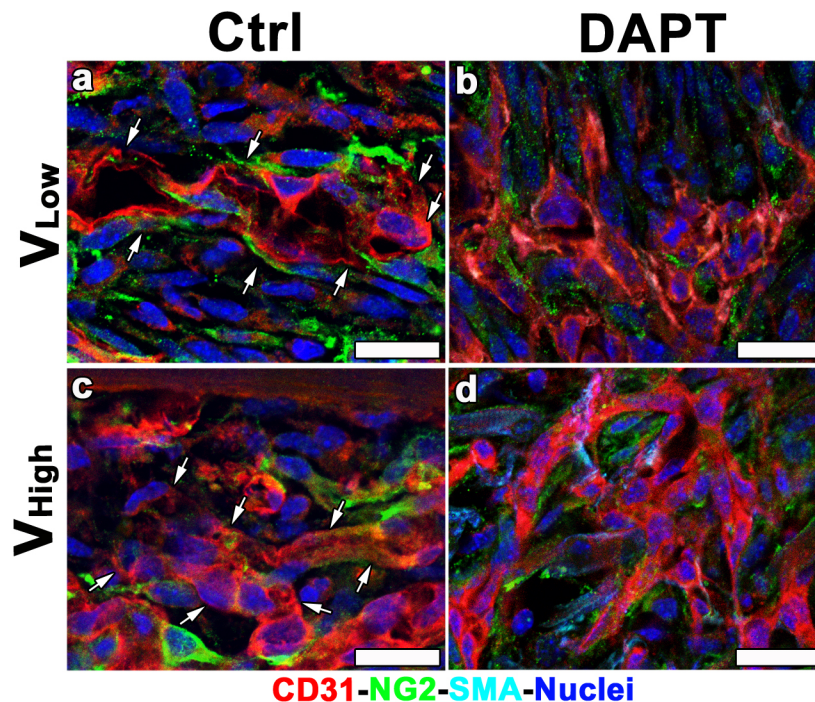
Figure 6. Inhibition of Notch signaling pathway impairs perivascular cells coverage. Transduced myoblasts, expressing either low or high VEGF levels, were implanted in hindlimbs of SCID mice that were then treated with DAPT. Four days after implantation, in untreated muscles (V_{Low}-Ctrl and V_{High}-Ctrl) (**a** and **c**), we observed vessels enlargments (arrows) associated with NG2-positive pericytes (green). DAPT-treated muscles showed instead disorganized endothelial structures (red) and very few pericytes (**b** and **d**). n=3 in all groups; size bar = 20 μm in all panels.

Notch inhibition affects vessels perfusion and functionality

To determine whether inhibition of Notch signaling could affect the functionality of VEGF-induced vessels, mice treated with DAPT or vehicle were injected intravenously with fluorescent tomato lectin, in order to stain all perfused vessels. Enlargements induced by both low and high VEGF levels were fully functional and perfused (Fig. 7a, c). In contrast, DAPT treatment impaired perfusion of the induced vascular structures, which were not connected to the circulation (Fig. 7b, d).
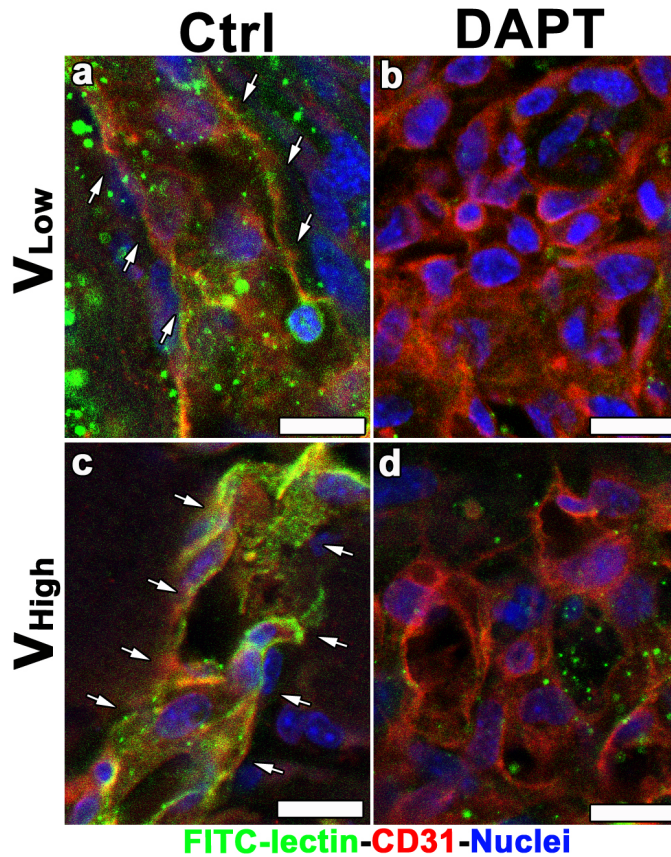
Figure 7. Notch inhibition impairs perfusion. Myoblasts, expressing either low or high VEGF levels, were implanted in hindlimbs of SCID mice. Animals were treated with DAPT and vehicle and after four days intravascular lectin staining was performed. In control muscles, at both VEGF doses, vessels enlargements were fully perfused (**a** and **c**). In DAPT treated muscles, disorganized endothelial structures were not perfused (**b** and **d**). n=3 in all groups; size bar = 20 μm in all panels.

Computational modeling of Notch signaling regulation in intussusceptive angiogenesis

To understand the molecular mechanism by which Notch signaling is regulated during intussusceptive angiogenesis, we complemented our experimental observations with a recently developed theoretical single-agent based computational model (ABM) [23]. ABMs simulate the behavior of the system that derives from the coordinated performance of

90

single cells ("agents"), which behave autonomously according to a set of "rules" derived from experimental findings. In this case, the presence or absence of VEGF gradients in our system was modulated in response to three different increasing VEGF concentrations. As shown in Fig. 8a, in the setting of Dll4/Notch1 lateral inhibition, described in Chapter 1, sufficiently low VEGF levels are predicted to lead to VEGF gradients in the microenvironment, the generation of a salt and pepper pattern of Notch1 activation, the selection of alternate tip and stalk cells and sprouting angiogenesis. In high VEGF concentrations, instead, the microenvironment become saturated, VEGF gradients are abolished and the model predicts an oscillation of patches of endothelial cells between synchronous all tip and all stalk states. On the other hand, it is known that activated Notch can also directly induce Dll4 expression in the same cell, as well as inhibiting it via VEGFR-2 down regulation [24]. This alternative process is called "lateral induction". As shown in Fig. 8b, in a setting of lateral induction the computational model predicts that, as the VEGF dose increases, so does the expression of Dll4 signaling, which causes increased Notch1 activation in the neighboring cells and a further increase in Dll4, which signals back to Notch1 in the first cell in a positive feedback mechanism. If Dll4 levels increase sufficiently by lateral induction, the model predicts that oscillations would be banished and that the system would instead stabilize with all cells in a high Dll4/high NICD state and inhibited from acquiring a tip cell phenotype. Lateral inhibition and lateral induction are taking place at the same time in all cells, but the system will globally behave according to one ot the other set of rules. The conditions under which either process prevails are unknown. Therefore, we set out to verify experimentally the testable

predictions made by the computational model in order to investigate the mechanism by which VEGF over-expression in skeletal muscle leads to intussusceptive angiogenesis.
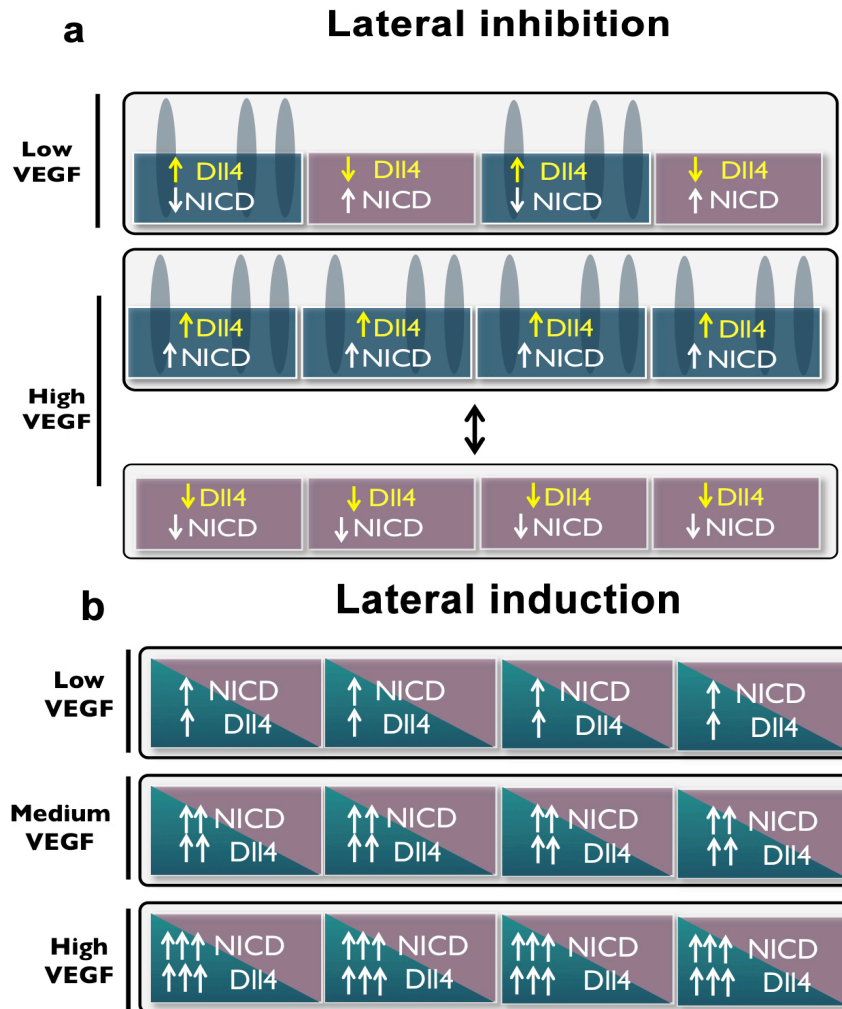
Figure 8. Computational predictions for Notch regulation in intussusceptive angiogenesis. Single-agent based computational modeling predicts in the first scenario of lateral inhibition, the generation of a salt and pepper pattern phenotype at low VEGF doses or synchronous oscillations between all tip and all stalk states at high VEGF doses (**a**). In a setting of lateral induction, the model predicts a dose-dependent increase in Dll4 expression and NICD in all cells at increasing VEGF levels, with stable expression of Dll4 in individual patches of endothelial cells within each VEGF dose (**b**).

Validation of computational predictions *in vivo*

Results described above and in Chapter 3 show that no filopodia-bearing endothelial cells can be identified in skeletal muscle vessels after VEGF over-expression and therefore the scenario that predicts the generation of a salt and pepper pattern of Notch1 activation and sprouting must be rejected. In the presence of high VEGF levels and the abolition of microenvironmental VEGF gradients, the model predicts the generation of endothelial cell patches synchronously displaying Dll4 expression and Notch1 activation both with lateral inhibition and lateral induction (Fig. 8). However, the key difference lies in the fact that these patches oscillate between low and high Dll4 expression in the first setting, while they are stable in the case of lateral induction. Therefore, to distinguish between the two scenarios, we performed quantification of Dll4 protein levels in endothelial patches *in vivo*. In fact, individual vascular structures in the injected muscle behave independently. Therefore, if Dll4 expression was oscillating in individual endothelial patches, quantification of Dll4 protein should reveal heterogeneous values in different vascular structures of each sample. On the other hand, if lateral induction was the prevailing process, homogeneous amounts would be expected in different vascular structures of each sample, while the absolute amount would be expected to increase with VEGF dose. Myoblasts clones expressing three different VEGF levels were injected into the hindlimbs of SCID mice (Low VEGF= 5 ng/10^6 cells/day; Medium VEGF=60 ng/10^6 cells/day; High VEGF= 120 ng/10^6 cells/day). Four days after injection, criosections of injected muscles were stained for Dll4 and PECAM. Z-stacks of the entire volume of single vessel enlargments showing Dll4 expression were captured maintaing the same acquisition settings for all samples analyzed. The amount of Dll4 protein was measured

by quantifying the staining intensity in individual endothelial patches and normalized by the endothelial volume of the structure, measured from the PECAM staining, to yield a value for Dll4 intensity/vascular structure. The results showed a VEGF dose-dependent upregulation of Dll4 protein levels, as expected. However, Dll4 intensity was remarkably homogeneous between individual enlarged vascular structures within each VEGF dose (Fig. 9). These findings suggest that Dll4 expression does not oscillate in individual endothelial patches and that therefore, synchronous and stable Notch1 activation in contiguous endothelial cells in intussusceptive angiogenesis, takes place by lateral induction. These results are currently being confirmed at the mRNA level by in situ hydridization (ISH).
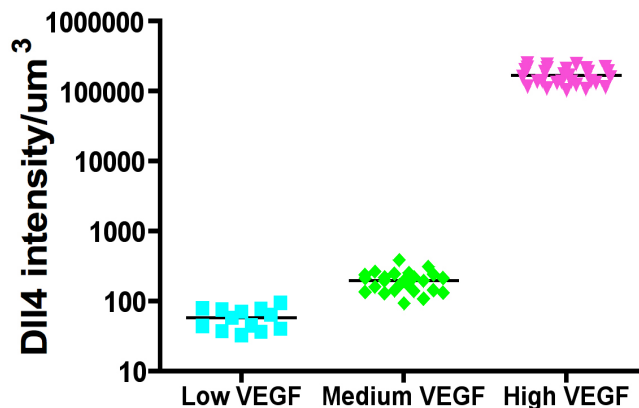
Figure 9. Quantification of Dll4 protein levels *in vivo*. Results show a dose-dependent upregulation of Dll4 protein levels at increasing VEGF doses and lack of oscillations of Dll4 expression within each VEGF dose.

4.4 Discussion

Sprouting angiogenesis is the best-known mechanism of vascular growth in adults. In the last decade, the molecular determinants of this process have been largely investigated in a variety of experimental models, such as tumors and in particular in the mouse retina. The Notch signaling pathway plays a fundamental role in sprouting angiogenesis because it tightly controls the endothelial specification in tip and stalk cells. We recently found that $VEGF_{164}$ over-expression at therapeutic doses in skeletal muscle does not induce angiogenesis by sprouting, but rather by a different mode of vascular growth, referred to as splitting angiogenesis or intussusception (as described in Chapter 3).

Here, taking advantage of the same highly controlled cell-based gene delivery platform previously used, we investigated how Notch signaling is regulated in intussusception. We found that Dll4 did not activate Notch1 according to the previously described "salt and pepper" pattern that regulates sprouting angiogenesis. Rather, 4 days after myoblast clone implantation, Notch1 was reciprocally activated in contiguous endothelial cells that simultaneously expressed also Dll4 in vascular enlargements both with low and high VEGF doses. Pharmacological inhibition showed that synchronous Notch1 activation in contiguous endothelial cells determines the initial morphogenic event of vascular enlargement rather than sprouting. Furthermore, the experimental validation of testable predictions generated by a computational model of Notch signaling in VEGF-stimulated endothelial cells suggests that Notch activation during intussusception is not regulated by the classical mechanism of lateral inhibition. During lateral inhibition, the first cell that responds to a VEGF gradient becomes a tip cell, upregulates Dll4 and activates Notch in the adjacent cell, which in turn is inhibited from becoming a tip cell and becomes a stalk

cell instead. In the stalk cell, activated Notch1 reduces VEGF responsiveness by down-regulating VEGFR-2 expression, which causes reduced activation of Dll4 promoter. Dll4 downregulation also avoids Notch activation in neighboring tip cells. Our findings instead suggest that during vessel enlargement and intussusception induced by VEGF over-expression, Notch activity is regulated by lateral induction. Lateral induction of Notch signaling has been documented in several physiological systems [25-28] and relies on the ability of activated NICD to directly promote Notch ligand expression in the same cell, thereby propagating the activating signal to adjacent ones [29]. More recently, Caolo and coworkers showed that VEGF-induced Dll4 up-regulation is Notch activation-dependent and is directly due to the ability of the Notch intracellular domain (NICD) to transactivate the Dll4 promoter [30]. Other studies showed that lateral induction controls the interaction between endothelium and mural cells by regulating the expression and activation of Jagged-1 and Notch3 [31, 32]. However, recent studies that investigated the regulation of Dll4/Notch signaling after ischemia, reported that spontaneous reparative angiogenesis after ischemia in skeletal muscle occurs by sprouting and is regulated by lateral inhibition [33]. On the other hand our results suggest that lateral induction is the mechanism by which Notch signaling induces vessel enlargement and intussusception after VEGF over-expression at therapeutic doses in skeletal muscle. A key parameter to consider in order to explain this apparent contradiction is VEGF dose. In fact, as already discussed in Chapter 3, the endogenous VEGF levels achieved in response to ischemia are much lower than even the lowest dose delivered by our cell-based platform, but such over-expression is necessary to achieve therapeutic efficacy [18]. If Notch activation can lead to both lateral inhibition and lateral induction, which mechanism prevails at

different VEGF doses? In order to address this open question, we would like to propose a possible model to help define future experiments. We speculate that a differential ability of activated NICD to start the two processes could provide a basis for the switch from prevailing inhibition to prevailing induction at increasing VEGF doses (Fig. 10).
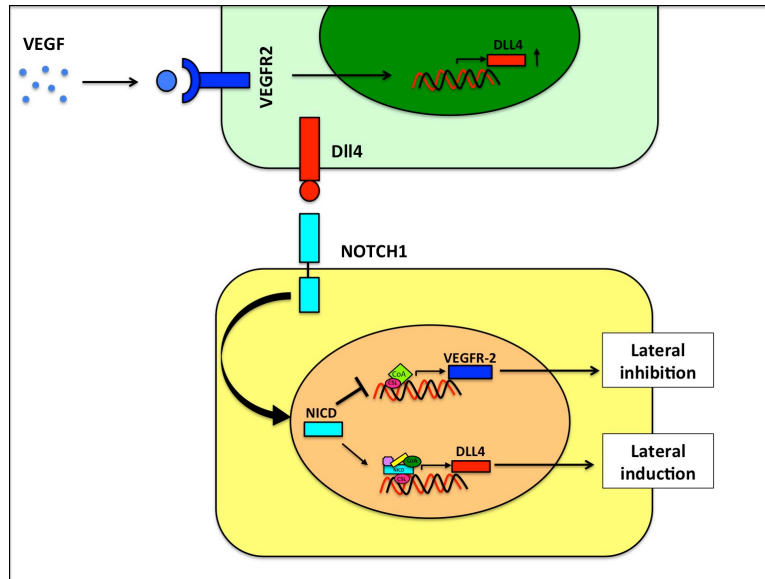
Figure 10. **Regulation of Notch signaling by lateral inhibition and lateral induction.**

In fact, if we postulate that maximal inhibition of VEGFR2 promoter activity by Notch is achieved already at low and moderate NICD levels that result from low Dll4 expression at low VEGF levels, while the direct activation of Dll4 expression by NICD requires higher levels of Notch activation achieved at higher VEGF levels, the following scenarios would result:

1) At low VEGF doses, low levels of Dll4 are induced by activation of VEGFR2, leading to moderate Notch1 activation and NICD translocation to the nucleus in the neighboring cell. If the postulates above hold true, this would cause efficient

repression of VEGFR2 expression and consequent downregulation of Dll4 expression, which would not be significantly compensated by the direct activation of Dll4 promoter by NICD. In this scenario, the net effect would be lateral inhibition of Dll4 expression leading to a salt-and-pepper pattern and selection of tip and stalk cells.

2) At high VEGF doses, in the other hand, high Dll4 expression causes robust NICD activation in the neighboring cells. As VEGFR2 repression was already maximal at low VEGF doses, no further loss of Dll4 stimulation would take place by this route, while the high level of NICD1 would now robustly activate Dll4 promoter. In this scenario, the net effect would be lateral induction of Dll4 expression, leading to simultaneous expression on neighboring cells, reciprocal Notch1 activation, abolition of tip cell formation and circumferential enlargement of vessels instead of sprouting.

Such postulated differential ability of NICD to repress VEGFR2 and activate Dll4 expression could directly derive from a different affinity of NICD for the binding to the respective promoters or can involve the recruitment of co-transcription factors that can differentially modulate the transcriptional activity. However, it is also conceivable that equal effects on the downregulation of VEGFR2 promoter activity and on the upregulation of Dll4 promoter activity may have disparate effects on the final Dll4 protein level. In fact, when VEGF activates VEGFR2, it triggers a kinase-mediated signalling cascade that causes the amplification of the transduced signal. As a consequence, even few activated molecules of VEGFR2 could be able to efficiently stimulate Dll4 promoter activity. Thus, in presence of low NICD levels, the downregulation of VEGFR2 promoter

activity would actually remove a large stimulus on Dll4 promoter. On the other hand, NICD stimulates Dll4 promoter directly with no amplification of the signal and therefore it may require higher doses to compensate efficiently the loss of VEGFR2 stimulation. It should be underlined that this model is speculative in nature and only provides a plausible scenario. The usefulness lies in the fact that it generates testable hypotheses. We would, therefore, propose to experimentally determine, by using biochemical assays, the relative strength and affinity of NICD binding to both VEGFR2 and Dll4 promoter at increasing VEGF doses in order to definitively elucidate the mechanism by which VEGF dose controls Notch signaling and the switch between intussusception and sprouting.

Bibliography

1.   Ozawa CR, Banfi A, Glazer NL, Thurston G, Springer ML, Kraft PE, McDonald DM, Blau HM. Microenvironmental vegf concentration, not total dose, determines a threshold between normal and aberrant angiogenesis. *The Journal of clinical investigation*. 2004;113:516-527

2.   Makanya AN, Hlushchuk R, Djonov VG. Intussusceptive angiogenesis and its role in vascular morphogenesis, patterning, and remodeling. *Angiogenesis*. 2009;12:113-123

3.   Gerhardt H, Golding M, Fruttiger M, Ruhrberg C, Lundkvist A, Abramsson A, Jeltsch M, Mitchell C, Alitalo K, Shima D, Betsholtz C. Vegf guides angiogenic sprouting utilizing endothelial tip cell filopodia. *J Cell Biol*. 2003;161:1163-1177

4.   Dejana E, Tournier-Lasserve E, Weinstein BM. The control of vascular integrity by endothelial cell junctions: Molecular basis and pathological implications. *Dev Cell*. 2009;16:209-221

5.   Suchting S, Freitas C, le Noble F, Benedito R, Breant C, Duarte A, Eichmann A. The notch ligand delta-like 4 negatively regulates endothelial tip cell formation and vessel branching. *Proceedings of the National Academy of Sciences of the United States of America*. 2007;104:3225-3230

6.   Hellstrom M, Phng LK, Hofmann JJ, Wallgard E, Coultas L, Lindblom P, Alva J, Nilsson AK, Karlsson L, Gaiano N, Yoon K, Rossant J, Iruela-Arispe ML, Kalen M, Gerhardt H, Betsholtz C. Dll4 signalling through notch1 regulates formation of tip cells during angiogenesis. *Nature*. 2007;445:776-780

7.   Leslie JD, Ariza-McNaughton L, Bermange AL, McAdow R, Johnson SL, Lewis J. Endothelial signalling by the notch ligand delta-like 4 restricts angiogenesis. *Development*. 2007;134:839-844

8.   Ridgway J, Zhang G, Wu Y, Stawicki S, Liang WC, Chanthery Y, Kowalski J, Watts RJ, Callahan C, Kasman I, Singh M, Chien M, Tan C, Hongo JA, de Sauvage F, Plowman G, Yan M. Inhibition of dll4 signalling inhibits tumour growth by deregulating angiogenesis. *Nature*. 2006;444:1083-1087

9.   Siekmann AF, Lawson ND. Notch signalling limits angiogenic cell behaviour in developing zebrafish arteries. *Nature*. 2007;445:781-784

10. Phng LK, Gerhardt H. Angiogenesis: A team effort coordinated by notch. *Dev Cell*. 2009;16:196-208

11. Jakobsson L, Franco CA, Bentley K, Collins RT, Ponsioen B, Aspalter IM, Rosewell I, Busse M, Thurston G, Medvinsky A, Schulte-Merker S, Gerhardt H. Endothelial cells dynamically compete for the tip cell position during angiogenic sprouting. *Nat Cell Biol*. 2010;12:943-953

12. Roca C, Adams RH. Regulation of vascular morphogenesis by notch signaling. *Genes Dev*. 2007;21:2511-2524

13. Hofmann JJ, Iruela-Arispe ML. Notch signaling in blood vessels: Who is talking to whom about what? *Circ Res*. 2007;100:1556-1568

14. Springer ML, Blau HM. High-efficiency retroviral infection of primary myoblasts. *Somat Cell Mol Genet*. 1997;23:203-209

15. Misteli H, Wolff T, Fuglistaler P, Gianni-Barrera R, Gurke L, Heberer M, Banfi A. High-throughput flow cytometry purification of transduced progenitors expressing defined levels of vascular endothelial growth factor induces controlled angiogenesis in vivo. *Stem Cells*. 2010;28:611-619

16. Rando TA, Pavlath GK, Blau HM. The fate of myoblasts following transplantation into mature muscle. *Exp Cell Res*. 1995;220:383-389

17. Gueret V, Negrete-Virgen JA, Lyddiatt A, Al-Rubeai M. Rapid titration of adenoviral infectivity by flow cytometry in batch culture of infected hek293 cells. *Cytotechnology*. 2002;38:87-97

18. von Degenfeld G, Banfi A, Springer ML, Wagner RA, Jacobi J, Ozawa CR, Merchant MJ, Cooke JP, Blau HM. Microenvironmental vegf distribution is critical for stable and functional vessel growth in ischemia. *FASEB journal : official publication of the Federation of American Societies for Experimental Biology*. 2006;20:2657-2659

19. Banfi A, von Degenfeld G, Gianni-Barrera R, Reginato S, Merchant MJ, McDonald DM, Blau HM. Therapeutic angiogenesis due to balanced single-vector delivery of vegf and pdgf-bb. *FASEB journal : official publication of the Federation of American Societies for Experimental Biology*. 2012;26:2486-2497

20. Conboy IM, Rando TA. The regulation of notch signaling controls satellite cell activation and cell fate determination in postnatal myogenesis. *Dev Cell*. 2002;3:397-409

21. Conboy IM, Conboy MJ, Smythe GM, Rando TA. Notch-mediated restoration of regenerative potential to aged muscle. *Science*. 2003;302:1575-1577

22. Dovey HF, John V, Anderson JP, Chen LZ, de Saint Andrieu P, Fang LY, Freedman SB, Folmer B, Goldbach E, Holsztynska EJ, Hu KL, Johnson-Wood KL, Kennedy SL, Kholodenko D, Knops JE, Latimer LH, Lee M, Liao Z, Lieberburg IM, Motter RN, Mutter LC, Nietz J, Quinn KP, Sacchi KL, Seubert PA, Shopp GM, Thorsett ED, Tung JS, Wu J, Yang S, Yin CT, Schenk DB, May PC, Altstiel LD, Bender MH, Boggs LN, Britton TC, Clemens JC, Czilli DL, Dieckman-McGinty DK, Droste JJ, Fuson KS, Gitter BD, Hyslop PA, Johnstone EM, Li WY, Little SP, Mabry TE, Miller FD, Audia JE. Functional gamma-secretase inhibitors reduce beta-amyloid peptide levels in brain. *J Neurochem*. 2001;76:173-181

23. Bentley K, Gerhardt H, Bates PA. Agent-based simulation of notch-mediated tip cell selection in angiogenic sprout initialisation. *Journal of theoretical biology*. 2008;250:25-36

24. Lewis J. Notch signalling and the control of cell fate choices in vertebrates. *Seminars in cell & developmental biology*. 1998;9:583-589

25. Eddison M, Le Roux I, Lewis J. Notch signaling in the development of the inner ear: Lessons from drosophila. *Proceedings of the National Academy of Sciences of the United States of America*. 2000;97:11692-11699

26. Hartman BH, Reh TA, Bermingham-McDonogh O. Notch signaling specifies prosensory domains via lateral induction in the developing mammalian inner ear. *Proceedings of the National Academy of Sciences of the United States of America*. 2010;107:15792-15797

27. Saravanamuthu SS, Gao CY, Zelenka PS. Notch signaling is required for lateral induction of jagged1 during fgf-induced lens fiber differentiation. *Developmental biology*. 2009;332:166-176

28. Daudet N, Lewis J. Two contrasting roles for notch activity in chick inner ear development: Specification of prosensory patches and lateral inhibition of hair-cell differentiation. *Development*. 2005;132:541-551

29. Ross DA, Kadesch T. Consequences of notch-mediated induction of jagged1. *Experimental cell research*. 2004;296:173-182

30. Caolo V, van den Akker NM, Verbruggen S, Donners MM, Swennen G, Schulten H, Waltenberger J, Post MJ, Molin DG. Feed-forward signaling by membrane-bound ligand receptor circuit: The case of notch delta-like 4 ligand in endothelial cells. *The Journal of biological chemistry*. 2010;285:40681-40689

31. Liu H, Kennard S, Lilly B. Notch3 expression is induced in mural cells through an autoregulatory loop that requires endothelial-expressed jagged1. *Circulation research*. 2009;104:466-475

32. Manderfield LJ, High FA, Engleka KA, Liu F, Li L, Rentschler S, Epstein JA. Notch activation of jagged1 contributes to the assembly of the arterial wall. *Circulation*. 2012;125:314-323

33. Al Haj Zen A, Oikawa A, Bazan-Peregrino M, Meloni M, Emanueli C, Madeddu P. Inhibition of delta-like-4-mediated signaling impairs reparative angiogenesis after ischemia. *Circulation research*. 2010;107:283-293

Chapter | 5

Dose-dependent angiogenesis by human VEGF$_{165}$ and mouse VEGF$_{164}$ is species-specific

5.1   Introduction

Coronary artery disease and peripheral vascular disease are a major cause of morbidity and mortality in Western societies despite current medical and surgical treatment [1]. Therapeutic angiogenesis aims at inducing new blood vessels by the delivery of vascular growth factors in order to increase the perfusion of tissue distal to a vascular occlusion and it is a promising strategy for the treatment of many patients for whom there is currently no effective surgical or medical treatment. Vascular endothelial growth factor-A (VEGF) is the master regulator of angiogenesis [2]. VEGF gene therapy with different vectors has been investigated in several clinical trials for both peripheral and coronary artery diseases. However, despite initial positive results, placebo controlled phase II studies have not shown clear clinical efficacy [3]. Retrospective analyses found that a crucial problem is the difficulty to achieve sufficient angiogenesis in the target tissue at safe vector doses, together with the apparently narrow therapeutic window of VEGF in vivo. [3-5] It has been shown that the uncontrolled delivery of VEGF by a variety of methods leads to progressive vascular proliferation and eventually the growth of angioma-like vascular tumors [6-10]. VEGF remains tightly localized in the extracellular matrix [11]. Therefore, heterogeneous levels in tissue do not average with each other and even a low frequency of high VEGF-expressing cells is sufficient to induce aberrant angiogenesis [12]. We have previously found that the induction of normal or aberrant angiogenesis by mouse $VEGF_{164}$ depends strictly on the amount produced in the microenvironment around each producing cell and not on the total dose, so that normal, functional and stable angiogenesis can be reliably induced over a wider range of levels if a homogeneous

distribution can be achieved in the tissue [12, 13]. However, nothing is known about the dose-dependent effects of human VEGF, which is the actual agent used in clinical approaches for therapeutic angiogenesis, since the delivery of different titers of gene therapy vectors only influences the total dose, but cannot uncover the effects of specific microenvironmental expression levels.

Therefore, here we aimed at rigorously determining the in vivo dose-dependent effects of human $VEGF_{165}$ in the therapeutic target tissue, i.e. skeletal muscle. We took advantage of a highly controlled platform for VEGF expression in mouse muscle, based on clonal populations of transduced myoblasts homogeneously producing specific levels of either mouse $VEGF_{164}$ [12, 13] or human $VEGF_{165}$. By comparing the dose-dependent effects of human VEGF over-expression to those of the syngenic murine factor, we further sought to establish whether its safety profile can be reliably determined in the mouse, which is a convenient and widely used preclinical model.

5.2   Materials and methods

Vector Construction

A construct carrying a truncated version of the mouse CD8a gene and the mouse VEGF$_{164}$ gene joined by an IRES sequence was generated. For mouse CD8 the truncated version Lyt-2 , or Lyt-2.2 (trCD8a), occurs naturally by alternative splicing [14] spanning codons 1-222 and it includes the signal peptide, the full extracellular, and transmembrane regions, whereas the cytoplasmic region is truncated after the first two amino acids (221-222). The full retroviral construct (mV) was generated by cloning the cDNAs encoding mouse VEGF$_{164}$ and mouse trCD8a upstream and downstream of an encephalomyocarditis virus internal ribosomal entry sequence (IRES). The control construct (mCD8) contained the IRES and mouse trCD8a sequences but no sequence for VEGF.

Correspondingly, a similarly truncated version of the human CD8 gene was generated by PCR from the full-length transcript (a kind gift by Dan Littman) and the corresponding constructs containing the genes for human human VEGF$_{165}$, IRES and trCD8a (hV) and the control construct containing IRES and human trCD8a but no VEGF (hCD8) were cloned.

Cell Culture

Primary myoblasts isolated from C57BL/6 mice and transduced to express the β-galactosidase marker gene (lacZ) from a retroviral promoter [15] were further transduced at high efficiency with the 4 retroviral constructs described above for 4 rounds of infection as previously described [16]. Early passage myoblast clones homogeneously expressing specific levels of VEGF were isolated by randomly sorting single cells in 96-

wells, using a FACS Vantage SE cell sorter (Becton Dickinson, Basel, Switzerland). Cells were cultured in 5% CO_2 on dishes coated with bovine skin collagen 1 (Sigma-Aldrich Chemie GmbH, Steinheim, Germany), with a growth medium consisting of 40% F10, 40% low-glucose DMEM (Sigma-Aldrich) and 20% fetal bovine serum (HyClone, Logan, UT, USA) supplemented with 2.5 ng/ml of basic fibroblast growth factor (FGF-2) (Becton Dickinson, Bedford, MA 01730, USA), as previously described [17].

CD8 Detection by FACS

Expression of human trCD8a and mouse trCD8a was assessed by staining transduced myoblasts with specific APC-conjugated antibodies under experimentally determined optimal conditions. The mouse anti-human CD8 (clone 3B5; Caltag Laboratories Inc, Burlingame, USA) was used at 0.5μg of antibody/10^6 cells, at a dilution of 1:50. The rat anti-mouse CD8 (clone 53-6.7; Becton Dickinson) was used at 0.8μg of antibody/10^6 cells, at a dilution of 1:50. Data were acquired with a FACSCalibur flow cytometer (Becton Dickinson) and analyzed using FlowJo software (Tree Star, Ashland, Oregon).

Human and Mouse VEGF measurement by ELISA

The production of VEGF in cell culture supernatants was quantified using species-specific VEGF immunoassay ELISA kits (R&D Systems Europe, Abingdon, UK). One ml of fresh medium was incubated on myoblasts cultured in a 60 mm dish for four hours, then filtered and analyzed in duplicate. Results were normalized by the number of cells and expressed as ng of VEGF per 10^6 cells per day. At least four separate dishes of cells were assayed for each clone.

Myoblast Injection into SCID Mice

For the evaluation of angiogenesis in vivo, cells were implanted into 6-8 week-old immunodeficient SCID CB.17 mice (Charles River Laboratories, Sulzfeld, Germany) in order to avoid an immunological response to myoblasts expressing xenogenic proteins. Animals were treated in accordance with Swiss Federal guidelines for animal welfare and the study protocol was approved by the Veterinary Office of the Canton of Basel-Stadt (Basel, Switzerland). Myoblasts were dissociated in trypsin and resuspended in PBS with 0.5% BSA. 5×10^5 myoblasts in 5 μl were implanted into the posterior auricular muscle, midway up the dorsal aspect of the external ear or transcutaneously into the tibialis anterior muscle of the hind limb, using a syringe with a $29^1/_2$G needle.

Tissue Staining

In order to visualize the entire vascular network of the ear, we performed intravascular staining with a biotinylated *Lycopersicon esculentum* (tomato) lectin (Vector Laboratories, Burlingame, California) which binds the luminal surface of all blood vessels as previously described [12]. Briefly, 4 weeks after myoblast implantation, mice were anesthetized and lectin was injected intravenously through the femoral vein. Four minutes later the thoracic cavity was opened and the tissues were fixed by perfusing the animal with 1% paraformaldehyde and 0.5% glutaraldehyde in PBS, pH 7.4 at 120 mmHg of pressure via a cannula in the left ventricle. Ears were then removed, bisected in the plane of the cartilage, and stained with X-gal staining buffer (1 mg/ml 5-bromo-4-chloro-3-indoyl-b-D-galactoside, 5 mM potassium ferrocyanide, 0.02% Nonidet P-40, 0.01% sodium deoxycholate, 1mM $MgCl_2$, in PBS, pH 7.4). Lectin-coated vessels were stained

using avidin-biotin complex-diaminobenzidine histochemistry (Vector Laboratories), dehydrated through an ethanol series from 50% to 98%, cleared with toluene (Fisher Scientific, Wohlen, Switzerland) and whole-mounted on glass slides with Permount embedding medium (Fisher Scientific, Wohlen, Switzerland). To obtain limb muscle sections, animals were anesthetized and tissues were fixed by perfusion of 1% paraformaldehyde in PBS, pH 7.4 via a cannula in the left ventricle. The tibialis anterior muscle was harvested in one piece, embedded in OCT compound (Sakura Finetek, Torrance, California), cryoprotected in 10% sucrose overnight, frozen in freezing isopentane and cryosectioned. Tissue sections were then stained with X-gal (20 μm sections) or with H&E (10 μm sections) as described previously [15]. The 10 μm sections were immunostained as previously described [12]. The following primary antibodies and dilutions were used: rat monoclonal anti-mouse CD31 (clone MEC 13.3; BD Biosciences) at 1:100; mouse monoclonal anti-mouse α-smooth muscle actin (α-SMA) (clone 1A4; MP Biomedicals, Irvine, CA, http://www.mpbio.com) at 1:400; rabbit polyclonal anti-NG2 (Chemicon, Temecula, CA, http://www.chemicon.com) at 1:200. Fluorescently labeled secondary antibodies (Invitrogen, Basel, Switzerland) were used at a concentration of 1:200.

Vessel Measurements

Regions of myoblast engraftment were determined by identifying β-galactosidase positive muscle fibers on whole-mounted ears. Images were taken on an Olympus BX61 microscope. Vessel length density (VLD) was measured by manually tracing the total vessel length in 3-6 fields of vision per ear and dividing it by the area of the field of vision

and expressed in mm /mm². Image analysis was performed with the AnalySIS D software (Soft Imaging System Gmbh, Münster, Germany).

VEGF Protein, Genomic DNA and total RNA Assay in Muscle Tissue

Whole fresh mouse muscles were disrupted using a Qiagen Tissue Lyser (Qiagen) in 500μl of PBS+ 1% Triton X-100, supplemented with Complete Protease Inhibitor Cocktail (Roche), which was non-denaturing for proteins and did not lyse nuclei. After centrifugation, 200μl aliquots of the lysates were used for protein quantification and ELISA analysis. The remaining supernatant (on average 250 μl) was used to extract total RNA with the allPrep DNA/RNA/protein Mini kit (Qiagen), after supplementation with the denaturing buffer provided by the manufacturer. The pellet containing the whole nuclei was then disrupted and homogenized in the same lysis buffer using the Qiagen Tissue Lyser. Genomic DNA was extracted using the same kit following the manufacturer's instructions.

Quantitative Real Time-PCR

Total RNA was reverse-transcribed into cDNA with the Omniscript Reverse Transcription kit (Qiagen) at 37 °C for 60 minutes. Quantitative Real-Time PCR (qRT-PCR) was performed on an ABI 7300 Real-Time PCR system (Applied Biosystems). In order to quantify both the human $VEGF_{165}$ and mouse $VEGF_{164}$ transcripts and to compare their expression, a unique set of primers and probe sequences was designed with Primer Express software 3.0 (Applied Biosystems), based on a common sequence expressed by both the human and mouse VEGF retroviral constructs:

Exo V-forward: 5'-GCTCTCCTCAAGCGTATTCAACA;

Exo V-reverse: 5'-CCCCAGATCAGATCCCATACA;

Exo V-probe: 5'-FAM-CTGAAGGATGCCCAGAAGGTACCCCA-TAMRA.

Furthermore to detect the mouse VEGF$_{164}$ transcripts expressed from the endogenous gene, an additional set of specific primers and probe sequences were designed with Primer Express software 3.0 (Applied Biosystems):

Endo V-forward: 5'-GACGGGCCTCCGAAACC;

Endo V-reverse: 5'-TGGTGGAGGTACAGCAGTAAAGC;

Endo V-probe, 5'-FAM-AACTTTCTGCTCTCTTGGGTGCACTGGAC-TAMRA.

The cycling parameters were: 50°C for 2 minutes, followed by 95°C for 10 minutes and 40 cycles of denaturation at 95°C for 15 seconds and annealing/extension at 60°C for 1 minute. All primers were used at 400nM, the Exo V probe at 400nM and the Endo V-probe at 100nM. Reactions were performed in triplicate for each template, averaged, and normalized to expression of the 18S housekeeping gene (Applied Biosystem assay, Hs99999901_s1).

qRT-PCR was also performed on genomic DNA in order to quantify the number of myoblasts engrafted after implantation, by measuring the amount of stably integrated LacZ retroviral construct. A reference curve was constructed for each of the different myoblast clonal populations with a 10-fold dilution series between 1 and 10^6 cells, by using which the ΔCt data of each sample could be transformed into the corresponding absolute cell numbers. LacZ primer and probe sequences and reaction concentrations were previously published [18].

In vitro assay of endothelial cell activation

Human umbilical vein endothelial cells (HUVEC) were used between passage 3 and 5 and cultured as described previously [19]. Mouse aortic endothelial cells (MAEC) were obtained from E. Battegay (University Hospital of Zurich, Switzerland) and cultured in DMEM high glucose (Sigma-Aldrich) supplemented with 10% FBS (HyClone), 1mM sodium pyruvate (Gibco, Invitrogen), 0.1mM MEM Non Essential Amino Acids (Gibco, Invitrogen), 2mM glutamine (Gibco, Invitrogen), 100U/ml penicillin and 100 μg/ml streptomycin (Gibco, Invitrogen).

HUVEC were seeded into gelatin-coated six-well cell culture plates at 4×10^5 cells/well and grown to confluency for three days without further medium change. MAEC were seeded into six-well cell culture plates at 1.5×10^5 cells/well and grown to confluency. Then cells were serum starved and induced by the addition of 50 ng/ml human VEGF-A$_{165}$ or mouse VEGF-A$_{164}$ (R&D System) for 6 hours. Total RNA was extracted using RNeasy kit (Qiagen) and reverse-transcribed into cDNA with the Omniscript Reverse Transcription kit (Qiagen) according to the manufacturer's instructions. Quantitative real time PCR (qRT-PCR) was performed on an ABI 7300 Real-Time PCR system (Applied Biosystems). As internal standard, 18S gene expression level was used for normalisation (TaqMan Gene Expression Assay, Hs99999901_s1, Applied Biosystem). Vascular Cellular Adhesion Molecule (VCAM1) expression upon VEGF-A stimulation was measured using customized gene expression assays (TaqMan Gene Expression Assay, Hs01003372_m1 and Mm01320970_m1, Applied Biosystem).

Statistical analyses

Data are presented as means ± standard error of the mean. The significance of differences was evaluated using one-way analysis of variance (ANOVA), applying the Bonferroni correction for multiple comparisons. P value < 0.05 was considered statistically significant.

5.3   Results

Generation of mouse and human VEGF-expressing myoblasts

Primary mouse myoblasts, which already expressed LacZ from a different retroviral construct [15] were transduced with retroviruses expressing either mouse VEGF$_{164}$ (mV) or human VEGF$_{165}$ (hV) genes, linked to a truncated version of mouse or human CD8, respectively, as a marker to determine transduction efficiency by FACS [20, 21] (Fig. 1a). Negative control myoblasts expressed mCD8 or hCD8, but no VEGF. The CD8 in the retroviral constructs served Transduction efficiency was greater than 95% in all cases (Fig. 1b). The average VEGF expression, measured by ELISA, was 78.2±2.6 ng/10^6 cells/day and 82.4±5.4 ng/10^6 cells/day for the mV and hV populations, respectively.

In *vivo* angiogenesis by heterogeneous mouse or human VEGF levels

The primary transduced hV and mV populations were composed of cells expressing heterogeneous VEGF levels, depending on the number and genomic location of integrated vector copies. Four weeks after implantation into auricular muscles of SCID mice (n=8 per cell type), neither mCD8 nor hCD8 control cells affected the capillary networks around transduced fibers. On the other hand, mV myoblasts caused the growth of large numbers of aberrant, bulbous vascular structures, as previously described. Surprisingly, expression of similarly high and heterogeneous levels of human VEGF$_{165}$ by hV myoblasts induced a robust increase in the density of homogeneous normal capillaries around transgenic fibers, but no instances of aberrant vascular structures could be detected in any of the implanted tissues (Fig. 1c).
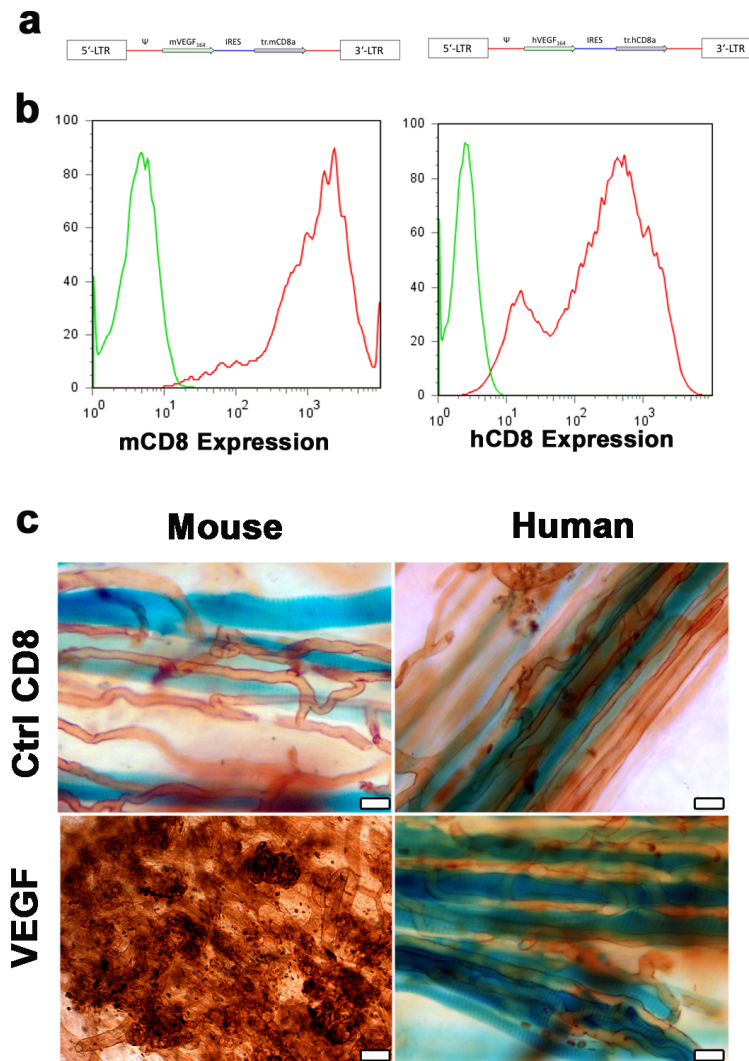
Figure 1. Heterogeneous expression of human VEGF$_{165}$ induces only normal angiogenesis. a Maps of the bicistronic retroviral vectors (pAMFG-VICD8) carrying the coding sequence of murine VEGF (mVEGF$_{164}$) or human VEGF (hVEGF$_{165}$) and of a truncated version of murine or human CD8a (tr.CD8a) linked through an IRES. **b** Heterogeneous and high levels of CD8a expression in the polyclonal populations of retrovirally transduced VICD8 myoblasts (red curve) were detected by flow cytometry and compared to non-transduced cells (negative control, green curve). **c** Whole-mount lectin staining (brown) of blood vessels 4 weeks after implantation of CD8 cells (Ctrl CD8) and VICD8 myoblasts expressing heterogeneous levels of murine or human VEGF (Poly VEGF) (n=5-8 for all groups). Myoblasts engraftment was revealed by X-Gal staining (blue). Heterogeneous murine VEGF levels caused the growth of aberrant structures whereas heterogeneous human VEGF levels induced only normal capillaries. Size bar = 50 μm in all panels.

**Distribution of VEGF expression levels in the hV and mV populations**

In order to determine why the heterogeneous hV population did not induce any aberrant angiogenesis, we asked whether the distribution of human VEGF expression levels by individual cells in the population might be different and possibly skewed towards lower values than that of the mouse VEGF myoblasts. Therefore, single cells were isolated to obtain clonal populations and their human VEGF production was measured and compared to that of mouse VEGF by similarly isolated mV clones, previously generated [20]. Twenty-one hV clones were randomly isolated by single cell FACS-sorting and found to secrete a wide range of $hVEGF_{165}$ levels (5.4 ± 0.9 to 254 ± 39 ng/10^6 cells/day). This range was similar to that of $mVEGF_{164}$ production by 15 mV clones (0.8 ± 0.1 to 142.55 ± 10 ng/10^6 cells/day). Analysis of the distribution of VEGF levels showed that both mV and hV populations secreted similarly spread levels over a wide range (Fig. 2).
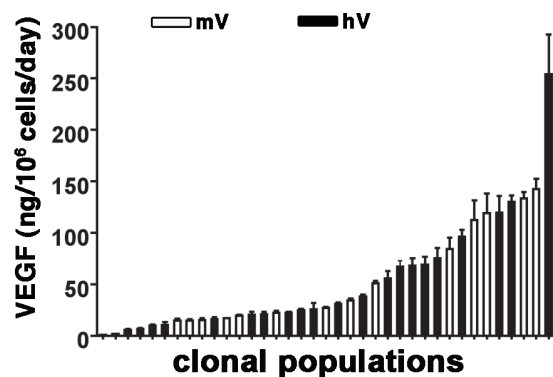
Figure 2. Distribution of VEGF levels in clonal populations of myoblasts expressing murine or human VEGF. Single myoblasts clones expressing either mouse or human VEGF were isolated from the polyclonal populations and their VEGF expression in vitro was quantified by ELISA showing that both populations had a similar distribution of VEGF expression levels in individual cells. White bars = murine VEGF (mV) expressing myoblasts, black bars = human VEGF (hV) expressing myoblasts.

116

Microenvironmental dose-dependent angiogenesis by mouse and human VEGF

To rigorously compare the dose-dependent effects of human $VEGF_{165}$ and mouse $VEGF_{164}$, hV and mV clones secreting matched VEGF levels were selected and injected into the ear and leg muscles of SCID mice. As shown in Fig. 3a, clones were chosen that produced either low or high mouse $VEGF_{164}$ levels, known to induce normal or aberrant angiogenesis, respectively (mV_{low} = 40.5±4 ng/10^6 cells/day and mV_{high} = 133.6±13.4 ng/10^6 cells/day). Matching hV clones produced similar and also higher levels of human $VEGF_{165}$ (hV_{low} = 32.2±2.8 ng/10^6 cells/day, hV_{high1} = 129.9±7.5 ng/10^6 cells/day and hV_{high2} = 253.7±44.8 ng/10^6 cells/day).
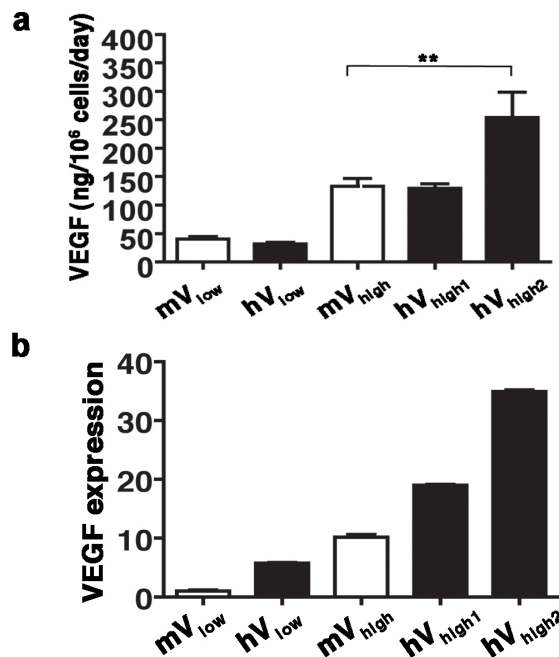
Figure 3. Human and murine VEGF production by selected clones. Five clones were selected: two clones expressing either mouse (mV_{low}) or human (hV_{low}) low VEGF levels and three clones expressing either mouse (mV_{high}) or human (hV_{high1}, hV_{high2}) high VEGF levels. In vitro VEGF expression was measured by ELISA **(a)** and further confirmed by qRT-PCR **(b)**. **P<0.01 for selected comparisons.

The quantification of the amount of secreted human and murine VEGF protein by ELISA requires the use of distinct species-specific antibody pairs, which may affect the precise comparison of VEGF production between the two families of clones. Therefore, the relative expression levels of all selected clones were independently quantified by qRT-PCR (n=4 per construct). A specific primer set was designed to recognize a viral construct-specific sequence, which is identical in the human and mouse expression cassettes, ensuring that results were comparable between all transduced populations. As shown in Fig. 3b, these results confirmed that in all cases the hV clones expressed similar or higher VEGF levels that the corresponding mV clones.

As shown in Fig.4a, four weeks after implantation in ear muscles, low levels of both human and mouse VEGF induced robust angiogenesis, comprising only homogeneous, normal capillaries. High mouse $VEGF_{164}$ expression gave rise to abundant aberrant vascular structures, as expected. However, a similarly high level of $hVEGF_{165}$ (clone hV_{high1}) induced only normal angiogensis. Remarkably, even the hV_{high2} clone, which secreted double the amount of human $VEGF_{165}$, did not induce any aberrant structures, but only normal and homogeneous capillary networks.

The amount of angiogenesis induced in the different conditions was quantified by measuring the vessel length density (VLD) in the cell implantation areas (n=4-7/group). As shown in Fig. 4b, low levels of both mouse and human VEGF caused a similarly large increase in VLD compared to control cells (106 ± 4 and 104 ± 5 mm/mm^2, respectively, compared to 38 ± 2 and 31 ± 6 mm/mm^2 with mCD8 and hCD8 cells; p<0.001). VLD in areas implanted with the mV_{high} clone was not significantly increased compared to control areas (38 ± 2 mm/mm^2), as normal capillary networks were replaced by large aberrant

vascular structures, which show heterogeneously dilated diameters, but do not contribute an appreciable increase in vessel length. However, the normal capillary networks induced by both clones expressing high levels of human VEGF$_{165}$ significantly increased VLD compared to control cells (79±6 mm/mm^2 and 120±2 mm/mm^2 respectively; p<0.001), to an extent similar to that induced by low VEGF levels.
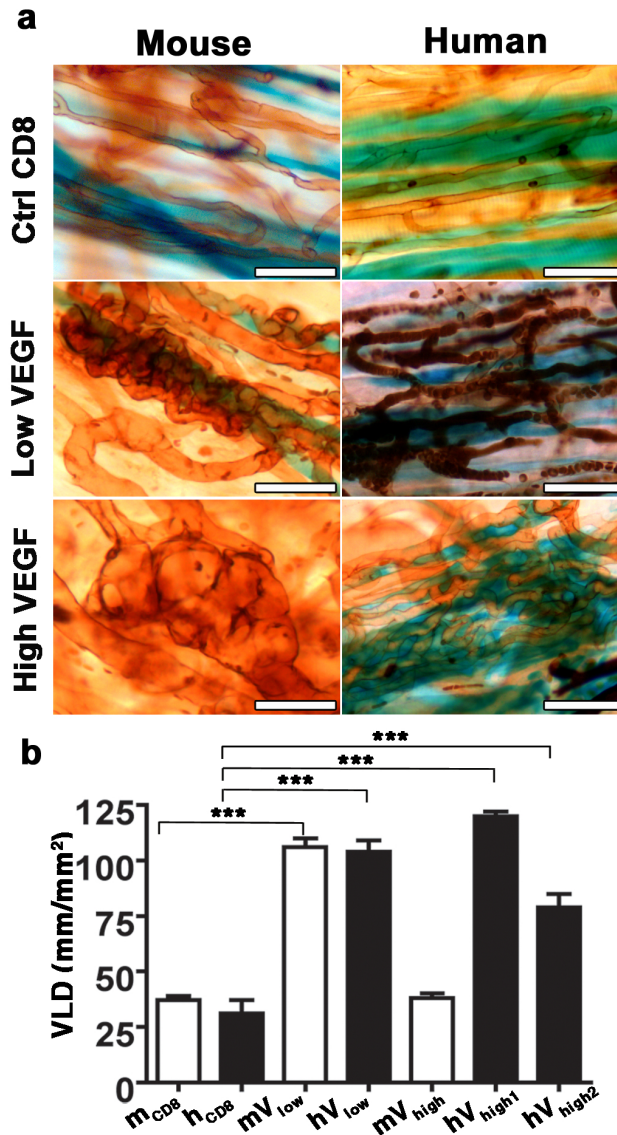
Figure 4. Human VEGF$_{165}$ induces only normal angiogenesis despite high levels of expression. a Whole mount lectin staining of control cells and mV and hV clonal populations. Low murine and human VEGF levels induced normal capillaries. High murine VEGF levels gave rise to aberrant bulbous vascular structures, but even higher human VEGF levels induced instead only normal angiogenesis (n=5-8 for all groups). Size bar = 50 μm in all panels. **b** Vessel length density quantification of induced angiogenesis by selected clones. ***P<0.001 for selected comparisons

Vascular maturation

The ear contains a thin muscle in a subcutaneous environment, which is amenable to whole-mount analyses and provides a convenient location to study in detail the 3-dimensional structure of induced vascular networks. However, as the target of therapeutic approaches are the leg muscles, we analyzed the morphology and maturation of vascular networks induced by specific levels of human and mouse VEGF also in the tibialis anterior muscles of SCID mice. As shown in Fig.5, four weeks after injection (n=4/group), low levels of both mouse and human VEGF caused an increased density of normal pericyte-covered capillaries around the transduced myofibers, compared to muscles implanted with control cells, while high levels of mouse VEGF induced aberrant angioma-like structures, devoid of pericytes and covered with a thick smooth muscle layer. However, in agreement with the results obtained in the ear muscles, expression of similar or even higher levels of human VEGF$_{165}$ only induced normal pericyte-covered capillary networks and no aberrant vascular structures.
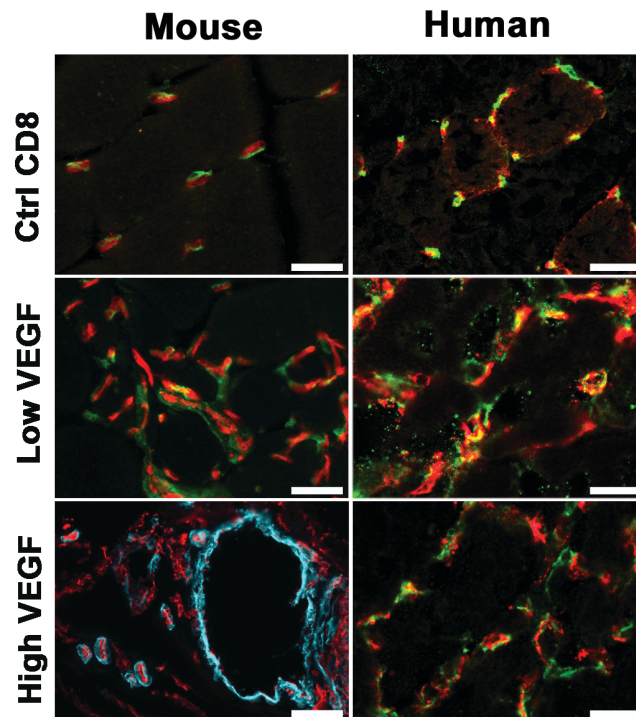
Figure 5. High human VEGF$_{165}$ levels induce normal and mature capillaries rather than angiomas. Immunofluorescent staining of vascular structures 4 weeks after implantation of control cells or mV and hV clones expressing low and high VEGF levels. Endothelium is stained in red (CD31), perycites in green (NG2) and smooth muscle cells in cyan (SMA). Mouse and human low VEGF levels induced normal perycite-covered capillaries. High mouse VEGF levels caused the growth of aberrant angioma-like vascular structures, covered by a thick layer of SMA$^+$ cells, while even higher human VEGF levels gave rise only to normal perycite-covered capillaries . Size bar = 50 µm in all panels.

In vivo kinetics of VEGF expression

In order to conclusively determine whether human and mouse VEGF had different dose-dependent effects, we sought to verify the possibility that the expression of human VEGF by the hV$_{high}$ clones could decrease more rapidly than that of mouse VEGF by the mV$_{high}$ clone after implantation in vivo, leading to a lower effective VEGF production in the tissue. Therefore, VEGF protein and mRNA levels were determined immediately after

injection of mV_{high}, hV_{high1} and hV_{high2} clones in tibialis anterior muscles, as well as at 7 and 14 days later (n=4 per each group and time-point). As expected, VEGF production dropped significantly in all cases during the first 7 days after implantation (Fig. 6), as about 90% of the myoblasts do not engraft and the retroviral promoter is downregulated. However, both protein and mRNA measurements confirmed that in vivo expression of human $VEGF_{165}$ was similar or higher than that of mouse $VEGF_{164}$ at all time-points (Fig. 6). The expression of endogenous VEGF was determined by qRT-PCR using specific primers spanning the 5'-UTR sequence, which is absent in the retroviral cassette, and it did not show any significant changes between groups at all time-points (data not shown).
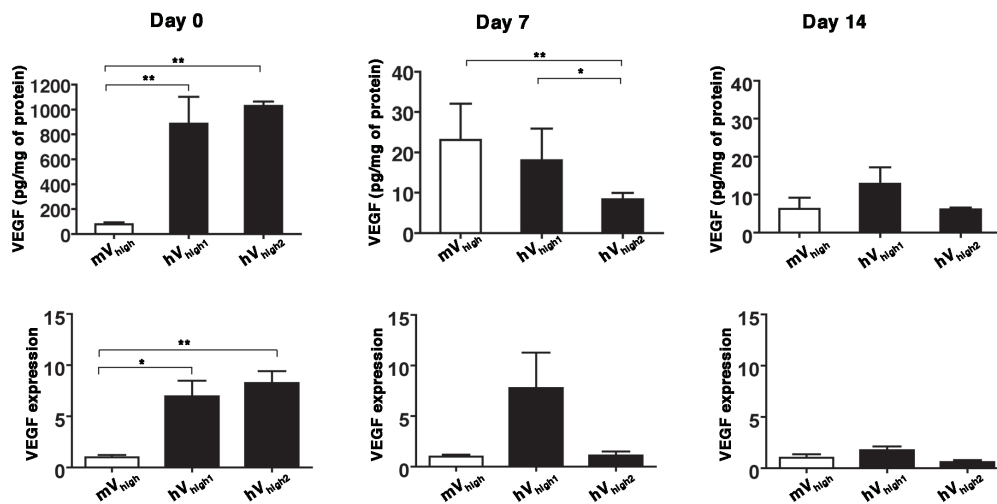
Figure 6. Human $VEGF_{165}$ expression persists at similar or higher levels than that of mouse VEGF over 2 weeks in vivo. In vivo expression by mV and hV clones was quantified immediately after cell injection (Day 0), after 1 (Day 7) or 2 weeks (Day 14) both by ELISA and qRT-PCR, confirming that expression of hV clones was similar or even higher than the corresponding mV clones up to 2 weeks after implantation. [*]P<0.05 for selected comparisons.

Species-specific VEGF-Induced Endothelial Cell Activation

Finally we asked whether human and mouse VEGF had an intrinsically different angiogenic potential or were instead less efficient than the syngenic factor in signaling through their receptor in mouse and human endothelial cells, respectively. Therefore, mouse aortic endothelial cells (MAEC) and human umbilical vascular endothelial cells (HUVEC) were stimulated with 50 ng/ml of either mouse $VEGF_{164}$ or human $VEFG_{165}$ and the relative signaling activation was assessed by measuring the induced expression of its target gene Vascular Cell Adhesion Molecule-1 (VCAM-1) [22]. As shown in Fig. 7, mouse VEGF was significantly more efficient than human VEGF in driving VCAM-1 expression in mouse endothelial cells, but human VEGF was more efficient on human endothelial cells, suggesting that human VEGF may display different dose-dependent effects in a mouse model due to a lower efficacy in activating signal transduction in mouse endothelial cells compared to mouse VEGF.
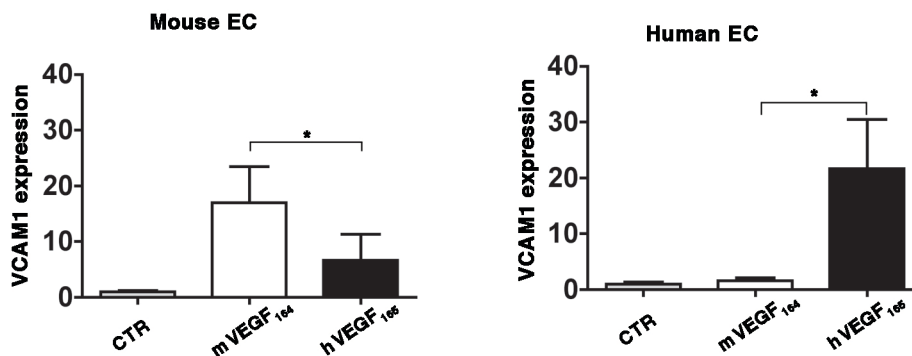
Figure 7. VEGF potency in activating mouse and human endothelial cells is species-specific. The induction of expression of the VEGF-A target gene VCAM1 was measured by qRT-PCR in human and murine endothelial cells after stimulation with recombinant murine and human VEGF (50 ng/ml), showing that the potency of VEGF is always higher on syngenic cells. *P<0.05 for selected comparisons.

5.4   Discussion

By taking advantage of a highly controlled cell-based platform for expression of specific VEGF levels in skeletal muscle, we could rigorously compare the dose-dependent effects of human and mouse $VEGF_{165/164}$ in a widely employed murine preclinical model. Although human $VEGF_{165}$ was similarly effective to mouse $VEGF_{164}$ in inducing normal angiogenesis at low doses, it differed dramatically from the syngenic factor in the potential to cause the growth of aberrant angioma-like vascular structures at higher doses. In fact, while clones expressing more than about 100 ng/10^6 cells/day of $mVEGF_{164}$ invariably caused the appearance of angiomas by 4 weeks, even 250 ng/10^6 cells/day of $hVEGF_{165}$ induced only the growth of physiological capillary networks. However, this is unlikely to reflect a fundamental biological difference between the human and murine factors, but rather may be the consequence of a lower potency of human $VEGF_{165}$ to stimulate the mouse VEGF receptors and vice versa, as suggested by our results in Fig. 7.

There are no studies directly comparing the species-specific effects of human and syngenic VEGF in preclinical animal models. Angioma formation has been reported extensively after $mVEGF_{164}$ expression in different murine tissues, such as skeletal and cardiac muscle, skin and fat [7, 9, 12, 23], in agreement with our results. On the other hand, the induction of angiomas by over-expression of $hVEGF_{165}$ has been described only rarely. There are no reports of $hVEGF_{165}$-induced angiomas in mouse tissues, while one study [8] described the appearance of angiomas in the heart of rats after injection of a high dose of a $hVEGF_{165}$ plasmid (500 μg DNA) in a single intramyocardial injection, probably leading to a very localized hotspot of expression. Rabbit $VEGF_{165}$ shares a greater degree of homology with the human sequence (14 aa difference) compared with mouse $mVEGF_{164}$

(19 aa difference). In the skeletal muscle of rabbits, delivery of a single high dose of hVEGF$_{165}$-AAV vectors (10^{11} particles) caused aberrant vascular growth, the formation of functional arterio-venous shunts and muscle fibrosis, but only after at least 6 months of sustained expression [24] [25]. One dose-escalation study investigated the effects of delivering from 10^9 to 10^{11} AV viral particles to rabbit skeletal muscle and found dose-dependent differences both in vessel morphology and functional improvement [26]. However, the short duration of expression afforded by the immune clearance of AV vectors prevented the evaluation of angioma formation. In human clinical trials, only one study reported the transient appearance of spider angiomas at a site downstream of the treated tissue after delivery of hVEGF$_{165}$ plasmid [27].

It is apparent that hVEGF$_{165}$ is capable of inducing angioma growth also in animal models if expressed at a sufficiently high level and a prolonged time. Therefore, our findings can in no way be taken as evidence that a tight control of VEGF levels would not be required in a clinical application with hVEGF$_{165}$ and have clear implications for the pre-clinical evaluation of VEGF-based strategies to treat ischemic conditions.

It has been recognized that the complexity of growth factor dosing may be pivotal for the lack of efficacy in VEGF gene therapy clinical trials [28] and it has been advocated that preclinical development of vectors should include the routine analysis of "STED" parameters: 1) Spread through the tissue; 2) Transfection efficiency; 3) Expression strength; and 4) Duration of expression [29]. Within this framework, our data suggest that, in a preclinical animal model, parameter "E" will depend not only on the amount of factor produced, but also on the species-specific potency of the human protein in that animal model. Therefore, the results of preclinical dose-escalation studies of the human factor in

animal models should be interpreted with caution, as species-specific differences may involve dose differences even of large magnitude.

In conclusion, our data suggest that only dose-finding Phase I clinical studies can accurately determine the safety profile of VEGF gene therapy approaches. In this respect, it would be advantageous to employ a tool that allows the controlled delivery of increasing doses, while also ensuring a homogeneous distribution of expression levels in vivo, in order to avoid hotspots and exploit the therapeutic window of VEGF [30]. We recently developed such a tool for cell-based VEGF gene delivery, whereby high-throughput FACS-purification of transduced progenitors allows the rapid generation of populations homogeneously expressing a pre-defined VEGF level [20, 21].

Bibliography

1.   Norgren L, Hiatt WR, Dormandy JA, Nehler MR, Harris KA, Fowkes FG, Bell K, Caporusso J, Durand-Zaleski I, Komori K, Lammer J, Liapis C, Novo S, Razavi M, Robbs J, Schaper N, Shigematsu H, Sapoval M, White C, White J, Clement D, Creager M, Jaff M, Mohler E, 3rd, Rutherford RB, Sheehan P, Sillesen H, Rosenfield K. Inter-society consensus for the management of peripheral arterial disease (tasc ii). *European journal of vascular and endovascular surgery : the official journal of the European Society for Vascular Surgery*. 2007;33 Suppl 1:S1-75

2.   Carmeliet P. Angiogenesis in health and disease. *Nature medicine*. 2003;9:653-660

3.   Gupta R, Tongers J, Losordo DW. Human studies of angiogenic gene therapy. *Circ Res*. 2009;105:724-736

4.   Yla-Herttuala S, Markkanen JE, Rissanen TT. Gene therapy for ischemic cardiovascular diseases: Some lessons learned from the first clinical trials. *Trends Cardiovasc Med*. 2004;14:295-300

5.   Karvinen H, Yla-Herttuala S. New aspects in vascular gene therapy. *Curr Opin Pharmacol*. 2010;10:208-211

6.   Carmeliet P. Vegf gene therapy: Stimulating angiogenesis or angioma-genesis? *Nature medicine*. 2000;6:1102-1103

7.   Lee RJ, Springer ML, Blanco-Bose WE, Shaw R, Ursell PC, Blau HM. Vegf gene delivery to myocardium: Deleterious effects of unregulated expression. *Circulation*. 2000;102:898-901

8.   Schwarz ER, Speakman MT, Patterson M, Hale SS, Isner JM, Kedes LH, Kloner RA. Evaluation of the effects of intramyocardial injection of DNA expressing vascular endothelial growth factor (vegf) in a myocardial infarction model in the rat--angiogenesis and angioma formation. *Journal of the American College of Cardiology*. 2000;35:1323-1330

9.   Springer ML, Chen AS, Kraft PE, Bednarski M, Blau HM. Vegf gene delivery to muscle: Potential role for vasculogenesis in adults. *Molecular cell*. 1998;2:549-558

10.   Pettersson A, Nagy JA, Brown LF, Sundberg C, Morgan E, Jungles S, Carter R, Krieger JE, Manseau EJ, Harvey VS, Eckelhoefer IA, Feng D, Dvorak AM, Mulligan RC, Dvorak HF. Heterogeneity of the angiogenic response induced in different normal adult tissues by vascular permeability factor/vascular endothelial growth factor. *Lab Invest*. 2000;80:99-115

11.   Park JE, Keller GA, Ferrara N. The vascular endothelial growth factor (vegf) isoforms: Differential deposition into the subepithelial extracellular matrix and bioactivity of extracellular matrix-bound vegf. *Mol Biol Cell*. 1993;4:1317-1326

12.   Ozawa CR, Banfi A, Glazer NL, Thurston G, Springer ML, Kraft PE, McDonald DM, Blau HM. Microenvironmental vegf concentration, not total dose, determines a threshold between normal and aberrant angiogenesis. *The Journal of clinical investigation*. 2004;113:516-527

13.   von Degenfeld G, Banfi A, Springer ML, Wagner RA, Jacobi J, Ozawa CR, Merchant MJ, Cooke JP, Blau HM. Microenvironmental vegf distribution is critical for stable and functional vessel growth in ischemia. *Faseb J*. 2006;20:2657-2659

14. Tagawa M, Nakauchi H, Herzenberg LA, Nolan GP. Formal proof that different-size lyt-2 polypeptides arise from differential splicing and post-transcriptional regulation. *Proc Natl Acad Sci U S A*. 1986;83:3422-3426

15. Rando TA, Blau HM. Primary mouse myoblast purification, characterization, and transplantation for cell-mediated gene therapy. *J Cell Biol*. 1994;125:1275-1287

16. Springer ML, Blau HM. High-efficiency retroviral infection of primary myoblasts. *Somat Cell Mol Genet*. 1997;23:203-209

17. Banfi A, Springer ML, Blau HM. Myoblast-mediated gene transfer for therapeutic angiogenesis. *Methods Enzymol*. 2002;346:145-157

18. Banfi A, von Degenfeld G, Gianni-Barrera R, Reginato S, Merchant MJ, McDonald DM, Blau HM. Therapeutic angiogenesis due to balanced single-vector delivery of vegf and pdgf-bb. *FASEB journal : official publication of the Federation of American Societies for Experimental Biology*. 2012;26:2486-2497

19. Witzenbichler B, Maisonpierre PC, Jones P, Yancopoulos GD, Isner JM. Chemotactic properties of angiopoietin-1 and -2, ligands for the endothelial-specific receptor tyrosine kinase tie2. *J Biol Chem*. 1998;273:18514-18521

20. Misteli H, Wolff T, Fuglistaler P, Gianni-Barrera R, Gurke L, Heberer M, Banfi A. High-throughput flow cytometry purification of transduced progenitors expressing defined levels of vascular endothelial growth factor induces controlled angiogenesis in vivo. *Stem Cells*. 2010;28:611-619

21. Wolff T, Mujagic E, Gianni-Barrera R, Fueglistaler P, Helmrich U, Misteli H, Gurke L, Heberer M, Banfi A. Facs-purified myoblasts producing controlled vegf levels induce safe and stable angiogenesis in chronic hind limb ischemia. *J Cell Mol Med*. 2011

22. Schweighofer B, Testori J, Sturtzel C, Sattler S, Mayer H, Wagner O, Bilban M, Hofer E. The vegf-induced transcriptional response comprises gene clusters at the crossroad of angiogenesis and inflammation. *Thromb Haemost*. 2009;102:544-554

23. Pettersson A, Nagy JA, Brown LF, Sundberg C, Morgan E, Jungles S, Carter R, Krieger JE, Manseau EJ, Harvey VS, Eckelhoefer IA, Feng D, Dvorak AM, Mulligan RC, Dvorak HF. Heterogeneity of the angiogenic response induced in different normal adult tissues by vascular permeability factor/vascular endothelial growth factor. *Laboratory investigation; a journal of technical methods and pathology*. 2000;80:99-115

24. Zacchigna S, Tasciotti E, Kusmic C, Arsic N, Sorace O, Marini C, Marzullo P, Pardini S, Petroni D, Pattarini L, Moimas S, Giacca M, Sambuceti G. In vivo imaging shows abnormal function of vascular endothelial growth factor-induced vasculature. *Human gene therapy*. 2007;18:515-524

25. Karvinen H, Pasanen E, Rissanen TT, Korpisalo P, Vahakangas E, Jazwa A, Giacca M, Yla-Herttuala S. Long-term vegf-a expression promotes aberrant angiogenesis and fibrosis in skeletal muscle. *Gene therapy*. 2011;18:1166-1172

26. Korpisalo P, Hytonen JP, Laitinen JT, Laidinen S, Parviainen H, Karvinen H, Siponen J, Marjomaki V, Vajanto I, Rissanen TT, Yla-Herttuala S. Capillary enlargement, not sprouting angiogenesis, determines beneficial therapeutic effects and side effects of angiogenic gene therapy. *European heart journal*. 2011;32:1664-1672

27.   Isner JM, Pieczek A, Schainfeld R, Blair R, Haley L, Asahara T, Rosenfield K, Razvi S, Walsh K, Symes JF. Clinical evidence of angiogenesis after arterial gene transfer of phvegf165 in patient with ischaemic limb. *Lancet*. 1996;348:370-374

28.   Yla-Herttuala S, Markkanen JE, Rissanen TT. Gene therapy for ischemic cardiovascular diseases: Some lessons learned from the first clinical trials. *Trends in cardiovascular medicine*. 2004;14:295-300

29.   Yla-Herttuala S. An update on angiogenic gene therapy: Vascular endothelial growth factor and other directions. *Current opinion in molecular therapeutics*. 2006;8:295-300

30.   Banfi A, von Degenfeld G, Blau HM. Critical role of microenvironmental factors in angiogenesis. *Current atherosclerosis reports*. 2005;7:227-234

Chapter | 6

Retroviruses versus Lentiviruses: the transition towards a clinical application for therapeutic angiogenesis

6.1 Introduction

Ischemic cardiovascular diseases are the most common cause of death in the Western world and, despite advances in medical and surgical therapy, their morbidity and mortality remain very high. Restoring blood supply by the delivery of growth factors (i.e.VEGF) by means of viral vectors is an attractive approach for patients with advanced coronary or peripheral artery disease that are not amenable to other treatment options.

We have previously found that, in order to achieve therapeutic vascular growth, the mode of VEGF expression *in vivo* should satisfy two requirements: 1) the dose must be controlled at the microenvironmental level, i.e. all transduced cells should express homogeneous levels in the therapeutic range, since VEGF binds to the matrix and hotspots do not diffuse, leading to angioma growth [1,2]; 2) expression should be sustained for about 4 weeks, in order for new vessels to stabilize and persist indefinitely [1,3,4] . Both these requirements can be achieved with the use of stably transduced progenitors, such as skeletal myoblasts, FACS-purifies to generate populations that homogeneously express a desired VEGF dose [5,6].

Retroviral vectors (RVs) have been extensively used to stably introduce therapeutic genes in different progenitor classes and tested in several clinical trials. Although successful in the treatment of different genetic diseases of the immune system, the use of retroviruses with hematopoietic stem cells led to clonal transformation of some transduced cells and the generation of leukemias in a proportion of the treated patients, due to insertional mutagenesis and activation of endogenous oncogenes by the strong retroviral LTR promoter. Although neoplasias only developed in transduced hematopoietic stem cells [7], but not in other progenitor classes [8], regulatory bodies in

132

Europe and the US are currently greatly restricting the use of retroviral vectors for clinical applications.

To overcome these safety concerns, new therapeutic strategies with transduced progenitors have been developed using self-inactivating lentiviral vectors (LVs), which possess a much lower oncogenic potential than retroviral vectors [9]. Furthermore, recent reports show that a cellular enhancer-promoter, such as that of Elongation Factor-1α (EF1α), can greatly reduce the genotoxic potential of integrating vectors [10]. Therefore, a significant protection against insertional mutagenesis can be achieved by combining the use of self-inactivating lentiviral vectors with that of a cellular enhancer-promoter such as EF1α.

In order to translate the myoblast-mediated gene transfer system we developed the last decade towards a clinically compliant platform for cell-based controlled VEGF$_{165}$ expression, we investigated the use of self-inactivating lentivectors. However, as integration sites and internal promoter differ dramatically between RV and LV, we asked whether and how the use of a different viral vector could modify the angiogenic effects of engineered cells. Therefore, we generated a library of LV-transduced clonal myoblast populations over-expressing specific doses of hVEGF$_{165}$ and compared them to similar populations transduced with RV, described in Chapter 5.

6.2   Materials and methods

Lentiviral vector cloning, transfection and lentivirus purification

A lentiviral vector expressing human $VEGF_{165}$ was generated as follows: pAMFG-hVICD8 and pAMFG-hICD8 (described in Chapter 5) retroviral vectors were digested with Xba and EcoRI restriction enzymes to extract the expression cassettes hVICD8 (human VEGF-IRES-truncated human CD8) and hICD8 (IRES-truncated human CD8). The recipient lentiviral vector pCDH-EF1a-MCS (CD502A-1, System Biosciences, CA) was digested with Xba and EcoRI and linked to the previously excised fragments to generate the final pCDH-EF1a-hVICD8 lentivector and the control vector pCDH-EF1a-hICD8. HEK 293TN cells (LV900A-1, System Biosciences, CA) were cultured in the presence of 0.01mM cholesterol and transfected using a $CaPO_4$-based protocol [11] with a mixture of the 3 plasmids pCDH-EF1a-hVICD8 or pCDH-EF1a-hICD8 (25.2 ug), pMDLg/pRRE (18.8 ug, Addgene plasmid 12251), pMD2.G (8.86 ug, Addgene plasmid 12259) and pRSV-Rev (6.3 ug, Addgene plasmid 12253). Viral supernatant was harvested 36-48 hours after transfection, purified and concentrated by ultracentrifugation.

Cell culture and lentiviral transduction protocol

Primary myoblasts isolated from C57BL/6 mice and transduced to express the β-galactosidase marker gene (lacZ) from a retroviral promoter [12] were further transduced at high efficiency with the 2 recombinant lentiviruses described above. Mouse myoblasts were seeded in 6 well-plate ($1x10^5$ cells/well) and infected for 4 hours at 37°C with hVICD8 and hICD8-expressing lentiviruses (MOI=25). Early passage myoblast clones

homogeneously expressing specific levels of VEGF were isolated by randomly sorting single cells in 96-wells, using a FACS Vantage SE cell sorter (Becton Dickinson, Basel, Switzerland). Expression of human trCD8a was assessed by staining transduced myoblasts with a specific APC-conjugated antibody under previously determined optimal conditions: the mouse anti-human CD8 antibody (clone 3B5; Caltag Laboratories Inc, Burlingame, USA) was used at a concentration of $0.5\mu g$ /10^6 cells, at a dilution of 1:50.

Isolated clones were cultured in 5% CO_2 on dishes coated with bovine skin collagen 1 (Sigma-Aldrich Chemie GmbH, Steinheim, Germany), with a growth medium consisting of 40% F10, 40% low-glucose DMEM (Sigma-Aldrich) and 20% fetal bovine serum (HyClone, Logan, UT, USA) supplemented with 2.5 ng/ml of basic fibroblast growth factor (FGF-2) (Becton Dickinson, Bedford, MA 01730, USA), as previously described [13].

Human VEGF$_{165}$ measurement by ELISA

The production of VEGF was quantified in cell culture supernatants using species-specific VEGF ELISA kits (R&D Systems Europe, Abingdon, UK). One ml of fresh medium was incubated on myoblasts cultured in a 60 mm dish for four hours, then filtered and analyzed in duplicate. Results were normalized by the number of cells and expressed as ng of VEGF/10^6 cells/day. At least four separate dishes of cells were assayed for each clone.

Myoblast Injection into SCID Mice

Single myoblasts clones expressing determined VEGF levels were implanted into 6-8 week-old immunodeficient SCID CB.17 mice (Charles River Laboratories, Sulzfeld,

Germany) in order to avoid an immunological response to myoblasts expressing xenogenic proteins. Animals were treated in accordance with Swiss Federal guidelines for animal welfare and the study protocol was approved by the Veterinary Office of the Canton of Basel-Stadt (Basel, Switzerland). Myoblasts were dissociated in trypsin and resuspended in PBS with 0.5% BSA. 5×10^5 myoblasts in 5 µl were implanted into the posterior auricular muscle, midway up the dorsal aspect of the external ear or transcutaneously into the tibialis anterior muscle of the hind limb, using a syringe with a $29^1/_2$G needle.

Tissue Staining

In order to visualize the entire vascular network of the ear, we performed intravascular staining with a biotinylated *Lycopersicon esculentum* (tomato) lectin (Vector Laboratories, Burlingame, California) which binds the luminal surface of all blood vessels as previously described [1]. Briefly, 4 weeks after myoblast implantation, mice were anesthetized and lectin was injected intravenously through the femoral vein. Four minutes later the thoracic cavity was opened and the tissues were fixed by perfusing the animal with 1% paraformaldehyde and 0.5% glutaraldehyde in PBS, pH 7.4 at 120 mmHg of pressure via a cannula in the left ventricle. Ears were then removed, bisected in the plane of the cartilage, and stained with X-gal staining buffer (1 mg/ml 5-bromo-4-chloro-3-indoyl-b-D-galactoside, 5 mM potassium ferrocyanide, 0.02% Nonidet P-40, 0.01% sodium deoxycholate, 1mM $MgCl_2$, in PBS, pH 7.4). Lectin-coated vessels were stained using avidin-biotin complex-diaminobenzidine histochemistry (Vector Laboratories), dehydrated through an ethanol series from 50% to 98%, cleared with toluene (Fisher

Scientific, Wohlen, Switzerland) and whole-mounted on glass slides with Permount embedding medium (Fisher Scientific, Wohlen, Switzerland).

Quantitative Real Time-PCR

RNA was extracted from cells using RNeasy kit (Qiagen) and from muscle using Trizol (Invitrogen), according to the manufacturer's instructions. RNA was reverse-transcribed into cDNA with the Omniscript Reverse Transcription kit (Qiagen) at 37 °C for 60 minutes. Quantitative Real-Time PCR (qRT-PCR) was performed on an ABI 7300 Real-Time PCR system (Applied Biosystems). In order to quantify both the human $VEGF_{165}$ and mouse $VEGF_{164}$ retroviral transcripts and to compare their expression, a unique set of primers and probe sequences was designed with Primer Express software 3.0 (Applied Biosystems), based on a common sequence expressed by both the human and mouse VEGF retroviral constructs:

IRES forward: 5'-GCTCTCCTCAAGCGTATTCAACA-3'

IRES reverse: 5'-CCCCAGATCAGATCCCATACA-3'

IRES probe: 5'-FAM-CTGAAGGATGCCCAGAAGGTACCCCA-TAMRA-3'

The cycling parameters were: 50°C for 2 minutes, followed by 95°C for 10 minutes and 40 cycles of denaturation at 95°C for 15 seconds and annealing/extension at 60°C for 1 minute. IRES primers and probe were used at 400nM. qRT-PCR was also performed on genomic DNA in order to quantify the number of myoblasts engrafted after implantation, by measuring the amount of stably integrated LacZ retroviral construct. A reference curve was constructed for each of the different myoblast clonal populations with a 10-fold dilution series between 1 and 10^6 cells, by using which the **Δ**Ct data of each sample

could be transformed in the corresponding absolute cell numbers. LacZ primer and probe sequences and reaction concentrations were previously published [14]. Reactions were performed in triplicate for each template, averaged, and normalized to expression of the GAPDH housekeeping gene (Applied Biosystems, Mm03302249_g1)

Viral copy number determination by qRT-PCR

Genomic DNA was extracted using DNeasy kit (Qiagen) according to the manufacturer's instructions. To calculate the number of viral copies integrated into the genome of target cells, RT-PCR was performed using the set of primers described above detecting a common sequence to retroviral and lentiviral vectors (IRES). Serial 10-fold dilutions of a recombinant plasmid in which the copy number was known were used as the positive control and standards for quantification in all real-time assays. Reactions were performed in triplicate for each template, averaged, and normalized to expression of the titin housekeeping gene, which is known to be present in 2 copies per genome:

TITIN forward: 5'- AAAACGAGCAGTGACGTGAGC-3'

TITIN reverse: 5'-TTCAGTCATGCTGCTAGCGC-3'

TITIN probe: 5'-FAM-TGCACGGAAGCGTCTCGTCTCAGTC-TAMRA-3'

The cycling parameters were: 50°C for 2 minutes, followed by 95°C for 10 minutes and 40 cycles of denaturation at 95°C for 15 seconds and annealing/extension at 60°C for 1 minute. Titin primers and probe were used at 200nM. IRES primers and probe were used at 400nM.

6.3 Results

Generation of lentivirally transduced mouse myoblasts and distribution of hVEGF$_{165}$ expression levels in single clones

In order to evaluate the effect of a lentiviral-based vector type and design on the expression of the therapeutic molecule, human VEGF$_{165}$, we generated a library of lentivirally transduced myoblast clones (hLV). Mouse myoblasts were infected at high efficiency with hVEGF$_{165}$-expressing lentivirus. One single round of transduction (MOI=25) resulted in more than 90% of positively transduced cells (Fig. 1a).
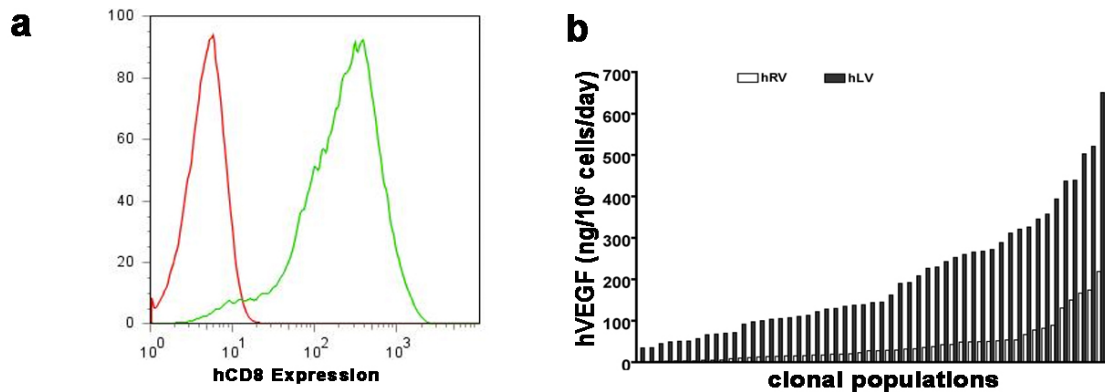
Figure 1. **Distribution of VEGF levels in clonal populations of myoblasts expressing human VEGF from a lentiviral vector (hLV) or retroviral vector (hRV). (a)** Heterogeneous and high levels of CD8a expression in the polyclonal population of lentivirally transduced VICD8 myoblasts (green curve) were detected by flow cytometry and compared to non-transduced cells (negative control, red curve). **(b)** Single myoblast clones expressing human VEGF were isolated from the polyclonal populations and their VEGF expression in vitro was quantified by ELISA showing that the lentivirally transduced population displayed a wider distribution of VEGF expression levels compared to retrovirally transduced cells. White bars = retrovirally transduced (hRV) human VEGF$_{165}$-expressing myoblasts, black bars = lentivirally transduced (hLV) human VEGF$_{165}$-expressing myoblasts.

Fifty-one hLV clones were randomly isolated by single cell FACS-sorting and found to secrete a wide range of $hVEGF_{165}$ levels (34.4 ± 8.4 to 650 ± 100 ng/10^6 cells/day). This range reached much higher levels than with hRV clones, previously isolated and characterized (5.4 ± 0.9 to 254 ± 39 ng/10^6 cells/day), as described in Chapter 5. Analysis of the distribution of VEGF levels showed that both hLV and hRV clones secreted spread levels over a wide range (Fig. 1b), although lentivectors enriched for higher VEGF levels as compared to hRV clones.

Viral copy number analysis of hLV and hRV $VEGF_{165}$-expressing clones

Retroviruses and lentiviruses differ from each other with respect to their integration profile in target cells. While retroviruses cluster in proximity of transcriptional unit start sites, lentiviruses often integrate within the whole transcriptional unit. To evaluate the possibility of modulating the distribution of VEGF expression levels within a polyclonal population by regulating the number of viral copies integrated into the genome of each target cell, we performed qRT-PCR to compare the viral copy number in single clones isolated from a population of retrovirally (hRV) or lentivirally (hLV) transduced mouse myoblasts. We found that hLV clones had significantly higher numbers of viral genomes per cell, demonstrating that lentivectors have a propensity to integrate in multiple copies compared to retrovectors (Fig. 2). We reasoned that, if lentivectors showed a consistent level of expression per integrated copy, then it would be possible to generate populations of genetically modified cells producing a sufficiently homogeneous range of levels just by controlling the multiplicity of infection during transduction, possibly avoiding the need for FACS purification. The viral copy number value obtained for each clone was therefore

correlated with the corresponding VEGF expression level measured by ELISA. As expected, both populations (hRV and hLV) showed that the same copy number yielded a wide range of VEGF expression levels in both populations and that lentivectors produced a less variable distribution than retrovectors. These results suggest that optimizing the transduction conditions to control the number of viral copies integrated into each target cell would not result in polyclonal populations expressing pre-determined VEGF expression levels with sufficient homogeneity.
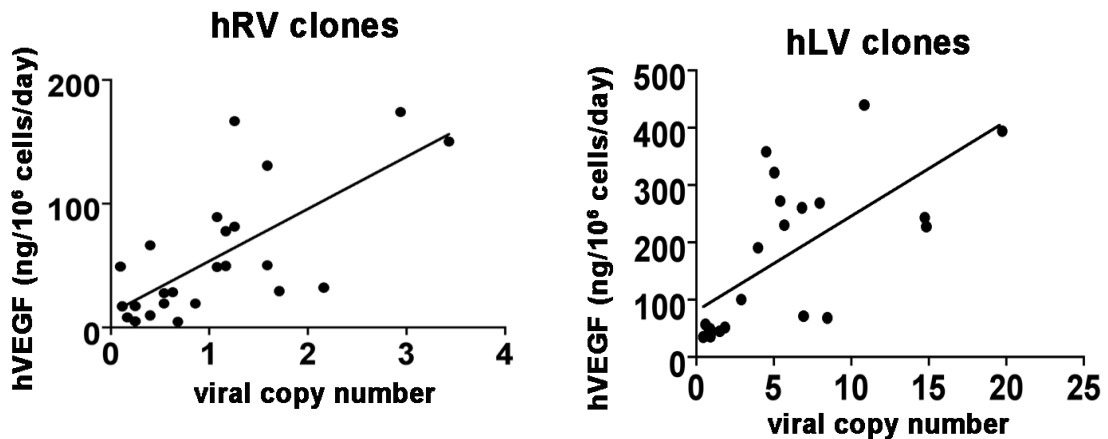
Figure 2. **Correlation between hVEGF$_{165}$ expression and viral copy number in retrovirally (hRV) and lentivirally (hLV) myoblasts.**
Viral copy number was calculated in single hRV and hLV clones (n=21 for both groups) and correlated to the corresponding VEGF expression level *in vitro*, measured by ELISA. A direct correlation was found to exist in both groups (p<0.0001), but with a widespread distribution of levels at each copy number.

In vivo kinetics of hVEGF$_{165}$ expression by hLV and hRV clones

As well as on the copy number, the effective level of expression in *vivo* depends also on whether and how much the viral promoter activity is affected by *in vivo* conditions, potentially leading to a loss of expression or even greater factor release. As this is a critical parameter influencing the safety and the efficacy of the vector, the cellular

promoter elongation factor 1α (EF1α), that drives the expression in the third-generation lentiviral vectors used here, could influence expression kinetics of VEGF$_{165}$ *in vivo* compared to the viral LTR promoter in retroviral vectors. We selected 4 clones, belonging to either the hRV or the hLV pool, that secreted matching low and high VEGF levels *in vitro* (hRV$_{low}$ = 32.2±2.8 ng/10^6 cells/day; hRV$_{high}$ = 253.8±44.8 ng/10^6 cells/day; hLV$_{low}$ = 34.8±2.2 ng/10^6 cells/day; hLV$_{high}$ = 268±16.6 ng/10^6 cells/day) and cells were injected in the tibialis anterior muscles of SCID mice. mRNA levels of the viral-encoded hVEGF$_{165}$ were determined immediately after injection (d0), as a baseline value, and 7 and 14 days later. VEGF expression was normalized by the number of surviving cells in each sample, determined by qRT-PCR for the LacZ marker on genomic DNA, as described in Chapter 5, so that the results reflected the intrinsic activity of the vector promoters in each cell. We found a rapid and drastic decrease of the VEGF expression per cell with both hRV clones already 1 week after implantation, which was further diminished by the 2 weeks time-point. In contrast, both hLV clones did not suffer any switch off and the presence of a cellular promoter allowed a constant VEGF expression in each cell up to 2 weeks after implantation (Fig. 3).
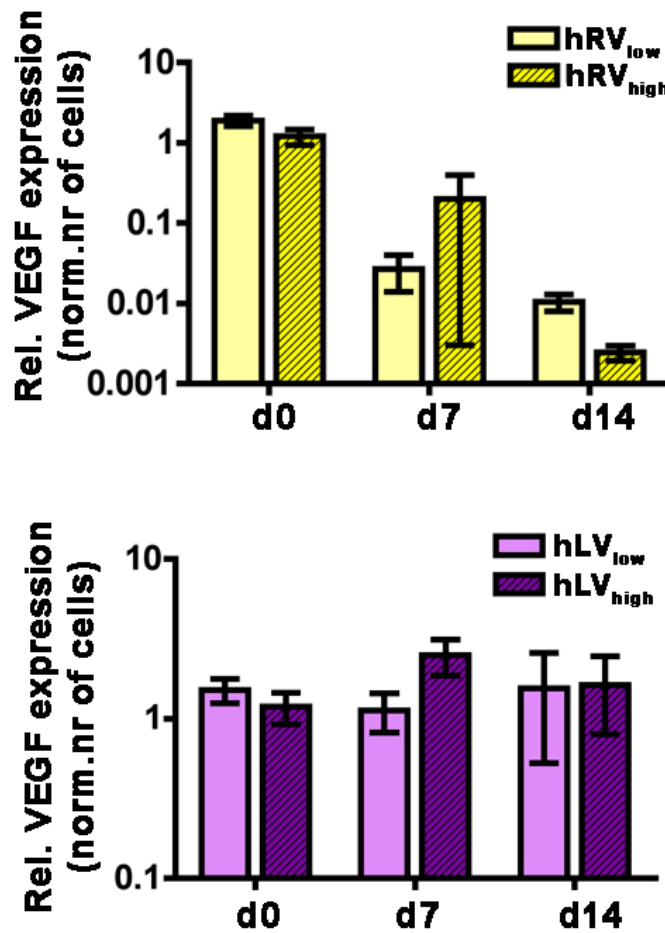
Figure 3. *In vivo* **kinetics of hVEGF$_{165}$ expression by retrovirally (hRV) and lentivirally (hLV) transduced myoblasts.**

In vivo VEGF$_{165}$-expression of hRV and hLV clones was quantified immediately after cell injection (Day 0) or after 1 (Day 7) or 2 weeks (Day 14) by qRT-PCR and normalized by the number of injected cells surviving in each sample. VEGF expression by hRV clones rapidly decreased already 7 days after myoblasts implantation, whereas VEGF levels of expression by hLV clones was sustained until 2 weeks after injection (n=4 per each group).

Microenvironmental dose-dependent angiogenesis by hLV clones

Since lentiviral vectors ensured a more sustained expression *in vivo*, we investigated

whether lentivirally transduced cells would induce aberrant angiogenesis at lower levels

of human VEGF$_{165}$ than those expressing from retroviral vectors described in Chapter 5.

Selected clones spanning the whole range of hVEGF$_{165}$ levels were injected into the ears of SCID mice and the morphology of newly induced capillaries was visualized by lectin intravascular staining. Four weeks after implantation, hLV clones expressing increasing VEGF$_{165}$ levels up to 450 ng/10^6 cells/day induced a clear angiogenesis, but this was comprised only of normal capillaries. However, the clone producing the highest level of 650 ng/10^6 cells/day, caused the growth of large aberrant angioma-like structures already 10 days after implantation, as shown by hematoxylin and eosin staining in Fig. 4.
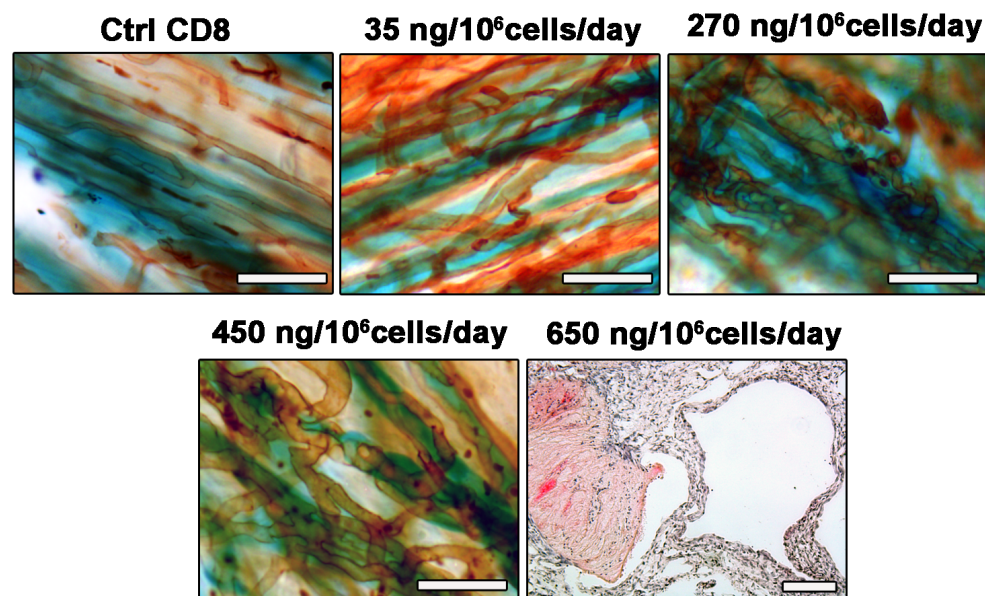
Figure 4. **Morphological analysis of hLV clones at several VEGF doses *in vivo*.**
Whole mount lectin staining showed that human VEGF expressed by a lentivector induced only normal capillaries until a dose of 450 ng/10^6 cells/day. However, injecting the highest hLV producer clone (650 ng/10^6 cells/day) induced the growth of aberrant bulbous vascular structures (hematoxylin and eosin staining) already 10 days after implantation (n=5-8 for all groups). Size bar = 50 μm in all panels.

6.4 Discussion

Oncogenicity concerns regarding retroviral vectors (RV) usage in clinical practice caused recent changes in regulatory requirements that prompted us to implement the use of self-inactivating lentiviral vectors to establish a clinically compliant cell-based platform for $VEGF_{165}$-expression. Lentiviral vectors (LV) offer a much improved safety profile and were approved for use in 24 gene therapy clinical trials in Europe and the USA in 2009 (www.wiley.co.uk/genetherapy/clinical). In this study we compared the integration profile of LV- and RV-transduced clonal populations over-expressing different $VEGF_{165}$ levels and we found that LV integrate in larger copy numbers per cell, leading to significantly higher VEGF levels than RV. We also found that there is no strict correlation between a given viral copy number and a specific VEGF level, suggesting that controlling the number of viral copies integrated in each cell would not be sufficient to avoid a wide heterogeneity in the VEGF levels expressed by the transduced population, including potentially toxic ones.

Besides the different integration profile, we found that LV employing a cellular promoter allowed a sustained VEGF expression *in vivo* up to 2 weeks after implantation. On the contrary, RV displayed a rapid loss of VEGF expression already 1 week after implantation, most likely due to the silencing of the viral LTR promoter, which is known to be more prone to methylation events [15]. Overall, LV-based expression led to features that are predicted to make the control of VEGF dose *in vivo* more difficult. In fact, our results showed that, compared to retroviral vectors, lentiviral transduction can easily lead to integration of multiple copies in the same cell and to higher levels of transgene expression which persist unabated *in vivo*. In order to overcome these limitations, it could

be advantageous to apply the high-throughput FACS-based technology we recently developed to rapidly purify populations homogeneously expressing desired VEGF levels [6]. To maximize the efficiency of purification of cells expressing safe and therapeutic levels, it would be desirable to optimize the transduction protocol in order to reproducibly obtain a high efficiency of transduction while preserving a balanced distribution of expression levels, so that high and toxic levels are not overrepresented in the primary transduced population. Expression levels of the transgene increase linearly as the multiplicity of infection (MOI) increases. Therefore, a suitable strategy to ensure a high percentage of transduction while minimizing the number of integrated viral copies per cell would be to use a low MOI over repeated rounds of infection, rather than a single round with high MOI. Furthermore, besides reducing the MOI, to generate a transduced population expressing in average lower VEGF levels, it might be desirable to use a different cellular promoter. Indeed, EF1a is a constitutive cellular promoter of moderate strength [16], but others could be used with lower activity.

The fact that transgene expression sustained *in vivo* over time, raises a safety concern regarding the use of LV in a therapeutic angiogenesis setting. In fact, we cannot exclude that low but sustained VEGF levels can become toxic in the long term and cause the onset of side effects. For this purpose, long-term experiments aiming to investigate the effects of sustained VEGF expression for a longer time (4 months) are ongoing.

In conclusion, LV have an increased safety profile regarding insertional mutagenesis, but also have features that make it more difficult to control the effective dose of VEGF over-expression *in vivo* for therapeutic purposes. The use of FACS-purified populations

may allow the rigorous investigation of the therapeutic window of this approach in appropriate preclinical models (not rodent), or in phase I clinical trials.

References

1.   Ozawa CR, Banfi A, Glazer NL, Thurston G, Springer ML, Kraft PE, McDonald DM, Blau HM. Microenvironmental vegf concentration, not total dose, determines a threshold between normal and aberrant angiogenesis. *The Journal of clinical investigation*. 2004;113:516-527

2.   von Degenfeld G, Banfi A, Springer ML, Wagner RA, Jacobi J, Ozawa CR, Merchant MJ, Cooke JP, Blau HM. Microenvironmental vegf distribution is critical for stable and functional vessel growth in ischemia. *FASEB journal : official publication of the Federation of American Societies for Experimental Biology*. 2006;20:2657-2659

3.   Tafuro S, Ayuso E, Zacchigna S, Zentilin L, Moimas S, Dore F, Giacca M. Inducible adeno-associated virus vectors promote functional angiogenesis in adult organisms via regulated vascular endothelial growth factor expression. *Cardiovascular research*. 2009;83:663-671

4.   Dor Y, Djonov V, Abramovitch R, Itin A, Fishman GI, Carmeliet P, Goelman G, Keshet E. Conditional switching of vegf provides new insights into adult neovascularization and pro-angiogenic therapy. *The EMBO journal*. 2002;21:1939-1947

5.   Wolff T, Mujagic E, Gianni-Barrera R, Fueglistaler P, Helmrich U, Misteli H, Gurke L, Heberer M, Banfi A. Facs-purified myoblasts producing controlled vegf levels induce safe and stable angiogenesis in chronic hind limb ischemia. *Journal of cellular and molecular medicine*. 2012;16:107-117

6.   Misteli H, Wolff T, Fuglistaler P, Gianni-Barrera R, Gurke L, Heberer M, Banfi A. High-throughput flow cytometry purification of transduced progenitors expressing defined levels of vascular endothelial growth factor induces controlled angiogenesis in vivo. *Stem Cells*. 2010;28:611-619

7.   Baum C, Dullmann J, Li Z, Fehse B, Meyer J, Williams DA, von Kalle C. Side effects of retroviral gene transfer into hematopoietic stem cells. *Blood*. 2003;101:2099-2114

8.   Mavilio F, Pellegrini G, Ferrari S, Di Nunzio F, Di Iorio E, Recchia A, Maruggi G, Ferrari G, Provasi E, Bonini C, Capurro S, Conti A, Magnoni C, Giannetti A, De Luca M. Correction of junctional epidermolysis bullosa by transplantation of genetically modified epidermal stem cells. *Nature medicine*. 2006;12:1397-1402

9.   Montini E, Cesana D, Schmidt M, Sanvito F, Bartholomae CC, Ranzani M, Benedicenti F, Sergi LS, Ambrosi A, Ponzoni M, Doglioni C, Di Serio C, von Kalle C, Naldini L. The genotoxic potential of retroviral vectors is strongly modulated by vector design and integration site selection in a mouse model of hsc gene therapy. *The Journal of clinical investigation*. 2009;119:964-975

10.   Zychlinski D, Schambach A, Modlich U, Maetzig T, Meyer J, Grassman E, Mishra A, Baum C. Physiological promoters reduce the genotoxic risk of integrating gene vectors. *Molecular therapy : the journal of the American Society of Gene Therapy*. 2008;16:718-725

11.   Mitta B, Rimann M, Fussenegger M. Detailed design and comparative analysis of protocols for optimized production of high-performance hiv-1-derived lentiviral particles. *Metabolic engineering*. 2005;7:426-436

12. Rando TA, Blau HM. Primary mouse myoblast purification, characterization, and transplantation for cell-mediated gene therapy. *The Journal of cell biology*. 1994;125:1275-1287

13. Banfi A, Springer ML, Blau HM. Myoblast-mediated gene transfer for therapeutic angiogenesis. *Methods in enzymology*. 2002;346:145-157

14. Banfi A, von Degenfeld G, Gianni-Barrera R, Reginato S, Merchant MJ, McDonald DM, Blau HM. Therapeutic angiogenesis due to balanced single-vector delivery of vegf and pdgf-bb. *FASEB journal : official publication of the Federation of American Societies for Experimental Biology*. 2012;26:2486-2497

15. Ellis J. Silencing and variegation of gammaretrovirus and lentivirus vectors. *Human gene therapy*. 2005;16:1241-1246

16. Kim DW, Uetsuki T, Kaziro Y, Yamaguchi N, Sugano S. Use of the human elongation factor 1 alpha promoter as a versatile and efficient expression system. *Gene*. 1990;91:217-223

Summary and future perspectives

Angiogenesis is a complex process that requires a fine regulation of different cells and factors both in space and time. The angiogenic cascade can be initiated by a single growth factor, i.e. Vascular Endothelial Growth Factor (VEGF). VEGF is the master regulator of sprouting angiogenesis, the best-understood mode of vascular growth. Besides its role in physiological angiogenesis, VEGF has been also shown to be an important regulator of pathological angiogenesis. Several studies have investigated VEGF over-expression by means of both gene and cell-based approaches as a possible therapeutic strategy to rescue blood supply in ischemic conditions. However, the results of clinical trails have been disappointing and VEGF gene delivery has been found to have a narrow therapeutic window *in vivo*. In fact, as described in Chapter 2, in order to achieve therapeutic angiogenesis, VEGF dose needs to be rigorously controlled in the microenvironment around each producing cell. Using a myoblast-based delivery system, we previously found that VEGF over-expression in skeletal muscle can induce normal and aberrant angiogenesis strictly depending on its microenvironmental level and not on the total dose delivered [1]. By using the same highly controlled cell-based delivery platform as a tool, in Chapters 3 and 4 we aimed to investigate the cellular and molecular mechanisms by which different VEGF doses induce normal and aberrant angiogenesis in a therapeutically relevant tissue, i.e. skeletal muscle. We found that 4 days after myoblast implantation, VEGF over-expression caused a dose-dependent enlargement of pre-existing capillaries, which was associated with active endothelial proliferation and increased blood flow and shear stress. In these conditions, we could never observe filopodia or protrusions, typical of tip cells, suggesting that VEGF over-expression was not inducing angiogenesis by sprouting. Indeed, by corrosion cast analysis and serial semi-thin 3D reconstruction, we

found that by 4 days vessel enlargements showed the formation of transluminar pillars, typical of intussusception or splitting angiogenesis, and that by 7 days, depending on VEGF dose, enlarged vessels remodeled both to normal and aberrant vascular structures by intussusception rather than by sprouting. The key regulator of sprouting angiogenesis is the Notch1 pathway, which determines the proper specification of endothelial cells to acquire a tip or a stalk phenotype. Therefore, in Chapter 4 we investigated whether and how the Notch1 signaling pathway regulated intussusceptive angiogenesis in skeletal muscle. By 4 days, when both low and high VEGF levels induced enlarged vessels, we found activated Notch1 in stretches of contiguous endothelial cells, which simultaneously expressed also the Notch ligand Dll4, whereas the alternate pattern ("salt and pepper") of Dll4 expression in tip cells and Notch1 activation in stalk cells, which controls sprouting by lateral inhibition, was absent. Pharmacological inhibition of Notch signaling pathway disrupted initial vascular enlargements, which formed disordered aggregates of endothelial cells instead. Interestingly, the experimental validation of testable predictions generated by a computational model of Notch signaling in angiogenesis, suggests that the synchronous expression of Dll4 and Notch1 activation in contiguous endothelial cells, which leads to circumferential enlargement instead of sprouting, is due to a switch from prevailing lateral inhibition to prevailing lateral induction of Dll4 by Notch1. Furthermore, we also demonstrated that subsequent remodeling to either normal capillaries or aberrant-like vascular structures was independent of Dll4-Notch1 signaling. These results suggest that the pattern of activation of the Dll4/Notch1 axis determines whether VEGF induces angiogenesis by sprouting or intussusception. However, other Notch ligands and receptors might be involved in the dose-dependent transition between

normal and aberrant angiogenesis, such as Jagged 1 and Notch4, which are also expressed in the endothelium. Jagged 1 has been described as a potent proangiogenic regulator that acts by antagonizing Dll4-Notch signaling by competing with Dll4 for the binding to the receptor [2]. Based of these results, we would propose as a next step, to investigate whether Jagged1 is differentially expressed in response to various VEGF levels and if its sustained expression can correlate with an aberrant remodeling of VEGF-induced vasculature. On the other hand, several studies showed that constitutive Notch4 activation in the endothelium causes the development of brain arteriovenous malformations (BAVMs) [3]. Arteriovenous (AV) malformations are characterized by vessel enlargement and high-flow AV shunts which bypass flow into downstream capillary-networks. Recently, it has been also demonstrated that normalization of Notch signaling by repressing Notch4 expression results in the regression of these large-caliber, high-flow AV shunts. This regression requires restoration of EphB4 receptor expression in venous endothelial cells, highlighting the involvement of other signaling pathways in the regulation of AVMs [4]. The aberrant vascular structures induced by uncontrolled and high VEGF levels, share some similarities with the AVMs phenotype described above. Indeed, the induced hemangiomas are very dilated vessels covered by a thick layer of smooth muscle cells characterized by a turbulent high-flow rate and have been shown to behave functionally as AV shunts [5]. Based on these considerations and knowing that Notch1 does not play a role in the differential remodeling between normal and aberrant vasculature, it is reasonable to hypothesize that Notch4 might play a role in this subsequent stage of VEGF-induced angiogenesis. We plan to investigate whether sustained Notch4 activation could be the trigger for the growth of aberrant-like vascular structures. We will

determine the levels and kinetics of Notch4 expression and activation in skeletal muscles implanted with myoblast clones expressing different specific VEGF doses, as well as express high VEGF levels in Notch4 KO mice.

On the other hand, it is likely that several pathways may act in concert to determine the switch between normal and aberrant angiogenesis induced by increasing VEGF doses. Therefore, we plan to combine the unique and highly controlled model of VEGF dose- and time-dependent angiogenesis we developed with laser-capture microdissection to perform a stage-specific and VEGF-dose dependent analysis of the vascular mRNA and miRNA transcriptomes. We will micro-dissect vascular structures specifically in the areas of effect 4 and 7 days after implantation of clones expressing low and high VEGF levels. State-of-the-art bioinformatics analysis in collaboration with Hoffman-La Roche is expected to identify differentially regulated clusters of genes and miRNAs that will define the high-level pathways regulating the switch from normal to aberrant angiogenesis. The results of these experiments should contribute to unravel the molecular mechanisms that govern the induction of physiological and pathological angiogenesis after therapeutic over-expression of VEGF and to foster the development of more effective strategies for the treatment of several pathologies, such as peripheral artery diseases.

In a clinical application, the therapeutic molecule is human $VEGF_{165}$. However, the angiogenic effects of controlled doses of human $VEGF_{165}$ in skeletal muscle are almost unknown. Therefore, in Chapter 5 we generated a library of retrovirally transduced mouse myoblast clones over-expressing specific doses of human $VEGF_{165}$ and we investigated their angiogenic potential *in vivo*. Interestingly, we found that human $VEGF_{165}$ did not induce any aberrant vascular structures in mouse skeletal muscle even at

higher levels of expression than those sufficient for mouse VEGF$_{164}$ to cause angioma growth. Furthermore, we found that human VEGF$_{165}$ expression persisted at similar of even higher levels than that of mouse VEGF$_{164}$ over 2 weeks *in vivo*, suggesting that the different biological effect observed was not due to a progressive loss of expression of the transgene. Indeed, we found that human VEGF$_{165}$ was less potent than mouse VEGF$_{164}$ in activating VEGFR signaling in mouse endothelial cells, while the reverse was true in human endothelium. Therefore, VEGF dose-dependent effects are species-specific and cannot be reliably determined in rodent preclinical models. Further, in view of a clinical translation of cell-based VEGF gene delivery, in Chapter 6, we investigated how the use of lentiviruses, which are safer than retroviruses, would modify the ability to control VEGF dose *in vivo*. We developed a new library of clones over-expressing human VEGF$_{165}$ from a lentiviral vector and we evaluated whether and how vector type and design affected human VEGF$_{165}$ expression and its angiogenic potential in skeletal muscle. We found that lentiviral vectors integrated a greater number of copies in target cells compared to retroviruses, leading to higher VEGF levels of expression. Furthermore, we found that lentiviruses allowed a sustained VEGF expression *in vivo* up to 2 weeks after implantation, while retroviruses displayed a rapid loss of expression of the transgene already 1 week after myoblast implantation. Morphological analysis of vessels induced by lentivirally transduced mouse myoblasts expressing human VEGF$_{165}$ showed that aberrant angioma-like vascular structures were induced at extremely high VEGF levels (650 ng/10^6 cells/day). These results suggest that two different points should be considered in view of a clinical translation of cell-based VEGF gene delivery:

1) the validation of cell-based VEGF$_{165}$ over-expression for therapeutic purpose in

rodent pre-clinical models is not adequate, because it can mask deleterious side effects that could occur in patients, due to the species-specific potency of VEGF stimulation. On the other hand, the use of a lentiviral vector led to features that are expected to make the control of VEGF dose *in vivo* more difficult. Therefore, it would be necessary to test the angiogenic potential of human VEGF in more clinically reflective large animal models, such as rabbits or pigs, which are evolutionarily closer to the humans. The greater rate of homology shared by VEGF sequence in humans and these species, is expected to better reflect the effects of $VEGF_{165}$ over-expression at specific doses in patients. Nevertheless, a rigorous comparison of the dose-dependent effects of human and syngenic VEGF would be required to validate these preclinical models.

2) On the other hand, in order to design rigorous dose-escalation phase I clinical trials, it would be necessary to rely on an effective strategy to ensure controlled expression of specific VEGF doses with a homogeneous distribution *in vivo*. Such requirements may be conveniently satisfied by flow cytometry-based technology that we recently developed to allow the high-throughput purification of transduced progenitor populations homogeneously expressing pre-defined VEGF levels [6].

Bibliography

1.   Ozawa CR, Banfi A, Glazer NL, Thurston G, Springer ML, Kraft PE, McDonald DM, Blau HM. Microenvironmental vegf concentration, not total dose, determines a threshold between normal and aberrant angiogenesis. *The Journal of clinical investigation*. 2004;113:516-527

2.   Benedito R, Roca C, Sorensen I, Adams S, Gossler A, Fruttiger M, Adams RH. The notch ligands dll4 and jagged1 have opposing effects on angiogenesis. *Cell*. 2009;137:1124-1135

3.   Murphy PA, Lam MT, Wu X, Kim TN, Vartanian SM, Bollen AW, Carlson TR, Wang RA. Endothelial notch4 signaling induces hallmarks of brain arteriovenous malformations in mice. *Proceedings of the National Academy of Sciences of the United States of America*. 2008;105:10901-10906

4.   Murphy PA, Kim TN, Lu G, Bollen AW, Schaffer CB, Wang RA. Notch4 normalization reduces blood vessel size in arteriovenous malformations. *Science translational medicine*. 2012;4:117ra118

5.   Zacchigna S, Tasciotti E, Kusmic C, Arsic N, Sorace O, Marini C, Marzullo P, Pardini S, Petroni D, Pattarini L, Moimas S, Giacca M, Sambuceti G. In vivo imaging shows abnormal function of vascular endothelial growth factor-induced vasculature. *Human gene therapy*. 2007;18:515-524

6.   Misteli H, Wolff T, Fuglistaler P, Gianni-Barrera R, Gurke L, Heberer M, Banfi A. High-throughput flow cytometry purification of transduced progenitors expressing defined levels of vascular endothelial growth factor induces controlled angiogenesis in vivo. *Stem Cells*. 2010;28:611-619

Personal information

Name	**Marianna Trani**
Date of birth	7th March 1984
Private address	Lothringerstrasse 104
	4056 Basel
	Switzerland
Nationality	Italian
E-mail	marianna.trani@gmail.com
	tranim@uhbs.ch
Mobile telephone	+393403208987
	+41796487297

1

Working experiences

February 2009 – current position

PhD Student in Biomedical Sciences

University Hospital of Basel, Department of Biomedicine, Laboratory of Cell and Gene Therapy (Dr. Banfi A.)

Main subject: The role of Notch signalling pathway in the regulation of vascular morphogenesis induced by VEGF through cell and viral-based delivery systems in skeletal muscle.

April 2008 – November 2008

Master Thesis Student

Ludwig Institute for Cancer Research in Uppsala, Laboratory of Apoptotic Signalling (Dr. Landstrom M.)

Main subject: Pro-apoptotic effect of aurothiomalate in prostate cancer cells.

April 2006 – October 2006

Bachelor Thesis Student

University of Bologna, Department of Biochemistry, Laboratory of molecular biology (Prof. Capranico G.)

Main subject: Effects of the camptothecin on the RNA polimerase II in transcribed genes of human cells expressing reduced levels of DNA topoisomerase.

Education

October 2006 – December 2008

Master Degree in Pharmaceutical Biotechnology -University of Bologna- (final mark: 110/110 cum laude)
Experimental thesis: **"***Pro-apoptotic effect of aurothiomalate in prostate cancer cells"*

October 2003 – October 2006   **Bachelor Degree in Biotechnology- University of Bologna -**(final mark: 110/110)

Experimental thesis: "*Effects of the camptothecin on the RNA polimerase II in transcribed genes of human cells expressing reduced levels of DNA topoisomerase I*"

Skills and competences

2

- Ability to work independently and in international teams
- Competent with most scientific databases (NCBI, SwissProt, SGD, UCSC) and softwares
- Problem solving and good organizational skills
- Willingness to learn and develop new skills

Language skills

Italian: mother tongue

English: excellent writing and oral skills

French: good writing and oral skills

Conferences

Poster presentation: 18th Meeting of European Society of Gene and cell therapy (22-25 October 2010, Milan)

Poster presentation: EC8 Zurich (15-18 June 2011)

Poster presentation (Best Poster Award): International Vascular Biology Meeting (2-5 June 2012, Wiesbaden)

Publications

- Gianni-Barrera R, **Trani M**, Reginato S, Banfi A "To split or to sprout? VEGF, Notch and vascular morphogenesis" Biochem Soc Trans. 2011 Dec; 39(6):1644-8
- **Trani M**, Sorrentino A, Busch C, Landstrom M "Pro-apoptotic effect of aurothiomalate in prostate cancer cells", Cell Cycle. 2009 Jan 15;8(2):306-13
- Gianni-Barrera R, **Trani M**, Hlushchuk R, Heberer M, Djonov V, Banfi A "Dose-dependent VEGF$_{164}$ overexpression in skeletal muscle induces angiogenesis and vascular remodeling by intussusception and not by sprouting" (manuscript submitted)
- **Trani M**, Gianni-Barrera R, Mujagic E, Gurke L, Wolff T, Heberer M, Banfi A " Dose-dependent angiogenesis by VEGF is species-specific" (manuscript submitted)
- **Trani M**, Gianni-Barrera R, Reginato S, Bentley K, Heberer M, Gerhardt H, Banfi A "Dll4/Notch1 axis regulates intussusceptive angiogenesis in skeletal muscle by lateral induction" (manuscript in preparation)
- **Trani M,** Gianni-Barrera R, Heberer M, Banfi A "Retroviruses versus Lentiviruses: the transition towards a clinical application for therapeutic angiogenesis" (manuscript in preparation)